SUSTAINABLE GROUND WATER WITHDRAWAL ASSESSMENT THROUGH PUMPING TEST FOR WELL FIELD DESIGN AND HYDRAULIC MODELING APPLICATION USING WATERGEMS FOR RURAL WATER SUPPLY: A CASE STUDY OF SHILLA VILLAGE BESIDE THE DAMODAR RIVER

A thesis submitted towards partial fulfillment of the requirements
for the degree of

MASTER OF ENGINEERING

In Water Resources and Hydraulic Engineering

Course affiliated to Faculty of Engineering & Technology

Jadavpur University

Submitted by

KARTICK JANA

Exam Roll No: **M4WRE24020**

Reg. No.:**163873 of 2022-2023**

Under the guidance of

PROF. (DR.) ASIS MAZUMDAR

Professor and Director

School Of Water Resources Engineering, Jadavpur University

Dr. GOURAB BANERJEE

Assistant Professor

School of Water Resources Engineering, Jadavpur University

School of Water Resources Engineering

M.E. (Water Resources & Hydraulic Engineering) course affiliated to

Faculty of Engineering & Technology

Jadavpur University

Kolkata 700032, India

2024

M.E. (Water Resources & Hydraulic Engineering) course affiliated to
Faculty of Engineering & Technology
Jadavpur University
Kolkata, India

Certificate of Recommendation

This is to certify that the thesis entitled **"Sustainable Ground Water Withdrawal Assessment Through Pumping Test For Well Field Design And Hydraulic Modeling Application Using WaterGEMS For Rural Water supply:A Case Study Of Shilla Village Beside The Damodar River"** is a bonafide work carried out by **Mr.Kartick Jana** our supervision and guidance for partial fulfillment of the requirement for the Post Graduate Degree of Master of Engineering in Water Resources & Hydraulic Engineering during the academic session 2022-2024.

THESIS ADVISOR
Prof. (Dr.) Asis Mazumdar
Professor and Director
School of Water Resources Engineering
Jadavpur University
Kolkata-700032

THESIS ADVISOR
Dr. Gourab Banerjee
Assistant Professor
School of Water Resources Engineering
Jadavpur University
Kolkata-700032

DIRECTOR
Prof. (Dr.) Asis Mazumdar
Professor and Director
School of Water Resources Engineering
Jadavpur University
Kolkata-700032

DEAN
Faculty of Interdisciplinary Studies, Law & Management
Jadavpur University

M.E. (Water Resources & Hydraulic Engineering) course affiliated to
Faculty of Engineering & Technology
Jadavpur University
Kolkata, India

CERTIFICATE OF APPROVAL **

This foregoing thesis is hereby approved as a credible study of an engineering subject carried out and presented in a manner satisfactorily to warranty its acceptance as a prerequisite to the degree for which it has been submitted. It is understood that by this approval the undersigned do not endorse or approve any statement made or opinion expressed or conclusion drawn therein but approve the thesis only for purpose for which it has been submitted.

Committee of

Final Examination
for the evaluation
of the thesis

_____

_____

_____

** Only in case the thesis is approved.

DECLARATION OF ORIGINALITY AND COMPLIANCE OF ACADEMIC ETHICS

I hereby declare that this thesis contains literature survey and original research work by the undersigned candidate, as part of my **Master of Engineering** in **Water Resources & Hydraulic Engineering** in the Faculty of Interdisciplinary Studies, Jadavpur University during academic session 2022-2024.

All information in this document have been obtained and presented in accordance with academic rules and ethical conduct.

I also declare that, as required by these rules and conduct, I have fully cited and referenced all material and results that are not original to this work.

NAME : **KARTICK JANA**

EXAM ROLL NUMBER : **M4WRE24020**

THESIS TITLE : **Sustainable Ground Water Withdrawal Assessment Through Pumping Test For Well Field Design And Hydraulic Modeling Application Using WaterGEMS For Rural Water Supply: A Case Study Of Shilla Village Beside The Damodar River.**

SIGNATURE :

DATE :

ACKNOWLEDGEMENT

I express my sincere gratitude and thanks to my supervisor **Prof. (Dr.) Asis Mazumdar,** Professor and Director of School of Water Resources Engineering, Jadavpur University and **Dr. Gourab Banerjee,** Assistant Professor of School of Water Resources Engineering, Jadavpur University. Without their support and guidance, it was impossible for me to carry out this project.

I would also like to express my sincere gratitude to **Prof. (Dr.) Arunabha Majumder,** Emeritus Professor, School of Water Resources Engineering, **Prof. (Dr.) Pankaj Kumar Roy,** Professor, School of Water Resources Engineering, **Dr. Subhasish Das,** Associate Professor, School of Water Resources Engineering, and **Dr. Rajib Das,** Assistant Professor, School of Water Resources Engineering, Jadavpur University for their valuable suggestions.

Moreover, I would like to express my sincere thanks to my seniors **Mr. Nilanjan Saha**, **Mr. Rijurekha Dasgupta and Mr. Nikhil Das** for their support and help during my thesis work.

Thanks, are also due to all staff of School of Water Resources Engineering of Jadavpur University and the Regional center for their help and support.

In addition, I express my very profound gratitude to my family members for providing me with unfailing support and continuous encouragement throughout my years of study and through the process of researching and writing this thesis. This accomplishment would not have been possible without them.

Most significantly I would like to express my gratitude, thanks and gratefulness to my parents without whom I would not be able to do anything in my life.

Date : **31st May, 2024**

KARTICK JANA

Examination Roll No- M4WRE24020

ABSTRACT

This research work presents a comprehensive assessment of the hydrogeological characteristics and the design of a sustainable water supply system for Shilla village, Galsi-1, Purba Bardhaman located beside the Damodar River in West Bengal. The study involves conducting pumping tests to determine key aquifer properties such as transmissivity and storativity, alongside Vertical Electrical Sounding (VES) surveys to delineate subsurface lithology and aquifer geometry. The results indicate a stratified subsurface with significant clay and sand layers, crucial for aquifer characterization and well field design. The pumping tests revealed an average transmissivity 2414 m^2/day and storativity of 0.1209, with recuperation tests showing an average transmissivity of 2795 m^2/day. Based on these findings, a well field design comprising ten strategically spaced wells, each well having capacity of 800 m^3/day, was proposed to meet the water demand without exceeding specified drawdown limits of 2.55m. Mechanical analysis suggested the need for artificial gravel packs around the pumping wells due to the Coefficient of Uniformity (Cu) values ranging from 1.8 to 2.4. Hydraulic modeling using WaterGEMS software enabled the simulation and optimization of the water distribution network, ensuring efficient supply to the target areas. The minimum pressure at the extreme consumer end (J-244) was found to be 8.25m of H2O, exceeding which is within the CPHEEO manual limit ($\geq$ 7m of H2O). Projected water demand for Shilla village up to the year 2052 was estimated, guiding the future planning of the water supply scheme. The findings underscore the importance of integrated hydrogeological assessment and advanced hydraulic modeling in developing sustainable water supply systems for rural areas.

Keywords : Sustainable groundwater withdrawal, pumping test, Vertical Electrical Sounding (VES), Well field design, WaterGEMS, Damodar River, Shilla village.

CONTENTS

CHAPTER 1- INTRODUCTION....14
1.1 Background of the study:....14
1.2 Study area:....15
1.3 Research Gap:....16
1.4 Research objective:....17
1.5 Brief Methodology Of The Study:....17
1.6 Proposed outcome:....17
1.7 Outline of the Thesis :....18
CHAPTER 2- LITERATURE REVIEW....19
2.1 National and International literature review:....19
CHAPTER 3- DETAILS OF STUDY AREA....29
3.1 Study Area:....29
3.2 Population of Rural and Urban:....30
3.2.1Population of Bardhaman:....30
3.3 Geomorphology and soil characteristics:....30
3.4 Rainfall and Temperature:....32
CHAPTER 4- THEORETICAL CONCEPTS OF DIFFERENT TOPICS....33
4.1 FUNDAMENTALS OF GROUNDWATER FLOWAND WELL HYDRAULICS:....33
4.1.1Types of groundwater:....33
4.1.2 Groundwater and the Hydrologic Cycle:....34
4.1.3 Vertical Distribution of Groundwater....34
4.1.4 Aquifer Properties Affecting Ground Water:....38
4.1.5 2-D Approximations in unconfined aquifers:....47
4.1.6 Steady-State Well Hydraulics:....49
4.1.7 Well in a confined aquifer:....50
4.1.8 Well in a leaky confined aquifer:....55
4.1.9 Thiem's Method For Steady-State Flow In A Confined Aquifer:....58
4.1.10 Theis Solution For Transient Flow In A Fully Penetrating, Confined Aquifer:....59
4.1.11 Theis Type-Curve Method:....61
4.1.12 Estimating “T” And “S” Using Recovery Data (Theis, 1935)....66
4.1.13 Response Of An Unconfined Aquifer To Pumping:....68
4.1.14 Calculation Of Drawdowns By Correcting Estimates For A Confined Aquifer:....69
4.1.15 Determination Of Hydraulic Parameters Using Distance- Drawdown Data:....69
4.2 VERTICAL ELECTRICAL SOUNDING (VES) SURVEY....70
4.3 THEORY OF PUMPING TEST:....71
4.4 RECOVERY TEST:....76
4.5 Water GEMS -WATER DISTRIBUTION NETWORK TOOL:....77

4.6. DESIGN OF GROUNDWATER SYSTEMS 79
4.7 MECHANICAL ANALYSIS OF SOIL 80
CHAPTER 5- METHODOLOGY 83
5.1Overall Methodology Flow Chart 83
5.2. Literature Review 84
5.2.1 Data Collection: 84
5.2.2.Reconnaissance Survey: 84
5.3. Preparation of lithology of borehole: 85
5.4. Ves Test: 88
5.4.1 Data analysis and interpretation: 90
5.5 Pumping Tests & Recuperation Test 92
5.5.1 Pumping Tests: 92
5.5.2 Recuperation Test: 95
5.6 Estimation of sustainable withdrawal with well field design concept: 95
5.7 Mechanical analysis : 98
5.8 WaterGEMS: 100
CHAPTER-6 RESULT AND DISCUSSION 102
6.1 Lithological data analysis and result 102
6.2 Vertical Electrical Resistivity (VES) survey Result: 103
6.3 Pumping Tests And Recuperation Test result: 107
6.4 Well field design result: 114
6.5 Mechanical Analysis Result: 115
6.7: Hydraulic Analysis By WaterGEMS 127
CHAPTER-7 CONCLUSIONS, LIMITATION AND FUTURE SCOPE 133
REFERENCES 135
ANNEXURE-1 138
Output Parameters for Hydraulic Analysis 138
ANNEXURE-2 153
Output Parameters for Hydraulic Analysis 153

LIST OF TABLES	PAGE NO
Table 4.1 Characteristics of Some Common Earth Formation Materials	38
Table 4.2.: Porosity and Specific Yield of selected Formations	39
Table 4.3.: Typical values of coefficient of permeability and intrinsic permeability of some porous media	42
Table 4.4.: Values of ($\boldsymbol{u}$) for the different values of $\boldsymbol{u}$	60
Table 4.5: Grade Scale for Size Terms	81
Table 5. 1: VES Field Data measured at the stduy area in Silla, Bardhaman	91
Table5.2: Pipe head loss equations for full flow	101
Table 6.1: Interpretation of longitudinal conductivity and transverse resistivity from VES Data	103
Table6.2: Initial Data recorded just before starting the Pumping Test	107
Table 6.3: Results of pumping Test	111
Table 6.4 : Results of recuperation or recovery test at a glance	113
Table 6.5: Mechanical Analysis of Main Well (depth 10 m to 30 m)	115
Table 6.6: Mechanical Analysis of Main Well (depth 30 m to 50 m)	116
Table 6.7: Mechanical Analysis of Observation Well-1 (depth 10 m to 18 m)	117
Table 6.8: Mechanical Analysis of Observation Well-1 (depth 18 m to 30 m)	119
Table 6.9: Mechanical Analysis of Observation Well-1 (depth 30 m to 45 m)	120
Table 6.10: Mechanical Analysis of Observation Well-2 (depth 10m to 25m)	121
Table 6.11: Mechanical Analysis of Observation Well-2 (depth 25m to 40m)	123
Table 6.12: Mechanical Analysis of Observation Well-3 (depth 6m to 25m)	124
Table 6.13: Mechanical Analysis of Observation Well-3 (depth 25m to 40m)	125
Table 6.14: Water demand for the water supply scheme Galsi-1 Block	127
Table 6.15: Water Demand Shilla Zone-1 Bamunara village	128
Table6.16: Details of Pipe diameter, Length and materials	130
Table 6.17: Details of Over head Reservoir	132

LIST OF FIGURES	PAGE NO
Figure 1.1: Location map of the study area	16
Figure3.1: Contour map of the Galsi-I area	29
Figure3.2: Land use land cover map of Galsi-I block	32
Figure4.1. Schematic representation of the Hydrologic Cycle (Freeze & Cherry, 1979)	33
Figure 4.2: Divisions of subsurface water (Subramanya, 2008) Saturated Formation	35
Figure4.3:Types of aquifers (U.S. Bureau of Reclamation, 1995)	37
Figure4.4 (a) Effluent Stream (b) Influent Stream (Subramanya, 2008)	37
Figure4.5 Illustrative sketches for defining storage coefficient of a confined aquifer(Todd & Mays, 2005)	40
Figure 4.6:Illustrative sketches for defining storage coefficient of an unconfined aquifer (Todd & Mays, 2005)	40
Figure 4.7.: Flow parallel to the stratification (Subramanya, 2008)	43
Figure 4.8.: Flow normal to the stratification (Subramanya, 2008)	44
Figure 4.9.: Control volume in a porous medium (Chin, 2013)	47
Figure 4.10.: (a) Actual case (b) Dupuit approximation (Chin, 2013)	48
Figure 4.11: Control volume in an unconfined aquifer (Chin, 2013)	49
Figure 4.12.: Control volume in a confined aquifer (Chin, 2013)	51
Figure 4.13: Fully penetrating well in a confined aquifer (Chin, 2013)	53
Figure 4.14: Fully penetrating well in an unconfined aquifer (Chin, 2013)	55
Figure 4.15: Fully penetrating well in a semi-confined aquifer (Chin, 2013)	58
Figure 4.16: Steady-state cone of depression in a confined aquifer, (a) sectional view, (b) map view	60
Figure 4.17: Ullastration of a nonleaky, confined aquifer being pumped by a fully penetratintg well (from Reed, 1980)	62

Figure. 4.18: Plot of ($\boldsymbol{u}$) versus $\boldsymbol{u}$, known as a type curve (Bruin & Hudson Jr., 1961)	63
Figure. 4.19.: Cooper-Jacob Approximation using Time-Drawdown Method	63
Figure. 4.20.: Cooper-Jacob Approximation using Distance-Drawdown Method	66
Figure. 4.21.: An example of the characteristic S shaped drawdown curve obtained from a test wth an unconfined aquifer	68
Figure 4.22: Different types of arrays used in resistivity sounding	70
Figure 4.23: This figure shows the impact of a pumping well on the water table and a neighbouring well (observation well) in an unconfined aquifer	72
Figure 4.24: Drawdown and recovery curves in a pumping well	77
Figure 5.1.: Flowchart for the overall methodology	83
Figure 5.2 : Location of the slim bores and pumping well/main well and three observation wells	86
Figure 5.3.: Preparation of lithology of borehole using STRATER software	88
Figure 5.4.VES survey at the study area	89
Figure 5.5: Electrode configuration of Schlumberger	90
Figure.5.6. Interpreted soil profile by ZOND IP 1D software	91
Figure.5.7:Layout of the main (pumping) well and three observation wells	93
Figure5.8: Conceptual arrangement of Wells	97
Figure5.9:WaterGEMS V8i Home screen	101
Figure 6.1 : Lithological details of the pumping well and three observation wells (OBS-1, OBS-2 and OBS-3)	102
Figure6.2: Resistivity and conductivity scale for water, clay, sand, gravel and rock (Palacky, G.V, 1987, Steve Nylund, 2012)	104
Figure6.3: A prepared smooth layer of the soil profile by ZOND IP 1D software	105
Figure.6.4 : Variation of Drawdown (s) at the main well with varying time (t) for pumping out water from the main well	106

Figure.6.5: Drawdown (s) versus time (t) data plotted for observation well-1	108
Figure.6.6: Drawdown (s) versus time (t) data for observation well-2	109
Figure 6.7: Drawdown (s) versus time (t) data for observation well-3	110
Figure 6.8 : Drawdown versus time curve representing recuperation data for Main well	111
Figure6.9: Time drawdown curve, Theis recovery for observation well-1	112
Figure 6.10: Time drawdown curve, Theis recovery for observation well-2	113
Figure 6.11: Conceptual arrangement of Wells	114
Figure 6.12: IS sieve aperture dimension (mm) versus cumulative % passing as per Sieve analysis for the main well (depth 10 m to 30 m)	116
Figure 6.13: IS sieve aperture dimension (mm) versus cumulative % passing as per Sieve analysis for Main Well (depth 30 m to 50 m)	117
Figure 6.14: IS sieve aperture dimension (mm) versus cumulative % passing as per sieve analysis for observation well-1 (depth 10 m to 18 m)	118
Figure 6.15: IS sieve aperture dimension (mm) versus cumulative % passing as per Sieve analysis for observation well-1 (depth 18m to 30m)	120
Figure 6.16: IS sieve aperture dimension (mm) versus cumulative % passing as per Sieve analysis for observation well-1 (depth 30m to 45m)	121
Figure 6.17: IS sieve aperture dimension (mm) versus cumulative % passing as per Sieve analysis for observation well-2 (depth 10m to 25m)	122
Figure6.18: IS sieve aperture dimension (mm) versus cumulative % passing as per Sieve analysis for observation well-2 (depth 25m to 40m)	124
Figure 6.19: IS sieve aperture dimension (mm) versus cumulative % passing as per Sieve analysis for observation well-3 (depth 6m to 25m)	125
Figure 6.20: IS sieve aperture dimension (mm) versus cumulative % passing as per Sieve analysis for observation well-3 (depth 25 m to 40 m)	126
Figure 6.21: Network Water Demand Shilla Zone-1 Bamunara village	130
Figure 6.22: Critical Path Profile (Critical Point To OHR Path) Lowest Point -J-245 Elevation Vs Hgl Vs Pressurefor Shillya- Zone-I-Bamunara	132

ANNEXURE-1:Output Parameters for Hydraulic Analysis

ANNEXURE-2;Output Parameters for Hydraulic Analysis

SYMBOLS

º=Degrees

ºC= Celsius degrees

cm= centimeter

d10= 10% effective size diameter

d60 =60% passing diameter

dc =collector size or grain diameter, grain size

log =logarithm

m =meter

Re=Reynolds number

Uc =uniformity coefficient

LIST OF ABBREVIATIONS

Acronym	Full Form
1-D	One-Dimensional
2-D	Two-Dimensional
3-D	Three-Dimensional
VES	Vertical electrical sounding

CHAPTER 1- INTRODUCTION

1.1 Background of the study:

Water is fundamentally the inherent necessity of mankind and an essential resource for human civilization. Access to safe and clean water plays a vital role in social and economic development and public health for any society. To meet the rising demand for water, groundwater reserves are often extracted in an unplanned manner, leading to the depletion of these resources. This unplanned and uncontrolled extraction of groundwater, coupled with water contamination, requires immediate remedial measures to optimize water withdrawal in our already water-stressed country. The annual utilizable water resources in India are 690 BCM from surface sources and 447 BCM from groundwater (CGWB Report, 2017). Despite possessing substantial surface water resources, India is highly dependent on groundwater for daily survival. Currently, India faces the challenge of fulfilling its water demand through the existing but depleting resources. To supplement its present resources, we must find unconventional solutions involving water recycling and reuse, rainwater harvesting, etc. It is possible to store 214 BCM of surplus monsoon runoff in groundwater reservoirs. We must return to practices that value and conserve each drop of water.India is home to approximately 17% of the world's population but only has 4% of the world's freshwater resources (Indian Institute of Tropical Meteorology, 2014). Managing these resources for such a vast population is a mammoth task. It is estimated that about 200,000 people die every year due to inadequate water, sanitation, and hygiene. In 2016, the per-person disease burden due to unsafe water and sanitation was 40 times higher in India than in China and 12 times higher than in Sri Lanka (NITI Aayog, 2019). The mismanagement of wastewater, which also contaminates groundwater, along with poor sanitation and hygiene habits, has led to a significant portion of the population suffering from waterborne diseases.Currently, nearly 820 million people in 12 major river basins of India are facing high to extreme water stress. Out of these, 495 million belong to the Ganga river basin, which generates nearly 40% of the country's GDP (NITI Aayog, 2019). The scarcity of water resources has many cascading effects, including risks to biodiversity, industry, the energy sector, and the carrying capacity of urban hubs. Although water management is a State subject, optimal utilization and management lie within the domain of the States. Considering these factors, the Nation must develop interventions that measure both outcomes and the efforts involved in achieving them.Two new indicators related to 24/7 piped water supply to villages and villages having individual household water meters are included in the index. These indicators fulfill the Government of India's mandate to achieve the objective of 24/7 piped water supply to both urban and rural areas. Groundwater is a critical resource for rural water supply, especially in regions where surface water availability is limited or unreliable. The sustainability of groundwater withdrawal is essential to ensure long-term availability for various uses, including drinking, irrigation, and industrial activities.In many rural areas of India, including Shilla Village beside the Damodar River, groundwater serves as the primary source of potable water. However, excessive and unregulated groundwater extraction can lead to declining water levels, reduced well yields, and deterioration of water quality. Shilla Village has been experiencing challenges

related to groundwater management due to increasing water demand driven by population growth and agricultural activities. To address these issues, it is imperative to conduct comprehensive assessments of groundwater withdrawal to design sustainable well fields and implement effective water supply systems.Pumping tests are essential tools for evaluating aquifer characteristics, determining the sustainable yield of wells, and designing efficient well fields. These tests provide critical data on aquifer properties, such as transmissivity and storativity, crucial for accurate hydraulic modeling and water resource management.Hydraulic modeling using advanced software like WaterGEMS allows for the simulation and optimization of water distribution systems. By integrating well field design with hydraulic models, it is possible to develop strategies for efficient groundwater extraction and distribution, ensuring a reliable and sustainable water supply for rural communities. This study aims to provide a comprehensive approach to sustainable groundwater management for rural water supply systems, combining empirical data from pumping tests with advanced hydraulic modeling techniques.

1.2 Study area:

The proposed study area shilla village falls under Block-Galsi-1, District- Purba Bardhaman ,West Bengal. The Shilla Piped Water Supply Scheme covers 26 (twenty six) nos. of mouzas of Block Galsi-l, P.S. galsi under Purba Bardhaman District in the state of West Bengal. The total area covered under the scheme is about 264 km^2 with a total population of 1,87,588 as per 2011 census and average population density of 712 persons per km^2. GPS location :23˚18’40”N, 87˚25’33”E.

Shilla village is located in Galsi- I subdivision of Barddhaman district in West Bengal, India. It is situated 19.4km away from sub-district headquarter Galsi. Barddhaman is the district headquarter of Shillya village. As per 2009 stats, Loaramgopalpur is the gram panchayat of Shilla village.

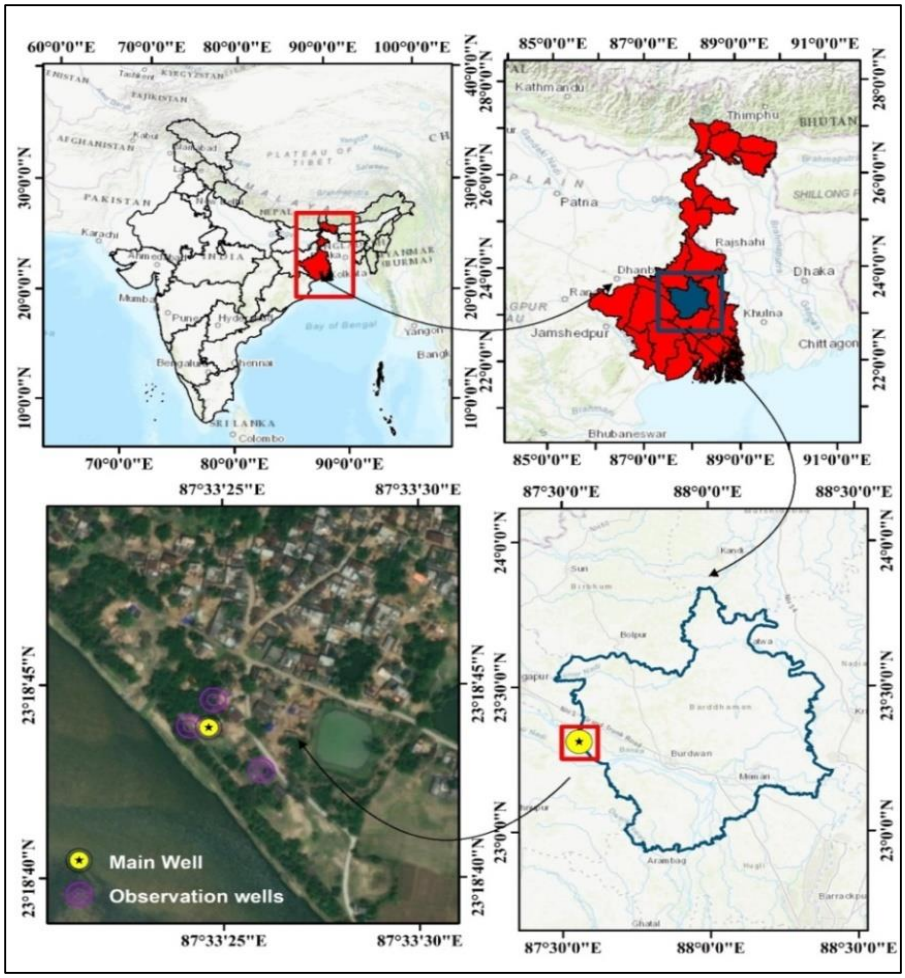


Figure 1.1: Location map of the study area.

1.3 Research Gap:

Despite the critical importance of sustainable groundwater management, there is a notable lack of comprehensive studies that integrate pumping test data with hydraulic modeling for rural water supply systems in regions like Shilla Village. Existing research primarily focuses on either groundwater assessment or hydraulic modeling independently, resulting in a fragmented understanding of water resource management. Key research gaps include the insufficient data on aquifer characteristics, which hinders accurate estimation of sustainable groundwater yields; the lack of integrated approaches that combine pumping test data with hydraulic modeling to optimize well fields and water distribution systems; the limited application of advanced hydraulic models like WaterGEMS in rural contexts; and the need for developing and validating sustainable groundwater withdrawal strategies tailored to the specific hydrogeological conditions of rural areas like Shilla Village.

1.4 Research objective:

The research objective of this thesis is to comprehensively assess the hydrogeological characteristics and design a sustainable water supply system for rural areas of West Bengal. This involves conducting a pumping test to determine aquifer properties, including transmissivity and storativity, to understand groundwater flow dynamics. Additionally, a Vertical Electrical Sounding (VES) survey will be conducted to delineate the subsurface lithology and aquifer geometry. The data obtained from these tests will inform the design of an optimized well field for groundwater extraction. Furthermore, the study will integrate the aquifer properties and well field design into Water GEMS modeling to simulate and optimize the water distribution network, ensuring reliable and efficient water supply to the target areas.

1.5 Brief Methodology Of The Study:

The methodology for this study adopts a comprehensive approach to assess hydrogeological characteristics and develop a sustainable water supply system for geogenically contaminated areas in West Bengal. The process begins with a literature review to understand existing research and practices in the field. Data collection involves conducting a pumping test to determine aquifer properties like transmissivity and storativity, crucial for understanding groundwater flow. A Vertical Electrical Sounding (VES) survey is conducted to map subsurface lithology and aquifer geometry. The collected data is then used to design an optimized well field for groundwater extraction. Subsequently, Water GEMS modeling is employed to integrate aquifer properties and well field design, allowing simulation and optimization of the water distribution network for reliable and efficient water supply. Data analysis includes interpreting the results of the pumping test and VES survey, as well as refining the Water GEMS model to meet the project objectives.

1.6 Proposed outcome:

In this study, the aim is to conduct a comprehensive assessment of the hydrogeological characteristics in geogenically contaminated areas of West Bengal. This includes examining aquifer properties such as transmissivity and storativity to gain insights into groundwater flow dynamics. The research outcomes are as follows:

- The evaluation of hydrogeological characteristics to understand groundwater dynamics in geogenically contaminated areas.
- The determination of aquifer transmissivity and storativity to assess groundwater flow rates and storage capacities.
- Using Vertical Electrical Sounding (VES) survey to map subsurface lithology and aquifer geometry.
- Developing an optimized well field design for groundwater extraction based on pumping test data and VES survey results.

- Integrating aquifer properties and well field design into Water GEMS modeling for simulating and optimizing the water distribution network.

1.7 Outline of the Thesis :

The thesis consists of seven chapters. Chapter 1 describes the overview of the research study, Chapter 2 contains literature review. Chapter 3 illustrates the study area and the research methodology. Chapter 4 reveals the governing equations and comprises the theoretical concept of Ground water dynamics. Chapter 5 contains Methodology Chapter 6 presents data analysis and result and discussion. Finally, the summery of the research study describes in conclusions and recommendations with limitation and the future scope of the study which are provided in chapter 7. References are given at end of the dissertation.

CHAPTER 2- LITERATURE REVIEW

2.1 National and International literature review:

The literature review shows that in the case of simple water distribution systems, optimization is extensively used. The design of large-scale water networks has some important features like the increasing population and the topography. Some papers focus on the details of a particular master planning study or actual water distribution systems. This section gives a detailed account/ description of the already accomplished research works/ case studies/ experimental and field works/ review papers in this domain ,that have been referred to/ cited in this present study.

Das (2006) carried out a pipe network analysis for a water treatment plant. As a case study, the total schematic drawing of the rising main for South 24 Parganas water supply scheme under Public Health Engineering Directorate, Government of West Bengal was considered. The network comprises of a clear water reservoir from which two pumps are supplying water to 24 numbers of zonal overhead reservoirs and two ground level reservoirs (for feeding 27 more overhead reservoirs) through the rising main. It was found that in this network, the time requirement taken for filling different overhead reservoir fully are not similar at all. Some of these fill up early and some other take a long duration.

Izquierdo et al. (2008) discussed about sensitivity analysis to assess the relative importance of pipes in water distribution networks. On the contrary, their designs are closely related to their hydraulic performance. Recognizing the sundry and relative importance of the different pipes in a water distribution network may help in assessing their impact on the hydraulic performance of the network. This information, in turn, will be helpful in the different aspects of a water distribution network make-up, namely design, planning, control and management.

Liana et al. (2008) studied mathematical modeling and computer simulation which are becoming one of the most important tools for water companies in their attempt to provide their high-quality service economically for both development and operations. The available sophisticated and accessible models permit the proper evaluation of network behaviour under normal and abnormal conditions and it allows these goals to be realized more fully than ever before. The result was obtained using two softwares EPANET and INFOWORKS WS, and the results were compared among each other. The obtained results were similar to the optimal design model for water distribution systems, considering the water quality aspect reported by Vuta and Popa (2006).

Koppel et al. (2009) discussed about calibration of a model of an operational water distribution system containing pipes of different age. The aim of the paper is to demonstrate that the Levenberg—Marquardt algorithm can give successful results when operational water distribution systems are calibrated with the proper selection of parameter increment for the calculation of partial derivatives.

Arunkumar et al. (2011) examined a study on water demand analysis of Public Water Supply in Municipalities using EPANET 2.0 software with the aim of providing effective planning,

development and operation of water supply and distribution networks which is one of the most essential components of urban infrastructure. Using EPANET 2.0 water model software, the demand for the Underserved and Un- served area is calculated. A framework for taking management decisions such as an extension of the supply network and location of new facilities was given.

Mukherjee et al. (2013) carried out a comparative study between hydraulic analysis outputs of pipeline network between software EPANET and HAMMER. The main objective here was to design a pipeline of water distribution network and insert the required input in both the software accordingly. The outputs which were considered for the above study were hydraulic grade line and pressure at junctions and flow and unit head loss for pipes. The comparative study was carried out with the help of statistical regression analysis by finding out correlation coefficient and probable error coefficient.

Sumithra et al. (2013) studied to suggest measures for improvement of the distribution system. The paper represents results of analysis carried out using computer package LOOP developed by World Bank and Bentley System, 2008, Water Gems for optimal design of distribution system including cost analysis and reorganization measures needed for the design year 2044. The analysis of zone-Ill of the distribution network indicates that existing pipes need to be rehabilitated to cater to the demand for the year 2044 and CI/AC/PVC pipes needs replacement for the year 2044. New pipelines are to be proposed to ensure the service standards of 135 lpcd with minimum residual head of 7 m. The network analysis with rate analysis with aid of software LOOP developed by World Bank and Bentley Water Gem has been made and Bentley water Gems is found to be extremely user friendly for addressing such systems with varying demand pattern, peak factor, pipe condition, water supply modes and design horizons. In additions it has graphical interface which facilitate analyses more effective and lesser time requires to reanalyse the network.

Pathan et al. (2015) carried out a study related to design of Water supply network with an objective of minimizing the overall cost while meeting the water demand requirements in the sufficient quantity, quality and at satisfactory pressure i.e. finding out such an optimal geometrical layout which delivers known demands from source to all individual consumers for a long period. In this paper design of water supply network duly considering optimization in addition to the cost minimization, minimum head requirement and minimum chlorine requirement is presented. Gradient method is one in which the pipe discharges and nodal heads are taken as the basic unknowns in equationting the Q-H equations. The nonlinear Q-H equations for the pipe head loss are linearised and solved by Gradient method. Water GEMS software algorithm is based on Gradient method gives optimal solution for the design of new as well as expansion of existing water supply network. The software also gives how the chlorine concentrations changes throughout the network. Water quality results are represented either using colour coding, tables or graphs and helps to discover what better initial values for chlorine concentration might be set in the network. Decision variables involves are pipe diameter, reservoir elevations and reservoir capacity etc. with flow as primary variable. A design is obtained duly considering minimum and maximum head and velocity criteria in order to

determine the actual supply form each node to all consumers. In this paper a part of Aurangabad city is designed and its water quality (chlorine) analysis is done by Water GEMS software.

Saha (2016) worked on the transient analysis of pipe networks using HAMMER software at the Mukutmanipur area of the Purulia piped water supply scheme. Sudden power failure, pump failure, valve failure were the main reasons behind the hydraulic transient in a water supply line. This work described the generation, propagation and reflection of pressure waves in liquid-filled pipe systems causing surge and water hammer. The hydraulic modelling of the clear water transmission main of the study area was first done and followed by the steady-state analysis of the same by Water GEMS software. Finally, the maximum transient pressured developed in the network and the factor of safety of the pipe experiencing the maximum transient pressure was checked as per Indian standards and American Water Work Association standards, respectively.

Mehta et al. (2017) studied on design of water distribution systems with an objective of minimizing the overall cost while meeting the water demand requirements at adequate pressures. However during operations of water supply systems, cases of pressure drops, Leakages and contamination occur and the main challenge is the lack of a simple tool to accurately predict zones of low pressures and areas where quality is compromised. This study will investigate the operations of Punagam area Water Distribution system in Surat city in terms of pressure Variations from the Treatment Works to the consumer points using WATERGEMS V8i software. The WATERGEMS V8i programme analyses the pressure at each node, track the flow of water in each pipe and height of the water in each tank during simulation. After simulation of existing water distribution network, results were presented in various forms and compared with the field actual data. This paper covers the water scarcity problems to consumer and the problem of leakage in the distribution system in particular with an explanation of its causes and its impact on various aspects of life and a clarification of the possibility of effectively using of geographic information systems to contribute in the management of this problem. The results obtained verified that the pressures at all junctions at all pipes are feasible enough to provide adequate water to the network of the study area. Simulated water pressure did not vary significantly with the actual values indicating that the pipes still had their hydraulic capacities even though some sections of the network need augmentation.

Bhoyar et al. (2017) carried out a Modelling and Optimization of water distribution system is addressed in this paper by Water GEMS and EPANET. A water distribution network is used to show the algorithm performance and the obtained results are compared with those given by using dynamic programming to solve the same problem under the same conditions. The work presented in this thesis has been driven by the need for reduced, while at the same time suitably accurate, models to imitate the complex and nonlinear nature of water distribution systems to optimize their operation. Water GEMS and EPANET are software that models the water transmission and distribution piping system. It is used to build a hypothetical model which is simulated and run to observe the performance of the network. Nagpur transmission network was designed and modelled for this study. The model is built from source- Pench Dam to the MBR in seminary hills. The models are later divided in 3 zones with assumed population. This system is

optimized for diameter and pressure.

Mehta et al. (2018) studied on design of water distribution nctworks to deliver water from a source in the adequate quantity and at satisfactory pressure to individual consumers. To solve any problem, design of new or upgradation of existing water distribution network is to be necessary. So, such type of problem can be solved using LOOP 4.0, STANET, EPANET 2.0, and WATERGEMS software. surat City facing problems like water scarcity and pressure fluctuation so for study purpose Punagam area is selected for analyzing the existing water distribution network using WATERGEMS V8i. The objective of our study is to analyze the existing water distribution network of Punagam area using WATERGEMS V8i and to recommend some measures if present network does

not fulfil the present and future demand. The results obtained verified that the pressures at all junctions and the flows with their velocities at all pipes are feasible enough to provide adequate water to the network of the study area.

Salunke et al. (2018) studied efficient water distribution networks based on advance computing systems include modern hydraulic modeling. In present study water distribution network of Bakori region of Wagholi is designed which is located at district Pune, State Maharashtra, India. For the design of BakoriPhata water distribution network, study of present population, population of the three decades, daily water demand, flow characteristics and also survey of the village is done with help of digital GPS .Water distribution network for the villages is analyzed and designed with help of Bentleys WATERGEMS software. Water distribution network systems are designed to deliver water from a source in the adequate quantity, quality and at satisfactory pressure to all individual consumers. Water distribution network are designed with an objective of minimizing the

overall cost while meeting the water demand requirements at adequate pressures. The system is a pipeline network consisting of one source node and several demand nodes is considered to find its optimal geometrical layout which delivers known demands from source to consumers over a long period of time.

Dumane et al. (2018) studied to fulfil the increasing demand day by day by designing efficient water distribution networks based on advance computing systems include modern hydraulic modeling and designing software. In present study water distribution network of Bakori region of Wagholi is designed which is located at district Pune, State Maharashtra, India. For the design of BakoriPhata water distribution network, study of present population, population of the three decades, daily water demand, flow characteristics and also survey of the village is done with help of digital GPS .Water distribution network for the villages is analyzed and designed with help of Bentleys WATERGEMS software. Water distribution network systems are designed to deliver water from a source in the adequate quantity, quality and at satisfactory pressure to all individual consumers. Water

distribution network are designed with an objective of minimizing the overall cost while meeting the water demand requirements at adequate pressures. The system is a pipeline network

consisting of one source node and several demand nodes is considered to find its optimal geometrical layout which delivers known demands from source to consumers over a long period of time.

Mehta et al. (2019) studied on hydraulic design and analysis of Rural Water Distribution System (WDS) for Nava shihora region of zone 1 of the state of Gujarat, India. Water supply distribution system is designed for this study for population estimated for future 30 years. LOOP 4.0 and Water Gems v8i software have been used and the results are compared to determine the economical size of pipes for water distribution system. The economical size of pipes of water supply distribution system is designed by considering the constraints; residual pressure at each node, velocity of flow in pipe, head loos in pipes, material of pipes, elevated service reservoir level, peak factor and available commercial pipe diameters. Further water distribution system has been analyzed for extended period simulation (EPS) for the present population scenario for intermittent water supply using Water Gems v8i. Further water supply system is analyzed the residual chlorine concentration at nodes and in the pipe links and also the total cost of water supply system of rural region is estimated.

Debnath (2019) studied the water distribution network of Bhogpur gram panchayat at Panskura-ll block in West Bengal by using WaterCAD software. The design and analyses of the water distribution network for Surface Water Based Water Supply Scheme at Panskura- Il (also referred to as Kolaghat Block), Zone-Ill (Bhogpur Gram Panchayet) of PurbaMedinipur district using WaterCAD software was discussed in this study. At the end of the analysis, it was found that the resulting pressures at all the nodes and the links velocities were satisfied enough to provide water to the study area.

Labhade et al. (2021) carried out a study of Nimgaon (Madh) village have done and Water Distribution Network (WDN) was designed, which was located at district Nashik, State Maharashtra, India. For the design of Nimgaon (Madh) water distribution network study of present population, forecast Population for the three-decade, daily water demand, flow and also survey of village Nimgaon (Madh) was done with the help of Auto Level. From the Level survey, map was created and also elevation and length of Pipeline required for the village was calculated. The node no. and pipe no. were denoted on map of villages. Water Distribution Network of village was designed with the Water Gems/Water Cad software and compared with manually result. It was found that software result was more accurate, save time and manpower than manual result. Water is essential element required for the sustenance of life. Demand for drinking is increasing on continual basis with corresponding increasing population. This ever-increasing demand can be fulfilled by designing efficient water distribution networks based on advance computing systems include modern hydraulic modeling and designing software.

Patil et al. (2023) carried out a study of a growing population country like India needs a sufficient amount of resources. Nowadays, most of our rural areas are not having a sufficient quantity of potable drinking water facilities, so the main objective of this study is to provide an efficient and optimal water distribution network design using LOOP and Water GEMS software by satisfying CPHEEO norms and Jal Jeevan Mission guidelines. The project is carried on

Awaradi village in Gokak taluk, Belagavi district. This project is carried out the designing rural drinking water with 55 LPCD. The population is forecasted for a design period of 30 years (2051) from 2021. The survey is carried out in the proposed village to collect ground data and area topographical profile. Then further hydraulic calculations are made with the use of LOOP 5.0 software and WaterGEMS Software. The velocity and head losses are high in the LOOP software design as compared with the WaterGEMS software. The pressure values are slightly more in the WaterGEMS software, but both the software results are meeting the CPHEEO norms as well as Jal Jeevan Mission guidelines with a pressure head of 7 m.

Dashti et al.(2022) studied emphasizes the critical need for accurate hydrodynamic parameter values in groundwater modeling and management, highlighting the importance of pumping tests in determining parameters like transmissivity, hydraulic conductivity, and storage coefficient. Two primary methods, analytical solutions with curve matching and numerical modeling, are commonly employed for parameter estimation. While graphical analyses of time-drawdown data are widely used, they can be time-consuming and approximate.The study explores the application of graphical type-curve methods, which are extensively used in water resources studies but relatively new in pumping test analysis. Through a review of literature from 2000 to 2022, the study categorizes papers into graphical, modeling, and hybrid approaches. Each approach is thoroughly examined to identify key characteristics and capabilities. The review aims to serve as a guide for researchers involved in pumping test analysis, offering insights into different methodologies and their effectiveness. The study focuses on estimating essential aquifer parameters, crucial for understanding groundwater dynamics. Specific capacity (C), transmissivity (T), and storativity (S) are fundamental parameters indicating groundwater availability and movement. These parameters are determined through aquifer performance tests (APT).

Kumbhar et al. (2019) in this study, 10 APTs were conducted across different locations within shallow basaltic aquifers. Key data such as well diameters, depths, and initial water levels were recorded. During the tests, water was continuously pumped out for 3 hours, and changes in water level were observed for drawdown and recuperation phases.The depth of the dugwells varied between 11 and 18.2 meters. Results from the aquifer performance tests revealed a wide range of specific capacity values, ranging from 16 to 583.36 liters per minute per meter. Analysis of pumping test data indicated storativity values between 1.8 and 13.7 meters per day and transmissivity values between 40.67 and 211.87 meters per day.These findings provide valuable insights into the characteristics of the studied aquifers and contribute to the understanding of groundwater behavior in the area.

Zahid et al. (2008) studied in Bangladesh's deltaic and floodplain regions, arsenic contamination in shallow groundwater (5-50m depth) has made accessing safe drinking water a critical concern. In Madaripur town, the municipal water supply faces quality degradation due to high levels of arsenic, iron, and chloride in the upper aquifer, along with salinity issues even at greater depths. This study identifies a 30-meter clay layer, acting as a confining unit between 130m to 160m below the land surface. This layer separates the deep aquifer, which generally

contains minimal arsenic concentrations, from the problematic shallow aquifer.

Utilizing aquifer-test data collected from a deep borehole, the study applies the Hantush-Jacob solution (1955) for a leaky confined aquifer. The analysis reveals that this solution provides the best fit to the data. The resulting curve matches observations from two wells, yielding key parameters: an average aquifer storage ranging from 0.0003 to 0.006, aquifer transmissivity of 4500 m^2/day, a vertical to lateral aquifer hydraulic conductivity ratio of 1.0, and a confining unit vertical hydraulic conductivity ranging from 0.044 to 0.93 m/day.This analysis confirms that the deep aquifer can supply significant quantities of water to wells with minimal drawdown, reducing the risk of drawing potentially contaminated water from the shallow aquifer. This characterization of the deep aquifer is crucial for sustainable drinking water use in Madaripur town and similar areas facing groundwater quality challenges.

Amah (2016) studied in five boreholes in the Akpabuyo Local Government Area of Cross River State underwent various pumping tests to assess hydraulic parameters. Results showed a range for transmissivity (T), hydraulic conductivity (k), and specific capacity (SC) from 485.0m^2/d to 1346.0m^2/d, 9.7m/d to 27.9m/d, and 0.02m^3/d/m to 346.m^3/d/m respectively. Additionally, mean static water level (SWL), saturated aquifer thickness (b), and borehole drilled depths (BDD) averaged at 30.29m, 48.0m, and 64.8m respectively. The litho-logs confirmed that these parameters were derived from unconfined gravelly sandy aquifers underlain by sandy clay (aquitard). Suggestions for future research include incorporating observation wells for storativity (S) computation and considering electrical resistivity techniques as a cost-effective alternative to pumping tests for estimating hydraulic parameters in the area.

Merritt (1986) explored the factors affecting the recovery efficiencies during ASR of fresh water into a saline limestone aquifer through the use of a finite difference model that was developed as a part of the study. Various arrangements of ASR wells were tested, although results were only given for a 5-well, cross-hair arrangement. He demonstrated that the pattern of fresh water in the aquifer was dependent upon which of the wells the water was pumped into, and similarly, the distribution at the end of an ASR cycle differed according to which wells were pumped. During particular combinations of injection and recovery residual fresh water remained in isolated zones between the wells after the extracted water had become too saline for potable usage. The recovery efficiency for the case where all wells were pumped was lower than the case where only the central well was pumped by a factor of six percent. This was in the absence of a regional hydraulic gradient. When the central well was first targeted followed by the peripheral wells the recovery efficiency was 10 percent higher than when injection occurred in all wells simultaneously, whilst the residual injectant in the aquifer was noticeably more contiguous.

Trefry et al. (1996) carried out the study the FEFLOW package to design efficient strategies for controlled injection of nutrient-rich solutions to stimulate microbial activity of a shallow aquifer contaminated by hydrocarbons. Schemes comprised of one-, two-, three-, four- and ninewells were tested to identify the best ‘curtain’ of bioclogging agents with minimal outlay of amendment solution and hydrologic disturbance. Not surprisingly, it was found that the fourand

nine- well systems yielded the most effective distributions of amendment, but at greater installation and operating costs than simpler systems.

Dillon et al. (2002) developed an approach for assessing the feasibility of alternative riverbank filtration schemes in alluvial sediments adjacent to surface water bodies, taking into account the removal of cyanobacterial toxins and the degree of mixing between fresh river water and more saline ambient groundwater. Using analytical expressions that predicted the minimum travel time between the surface water and the well, and the proportion of surface water extracted from the production well, a site was identified along the River Murray that met both criteria and minimised pumping costs. As will be shown later, these objectives are not too dissimilar to those of this study.

Fildebrandt et al. (2003) carried out a study a similar analytical approach to arrive at the appropriate separation distances between injection and recovery wells in the Bandung Basin in Indonesia, taking account of the travel time needed to achieve a given level of pathogen attenuation. A nomogram was developed that allowed prediction of the number of pathogen log removals from any set of design parameters. Miller et al., (2002) developed the ASR Risk Index (ASRRI), a computer program that evaluates the risk of contamination from trace organic or microbial contaminants based on the formulations and assumptions also used by Fildebrandt et al.

Stuyfzand et al. (2002) investigated the geochemical processes arising from prolonged injection of potable water into a deep sandy pyrite-rich aquifer and its recovery 98 m away at the Someren site in the Netherlands. The oxic zone around the injection well, which developed following 2.5 years of uninterrupted flushing of the aquifer with injectant, vanished due to reactions with pyrite and organic matter with associated leaching of iron and ammonium. Deposits of iron(hydr)oxides and organic matter around the injection well led to some reversible well clogging.

Abdullahi et al. (2014) studied new geophysical method for groundwater exploration in the crystalline rocks of Tudun Wada, Kano State, Nigeria, has been developed, offering a simple and quick approach. The study employed Electrical Resistivity method, specifically Vertical Electrical Sounding (VES) technique with Schlumberger array system, to evaluate groundwater potential in the area. The study area encompasses sedimentary rocks, igneous, and metamorphic formations, with alluvial deposits being common. Data from six VES stations, gathered using ABEM terrameter (SAS 300), was analyzed and tabulated. The analysis, conducted with the aid of computer software IPI2win, provided automatic interpretation of apparent resistivity. The VES results unveiled a heterogeneous subsurface geological sequence comprising topsoil, weathered layer, fractured basement, and fresh basement. Topsoil exhibited resistivity values ranging from 16Ωm to 550Ωm with varying thicknesses from 1.45m to 6.05m. The weathered layer displayed resistivity values between 14Ωm to 541Ωm and thicknesses spanning from 5.70m to 33.00m. Fractured basement resistivity ranged from 189Ωm to 785Ωm with thicknesses of 11m to 20m. The fresh or bedrock basement, with resistivity ranging from 1011Ωm to 3006Ωm, extends infinitely downwards. Consequently, the depth of the bedrock

from the earth's surface varied from 2m to 45m. Overall, the study demonstrates the effectiveness of the developed geophysical method for groundwater exploration in the crystalline rocks of the region, providing valuable insights into the subsurface geological structure and potential groundwater resources.

Chandra et al. (2009) carried out the study investigated geological discontinuities, specifically quartz reefs, in hard rock terrain using geophysical methods to explore and map potential aquifers. The electrical resistivity response of quartz reef intrusions in granite host rock was analyzed through synthetic simulation under various physical conditions. These conditions included fresh intrusive bodies with no alteration at contacts, fresh intrusive bodies with weathered-fissured contacts, and fissured intrusive bodies with weathered-fissured contacts. Electrical Resistivity Tomography (ERT) was conducted across and along the quartz reef at Kothur village, Hyderabad, India. Subsequently, 11 bore wells were drilled, followed by yield measurement, litholog collection, and electrical resistivity logging. The study found that geomorphology, ERT images, lithologs, resistivity logs, and well yields were consistent with each other. It confirmed the deepening of weathering fronts along the contacts of the quartz reef and granite, indicating suitable sites for groundwater occurrence. This observation was validated through drilling results, where a high-yielding bore well (18 m3/h) was found at low resistive zones within the quartz reef. The study facilitated the preparation of a 2D section illustrating the structural setup of the quartz reef in the granite host medium. Ultimately, it revealed that quartz reefs may serve as potential groundwater zones. The distribution of electrical resistivity of the geological discontinuity provided valuable input for groundwater flow modeling, particularly in three dimensions.

Taufiq et al.(2021) carried out the study the demand for freshwater is crucial for the development of a livable community, as it is required for various construction activities such as irrigating rice fields, building infrastructure, and daily consumption. To ensure good quality groundwater, specific parameters need to be determined, including groundwater depth, source thickness, and rock resistivity. In this study, the Vertical Electrical Sounding (VES) resistivity method with Schlumberger configuration was applied to assess these parameters in one of the Pamsimas Projects.The VES resistivity method involves injecting electric current into the earth and recording the potential difference produced at the surface, based on the electrical properties of subsurface rock. By measuring current and potential difference for different electrode spacings, resistivity variations in each layer beneath the measuring point can be determined. After conducting measurements at three points in Pandansari Village (PS-01, PS-02, PS-03), the results indicated the presence of water layers at different depths and resistivity values. PS-01 showed a water layer at 60-80 meters depth with a resistivity value of 36.750 Ωm, PS-02 indicated a water layer at 50-100 meters depth with a resistivity range of 18.7-40 Ωm, and PS-03 revealed a water layer at 30-60 meters depth with a resistivity value of 52.870 Ωm. Additionally, a 2D-pseudosection was generated to visualize the distribution of groundwater layers in the subsurface, revealing a groundwater thickness of 2050 meters at a depth of 40-80 meters. Based on these findings, PS-01 was identified as the optimal location for well exploitation in the South Pandansari Pamsimas Project.

Jatau et al. (2013) conducted the study in the Bomo area of Zaria, Kaduna state, employed Electrical Resistivity Investigation to examine the subsurface geology, aiming to determine bedrock depth and geologic layer thickness. Vertical Electrical Sounding (VES) using Schlumberger array was conducted at fifteen stations with ABEM terrameter (SAS 300) for data acquisition. Analysis was done using IPI2win software for automatic interpretation of apparent resistivity. Results indicated a heterogeneous subsurface geological sequence, comprising hard pan topsoil (clayey and sandy-lateritic), weathered layer, partly weathered/fractured basement, and fresh basement. Topsoil resistivity varied from 40Ωm to 450Ωm with thickness between 1.25 to 7.5 m. Weathered basement showed resistivity between 50Ωm to 593Ωm with thickness of 1.37 to 20.1 m. Fractured basement exhibited resistivity between 218Ωm to 520Ωm and thickness of 12.9 to 26.3 m. Fresh basement (bedrock) resistivity ranged from 1215Ωm to 2150Ωm with infinite depth. Depth to bedrock varied from 2.63 to 34.99 m.The study underscored the significance of these findings in civil engineering structures and groundwater prospecting.

CHAPTER 3- DETAILS OF STUDY AREA

3.1 Study Area:

The proposed study area shilla village falls under Block-Galsi-1, District- Purba Bardhaman ,West Bengal. The Shilla village has 26 (twenty six) nos. of mouzas of Block Galsi-l, P.S. galsi under Purba Bardhaman District in the state of West Bengal. The total area covered under the scheme is about 264 km^2 with a total population of 1,87,588 as per 2011 census and average population density of 712 persons per km^2. GPS location :23°18'40"N to 87°25'33"E.

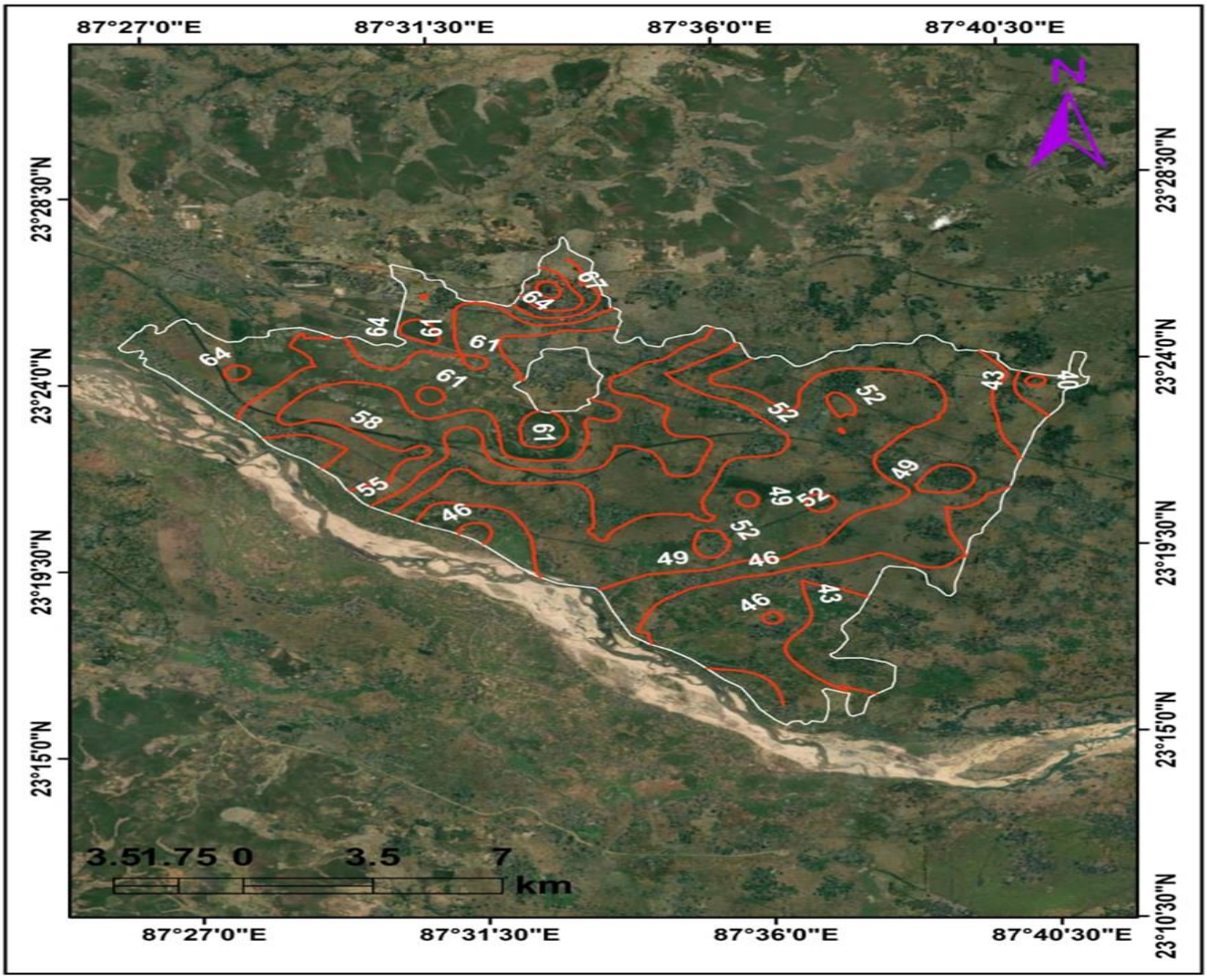


Figure3.1: Contour map of the Galsi-I area.

3.2 Population of Rural and Urban:

3.2.1Population of Bardhaman:

Bardhaman is a district in the West Bengal State of India. Total area of Bardhaman is 7,024 km² including 6,095.98 km² rural area and 928.02 km² urban area. As per 2011 stats, Bardhaman has a population of 77,17,563 peoples, out of which urban population is 30,78,299 while rural population is 46,39,264. The district has a population density of 1099 inhabitants per square kilometer. There are about 17,30,927 houses in the district, including 6,59,366 urban houses and 10,71,561 rural houses. When it comes to villages, there are about 2,418 villages in Bardhaman district

Population of Bardhaman District

Particulars	Rural	Urban	Total
Total Population	46,39,264	30,78,299	77,17,563
Male Population	23,73,787	15,93,102	39,66,889
Female Population	22,65,477	14,85,197	37,50,674
Population Density	761 / km²	3,317 / km²	1,099 / km²

3.3 Geomorphology and soil characteristics:

3.3.1 Topography

Purba Bardhaman district is a flat alluvial plain area that can be divided into four prominent topographical regions. On the north, the Kanksa Ketugram Plain lies along with the Ajay, which joins the Bhagirathi. The Bardhaman Plain occupies the central area of the district, with the Damodar on the south and the south-east. On the southern part is the Khandaghosh Plain. The Bhagirathi flows along the eastern boundary of the district, and the Bhagirathi Basin occupies the eastern part of the district. The undulating laterite topography of Paschim Bardhaman district extends up to the Ausgram area of this district.

The gradient is westerly to the west and to the east, it is northerly towards Ajay and southerly towards Damodar below the latitude. The Ajoy- Damodar inter-stream tract is made up of several stows consisting of vales and low convex spurs which run in almost all directions except north-east and thus lends a very complicated character to local relief.

3.3.2 Rivers

The river system in Barddhaman includes the Bhagirathi-Hooghly in the east, the Ajoy and its tributaries in the north and the Damodar and its branches in the south-west. Besides, there are innumerable Khals and old river beds all over the area.

The notable rivers and khals are Damodar, Bhagirathi, Ajay, Singaram, Kukua, Kunur, Tumuni, Khari, Banka, Chanda-kanki nala, Behula, Gangur, Brahmani, Khandesvari, Karulia nala, Dwaraka or Babla, Koiya nala, Kandarkahal, Kanadamodar, Kananadi, Ghea, Kakinadi etc.

3.3.3 Soil

Different types of soil are encountered in different topographical biological and hydrological as well as a geological conditions within the Purba Barddhaman district. Towards the east alluvial soil attains an enormous thickness in the low-level plains to the east. This alluvial soil is formed of alluvium brought down by the Ajay, Damodar, Bhagirathi, and numerous other rivers. These soils are sandy, well-drained, and slightly acidic in nature.

3.3.4 Water Resources

There are many tanks, wells, canals, swamps, and bills are found all over the district. Within the Damodar Valley region,there are around 17000 tanks.

3.3.5 Forest

The forest areas of the district are chiefly situated in the lateritic and red soil high lands in the Aushgram PS of Sadar Subdivision. In Ausgram P.S. the forest areas are interspersed with paddy fields.

3.3.6 Land use & land cover

The flora of the district is characterized by the arborescent species such as Simul, Neem, Amlaki, Aam, Jam,Narikel, Khejur, Tal, Bot, Aswattha, Palas, Krishnachuda, Amra, Peyara, Dumur, Ghentu or Bhat, Gulancha, Tulsi and other herbs.

The common aquatic and marsh weeds found in the jheels and swamps in the district are Kash, Bena, sola, Pond-weed, Kesar-dam, Kush, Pana, Mootha, Bara-pana, Hogla, Padma, etc.

The carnivora of the district comprise leopard, wolf, hyaena, jackal and other smaller species, but hyaenas and leopards are not common. Wolves are scarce, and are mostly met with in the jungles north of Kanksa. Wild pigs are numerous throughout the district and monkeys also abound including the variety known as Hanuman. Poisonous snakes are very common and include several kinds of cobra, the karait and the deadly Russell's viper. Other most frequently seen varieties are the Dhamna and various species of harmless grass snakes.

The common avifauna of the district are pea-fowl, jungle-fowl, jungle crow, house crow, treepie, common babbler, gold-fronted chloropsis, red-vented babul, red-whiskered bulbul, red spotted bluethroat, brown-backed robin, Shama, flycatcher, wood shrike, black drongo, tailor bird, streaked fantail warbler, golden oriole, common mayna, pied mayna, white-backed munia, white-throated munia, spitted munia, red munia, yellow-throated sparrow, house sparrow, woodpecker, India cuckoo, pied crested cuckoo, koel, parakeet, nilkantha, bee-eater, kingfisher, horned owl, spotted owlet, jungle owlet, griffon vulture, long-billed vulture, scavenger vulture, lagger falcon, small spotted eagle, brahminy kite, pariah kite, sparrow hawk, various types of pigeon and dove, goose, duck, teal, lapwing, white necked stork and several varieties of egret and heron. The low-lying swampy areas of Barddhaman being in line of migration provide a very good sheltering place for the migratory birds in winter.

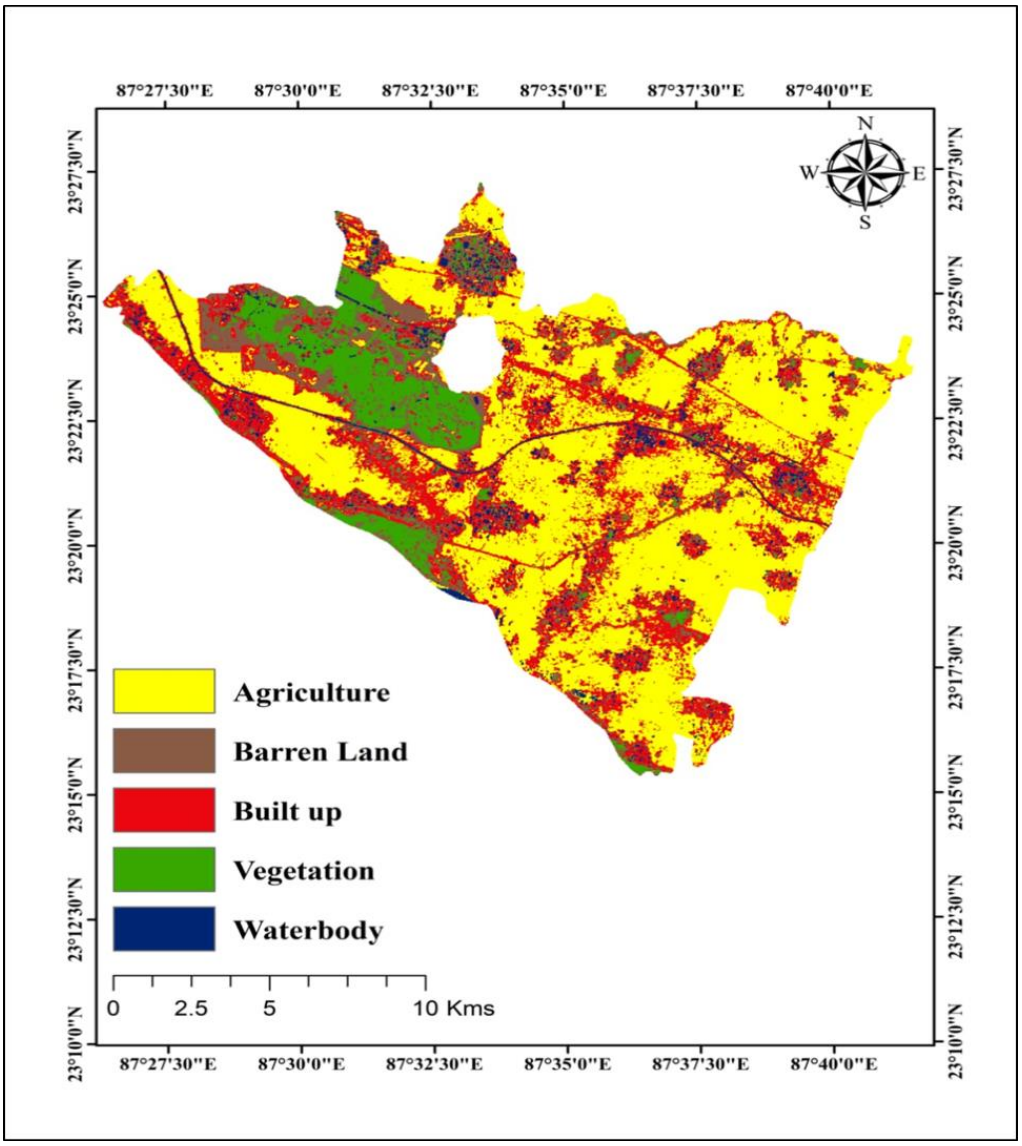


Figure3.2: Land use land cover map of Galsi-I block

3.4 Rainfall and Temperature:

Purba Bardhaman district in West Bengal receives an average annual rainfall of around 1400 mm while having 75% of it pouring down during the months of June to September. The district has a tropical hot and humid climate. The warmest month (with the highest average high temperature) is April (37.4°C). The months with the lowest average high temperature are January and December (26°C). Average high temperature in December: 26°C.

The month with the highest average low temperature is June (26°C). The coldest month (with the lowest average low temperature) is January (12°C).
Average low temperature in December: 12.5°C

CHAPTER 4- THEORETICAL CONCEPTS OF DIFFERENT TOPICS

4.1 FUNDAMENTALS OF GROUNDWATER FLOWAND WELL HYDRAULICS:

The underground water found in fully saturated soils and geologic formations below the water table is typically referred to as groundwater. Groundwater is not just an asset. It is a crucial aspect of the natural world; it causes issues with the ecosystem and, occasionally, provides a means for ecological remedies. It is a component of the hydrologic cycle, and knowing how it functions within this cycle is need to support integrated assessments in the evaluation of watershed resources, and in the evaluation of environmental contamination on a regional scale. When it comes to engineering, groundwater helps to such geotechnical issues including land subsidence and slope stability. Groundwater is also essential to comprehending a variety of several different geological process.

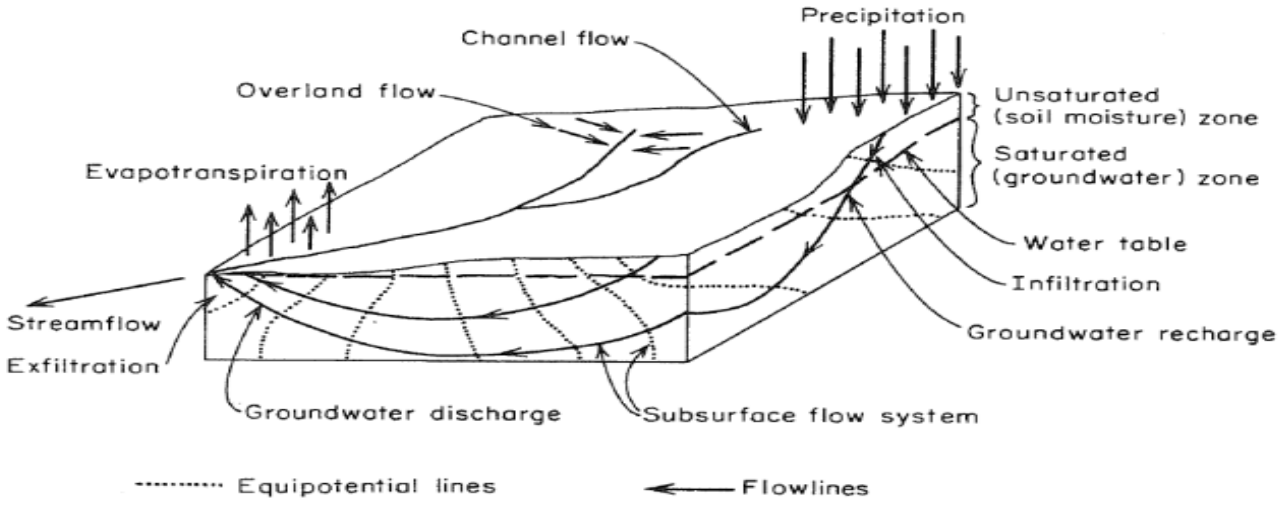


Figure4.1. Schematic representation of the Hydrologic Cycle (***Freeze & Cherry, 1979***)

4.1.1Types of groundwater:

Connate water refers to the groundwater that is trapped within the pore spaces of sedimentary rocks during their formation. As layers of sediment accumulate over time, pressure increases, squeezing water out of the sediment. However, some water remains trapped within the rock's pores, becoming connate water. This water is distinct from other groundwater sources because it is essentially "fossil water," having been isolated from the hydrological cycle for millions of years. Connate water is typically saline and can be found in reservoirs deep underground. It's an important consideration in various geological and hydrological studies, particularly in the exploration and extraction of oil and natural gas, as well as in understanding groundwater dynamics.

4.1.2 Groundwater and the Hydrologic Cycle:

The water cycle describes where water is on Earth and how it moves. Water is stored in the atmosphere, on the land surface, and below the ground. It can be a liquid, a solid, or a gas. Liquid water can be fresh or saline (salty). Water moves between the places it is stored. Water moves at large scales, through watersheds, the atmosphere, and below the Earth's surface. Water moves at very small scales too. It is in us, plants, and other organisms. Human activities impact the water cycle, affecting where water is stored, how it moves, and how clean it is.

Oceans store 96% of all water on Earth. Ocean water is saline, meaning it's salty. On land, saline water is stored in saline lakes. The rest of the water on Earth is fresh water. Fresh water is stored in liquid form in freshwater lakes, artificial reservoirs, rivers, and wetlands. Water is stored in solid, frozen form in ice sheets and glaciers, and in snowpack at high elevations or near Earth's poles. Water vapor is a gas and is stored as atmospheric moisture over the ocean and land. In the soil, frozen water is stored as permafrost and liquid water is stored as soil moisture. Deeper below ground, liquid water is stored as groundwater in aquifers. Water in groundwater aquifers is found within cracks and pores in the rock.

As it moves, water can change form between liquid, solid, and gas. Circulation mixes water in the oceans and transports water vapor in the atmosphere. Water moves between the atmosphere and the surface through evaporation, evapotranspiration, and precipitation. Water moves across the surface through snowmelt, runoff, and streamflow. Water moves into the ground through infiltration and groundwater recharge. Underground, groundwater flows within aquifers. Groundwater can return to the surface through natural discharge into rivers, the ocean, and from springs.

Climate change is actively affecting the water cycle. It is impacting water quantity and timing. Precipitation patterns are changing. The frequency, intensity, and length of extreme weather events, like floods or droughts, are also changing. Ocean sea levels are rising, leading to coastal flooding. Climate change is also impacting water quality. It is causing ocean acidification which damages the shells and skeletons of many marine organisms. Climate change increases the likelihood and intensity of wildfires, which introduces unwanted pollutants from soot and ash into nearby lakes and streams.

4.1.3 Vertical Distribution of Groundwater

(A) SATURATED ZONE: This zone, also known as groundwater zone, is the space in which all the pores of the soil are filled with water under hydrostatic pressure. The water table forms its upper limit and marks a free surface, i.e., a surface having atmospheric pressure.

(B) ZONE OF AERATION: In this zone the soil pores are only partially saturated with water. The space between the land surface and the water table marks the extent of this zone. The zone of aeration has three subzones:

(C) Soil Water Zone: This lies close to the ground surface in the major root band of the

vegetation from which the water is lost to the atmosphere by evapotranspiration.

(D) Intermediate Vadose Zone: This lies between the soil water zone and the capillary fringe. The thickness of the zone of aeration and its constituent subzones depend upon the soil texture and moisture content and vary from region to region. The soil moisture in the zone of aeration is of importance in agricultural practice and irrigation.

(E) Capillary Fringe: In this the water is held by capillary action. This zone extends from the water table upwards to the limit of the capillary rise.

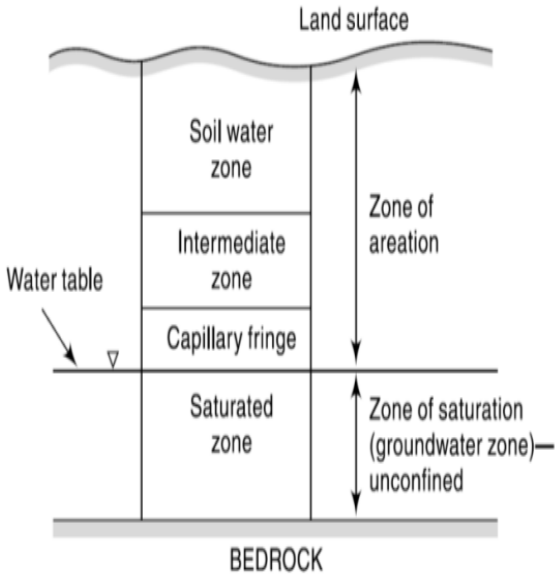


Figure 4.2 Divisions of subsurface water (***Subramanya, 2008***) Saturated Formation

All earth materials, from soils to rocks have pore spaces. Although these pores are completely saturated with water below the water table, from the groundwater utiliza- tion aspect only such material through which water moves easily and hence can be extracted with ease are significant. On this basis the saturated formations are classi- fied into four categories.

Aquifer: An aquifer is a saturated formation of earth material which not only stores water but yields it in sufficient quantity. Thus, an aquifer transmits water relatively easily due to its high permeability. Unconsolidated deposits of sand and gravel form good aquifers.

Aquiterd: It is a formation through which only seepage is possible and thus the yield is insignificant compared to an aquifer. It is partly permeable. A sandy clay unit is an example of aquitard. Through an aquitard appreciable quantity of water may leak to an aquifer below it

Aquiclude: It is a geological formation which is essentially impermeable to the flow of water. It may be considered as closed to water movement even though it may contain large amounts of water due to its high porosity. Clay is an example of an aquiclude

Aquifuge: It is a geological formation which is neither porous nor permeable. There are no

interconnected openings and hence it cannot transmit water. Massive compact rock without any fractures is an aquifuge.

The definitions of aquifer, aquitard and aquiclude as above are relative. A formation which may be considered as an aquifer at a place where water is at a premium (e.g. arid zones) may be classified as an aquitard or even aquiclude in an area where plenty of water is available.

The availability of groundwater from an aquifer at a place depends upon the rates of withdrawal and replenishment (recharge). Aquifers play the roles of both a transmission conduit and a storage. Aquifers are classified as unconfined aquifers and confined aquifers on the basis of their occurrence and field situation. An unconfined aquifer (also known as water table aquifer) is one in which a free water surface, i.e. a water table exists. Only the saturated zone of this aquifer is of importance in groundwater studies. Recharge of this aquifer takes place through infiltration of precipitation from the ground surface. A well driven into an unconfined aquifer will indicate a static water level corresponding to the water table level at that location.

The availability of groundwater from an aquifer at a place depends upon the rates of withdrawal and replenishment (recharge). Aquifers play the roles of both a transmission conduit and a storage. Aquifers are classified as unconfined aquifers and confined aquifers on the basis of their occurrence and field situation.

An unconfined aquifer (also known as water table aquifer) is one in which a free water surface, i.e., a water table exists. Only the saturated zone of this aquifer is of importance in groundwater studies. Recharge of this aquifer takes place through infiltration of precipitation from the ground surface. A well driven into an unconfined aquifer will indicate a static water level corresponding to the water table level at that location.

On the other hand, a confined aquifer (also known as artesian aquifer) is an aquifer which is confined between two impervious beds such as aquicludes or aquifuges. Recharge of this aquifer takes place only in the area where it is exposed at the ground surface. The water in the confined aquifer will be under pressure and hence the piezometric level will be much higher than the top level of the aquifer. At some locations, the piezometric level can attain a level higher than the land surface and a well driven into the aquifer at such a location will flow freely without the aid of any pump. A confined aquifer is called a leaky aquifer if either or both of its confining beds are aquitards.

Whether a stream feeds water into groundwater storage or the other way around depends on the location of the water table in relation to the water level in the stream. During times of low stream flows, if the stream's bed is below the groundwater table, the water surface may drop below the general the groundwater and the level of the water table both influence the stream's flow. These streams that are receiving Effluent streams are groundwater flows. These include streams and rivers that are perennial.

If, however, the water table is below the bed of the stream, the stream-water percolates to the groundwater storage and a hump is formed in the groundwater. Such streams which contribute to the ground water are known as influent streams. Intermittent rivers and streams which go dry

during long periods of dry spell (i.e., no rain periods) are of this kind.

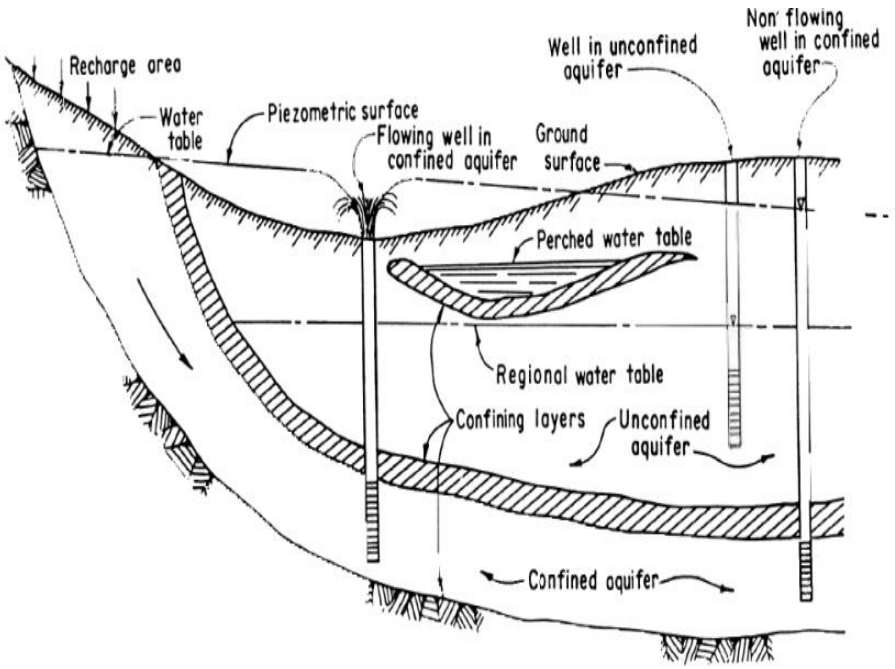


Figure4.3.Types of aquifers (***U.S. Bureau of Reclamation, 1995***)

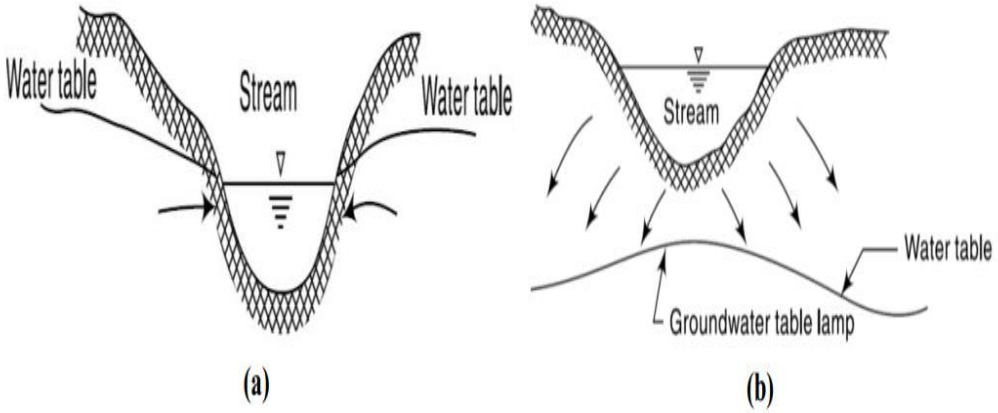


Figure4.4 (a) *Effluent Stream* **(b)** *Influent Stream* (***Subramanya, 2008***)

4.1.4 Aquifer Properties Affecting Ground Water:

Some of the important aquifer properties affecting ground water formations are:

Aquifer Material Properties

(1) Porosity: It gives a measure of the volume of void spaces in geological formations. It is defined as the ratio of pore volume to the bulk volume of the sample, given as

$$\boldsymbol{n} = \frac{V_v}{V} \quad \ldots\ldots \quad (4.1.)$$

where, $\boldsymbol{Vv}$ = volume and voids and $\boldsymbol{V}$ = total volume of aquifer material. Porosity represents the potential storage of an aquifer but does not indicate the amount of water a porous material will yield.

Table 4.1 Characteristics of Some Common Earth Formation Materials

Material	Specific yield (%)	Coefficient of Permeability (cm/s)	Porosity (%)	Porosity range classification
Clay	1-10	10^{-5} - 10^{-9}	45-55	
Silt	5-10	0.001-10^{-7}	35-50	High 5-20%
Sand fine	10-20	0.001-0.05	30-35	
Sand mixed	15-30	0.005-0.01	20-35	Medium 5-20%
Gravel	15-30	1-100	30-40	
Sand stone	5-15	0.001-0.0001	10-20	
Shale	0.5-5	10^{-10}-10^{-14}	1-10	Low 0-5%
Lime stone	0.5-5	0.001-0.00001	1-10	

Specific Yield and Specific Retention: While porosity gives a measure of the water-storage capability of a formation, not all the water held in the pores is available for extraction by pumping or draining by gravity. The pores hold back some water by molecular attraction and surface tension. The actual volume of water that can be extracted by the force of gravity from a unit volume of aquifer material is known as the ***specific yield*** ($\boldsymbol{Sy}$). The fraction of water held back in the aquifer is known as ***specific retention*** ($\boldsymbol{Sr}$). Thus, porosity,

$\boldsymbol{n} = \boldsymbol{Sy} + \boldsymbol{Sr}$ ……………………………………………………………………….(4.2.)

Both the parameters are dimensionless [$M^0L^0T^0$] and are expressed in percentage.

Table 4.2.: Porosity and Specific Yield of selected Formations

Formation	Porosity, %	Specific Yield, %
Clay	45-55	1-10
Sand	35-40	10-30
Gravel	30-40	15-30
Sandstone	10-20	5-15
Shale	1-10	0.5-5
Limestone	1-10	0.5-5

Storage Coefficient or Storativity:

The ***storage coefficient*** (or ***storativity***) is defined as the volume of water that an aquifer releases from or takes into storage per unit surface area of aquifer per unit change in the component of head normal to that surface.

For a vertical column of unit area extending through a confined aquifer, the storage coefficient, $\boldsymbol{S}$ equals the volume of water released from the aquifer when the piezometric surface declines a unit distance. The coefficient is a dimensionless quantity [$M^0 L^0 T^0$].

For most of the confined aquifers, $5 \times 10^{-5} \leq \boldsymbol{S} \leq 5 \times 10^{-3}$. This indicates that large pressure changes over extensive areas are required to produce substantial water yields.

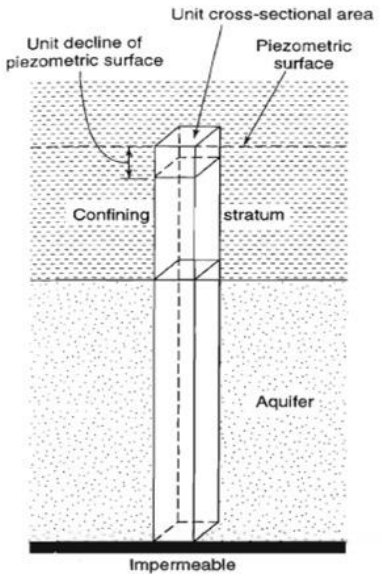


Figure4.5 Illustrative sketches for defining storage coefficient of a confined aquifer(Todd & Mays, 2005)

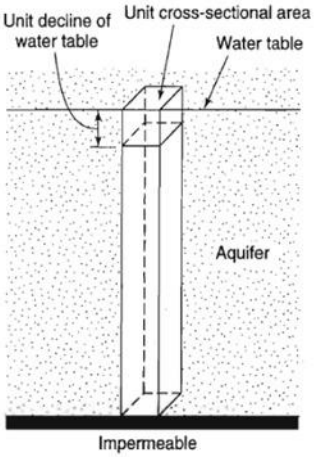


Figure 4.6 Illustrative sketches for defining storage coefficient of an unconfined aquifer (Todd & Mays, 2005)

Specific Storage: The ***specific storage, Ss*** of a saturated aquifer is the volume of water that a unit volume of aquifer releases from storage under a unit decline in hydraulic head, i.e.,

$$S = S_s \times b \quad \text{……(4.3.)}$$

where, ***b*** is the thickness of a confined aquifer.

It has a dimension of [L-1].

Specific Yield: t is defined as the volume of water that can be drained out by the force of gravity from a fully saturated aquifer per unit volume of aquifer material. It is expressed in percentage as

$$S_y=\frac{V_y}{V_b}\times 100$$

where V_y is the volume of water drained out, V_b the total volume of saturated sample. Since all the water from saturated sample cannot be removed by the action of gravity due to surface tension and molecular attraction between aquifer materials and water, specific yield is always less than porosity. For sand and gravel, specific yield is very high and for silt and clay it is low (Table 5.3); because smaller is the grain size of the aquifer material more is the number of grains per unit volume. The molecular attraction between water and aquifer material increases giving rise to less specific yield for silt and clay. Therefore grain size, shape, distribution, compaction, chemical and thermal conditions of the aquifer, time of drainage and other factors govern the specific yield from an aquifer. Specific yield for alluvial aquifer is 10-20%, i.e., from a fully saturated alluvial aquifer only 10-20% of total volume of soil equivalent of water can be drained out from the sample.

Specific Retention (S,): It is the volume of water which cannot be drained out from a saturated aquifer material by the force of gravity per unit volume of aquifer material. It is expressed in percentage as $S_r = \frac{V_r}{V_b}\times 100$ ……..(4.4)

Transmissibility: The ***transmissibility, T*** is the flow rate [*L2 T-1*] through a vertical strip of the aquifer of unit width extending through the saturated thickness under a unit hydraulic gradient. It indicates the capacity of an aquifer to transmit water through its entire thickness and is given by

$$\boldsymbol{T}=\boldsymbol{K}\times\boldsymbol{B}$$ …….(4.5.)

where, ***B*** is the saturated thickness of the aquifer.

Coefficient of Permeability: The ***coefficient of permeability*** (or ***hydraulic conductivity***) is defined as the velocity of flow through the total cross-sectional area of an aquifer subjected to a unit hydraulic gradient. It has a dimension of [LT^{-1}] and quantifies the ease with which the water will flow through the porous spaces of the aquifer. The parameter is a function of both the porous medium and the properties of the fluid. From the analogy of laminar flow through a conduit (***Hagen-Poiseuille Flow***) the coefficient of permeability, ***K*** can be expressed as

$$\boldsymbol{K}=(\boldsymbol{d}_{\mathrm{m}})^2\,\frac{\gamma}{\mu}$$……(4.6.)

where, ***C*** is a shape factor depending upon the shape of grains, packing, porosity and the grain-size distribution of the porous medium,

$\boldsymbol{d_m}$ is the mean size of particles of the porous medium,

$\boldsymbol{\gamma}$ is the unit weight of the fluid, and,

$\boldsymbol{\mu}$ is the coefficient of dynamic viscosity/ absolute viscosity of the fluid.

Often another parameter, $\boldsymbol{K}_0$, which is termed as the ***intrinsic permeability*** and is a function of the porous medium alone is defined as follows

$\boldsymbol{K}=\boldsymbol{K_0\gamma\mu}$ …(4.7.)

where, $\boldsymbol{K_0}=\boldsymbol{C}(\boldsymbol{d}_m)^2$……(4.8.)

It has a dimension of [L^2] and is expressed in darcys, where 1 darcy = 9.87×10^{-13} m^2.

Table 4.3.: Typical values of coefficient of permeability and intrinsic permeability of some porous media:

Sl. No.		**Material**		***K (cm/s)***	$\boldsymbol{K0}$ (darcys)
		Min.	***Max.***	***Min.***	***Max.***
			A. Granular Material		
1.	***Clean gravel***	1	100	10^3	10^5
2.	***Clean coarse sand***	10^{-2}	1	10	103
3.	***Mixed sand***	5×10^{-3}	10^{-2}	5	10
4.	***Fine sand***	10^{-3}	5×10^{-2}	1	50
5.	***Silty sand***	10^{-4}	2×10^{-3}	10^{-1}	2
6.	***Silt***	10^{-5}	5×10^{-4}	10^{-2}	5×10^{-1}
7.	***Clay***	$< 10^{-6}$			$< 10^{-3}$
			B. Consolidated Material		
1.	***Sandstone***	10^{-6}	10^{-3}	10^{-3}	1
2.	***Carbonate rock with secondary porosity***	10^{-5}	10^{-3}	10^{-2}	1
3.	***Shale***	10^{-10}		10^{-7}	
4.	***Fractured and weathered rock (aquifers)***	10^{-6}	10^{-3}	10^{-3}	1

Stratification of aquifers: Sometimes, the aquifer may be stratified, with varying permeabilities in each strata. Two kinds of flow conditions are possible in such a case.

(i) When the flow is parallel to the stratification

Equivalent transmissibility, $\boldsymbol{Teq}=\Sigma\boldsymbol{KiBii}$ ……(4.9.)

(ii) When the flow is normal to the stratification

Equivalent permeability, $\boldsymbol{Keq} = \Sigma \boldsymbol{Lii} \Sigma \boldsymbol{LiKii}$ ……..(4.10.)

Equivalent transmissibility, $\boldsymbol{Teq} = (\Sigma \boldsymbol{Lii}) \Sigma \boldsymbol{LiKii}$ ……..(4.11.)

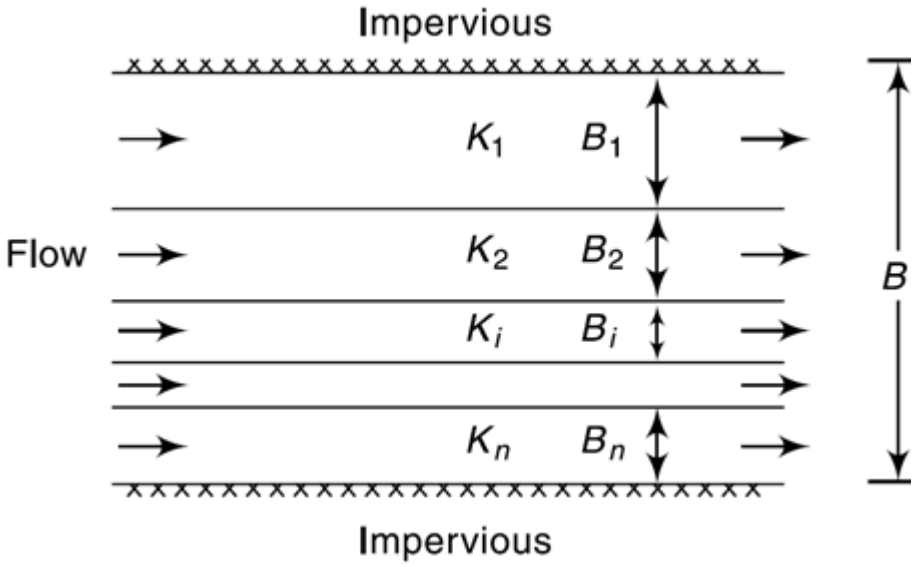


Figure. 4.7.: *Flow parallel to the stratification* (***Subramanya, 2008***)

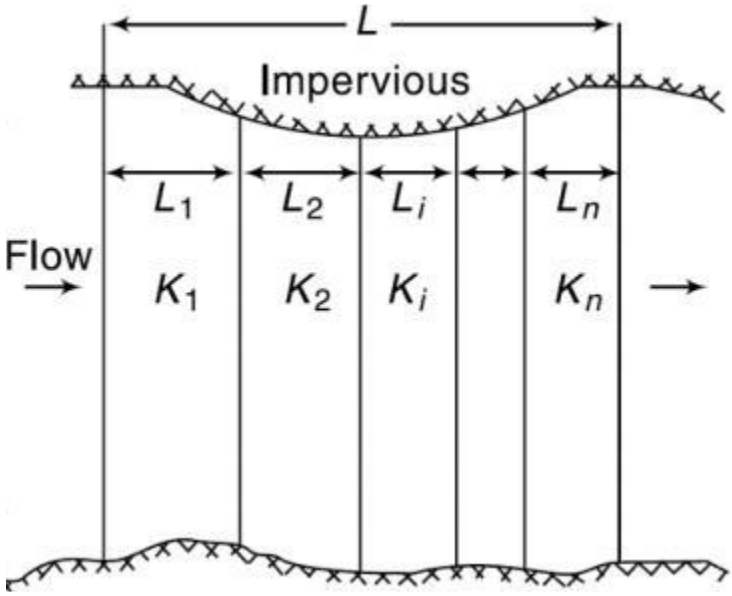


Figure.4.8: *Flow normal to the stratification* (***Subramanya, 2008***)

General 3-D Flow Equation in a porous medium: Consider the control volume . The net mass inflow rate to the control volume is given by

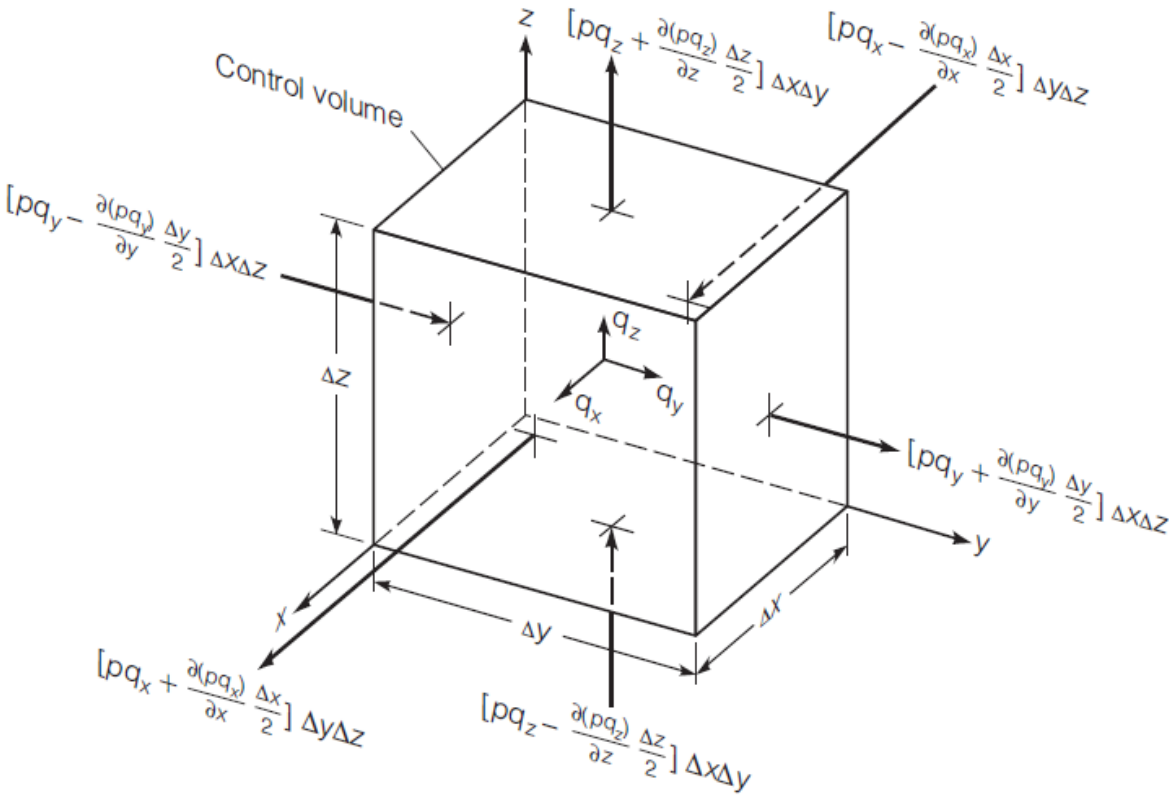


Figure. 4.9.: Control volume in a porous medium (**Chin, 2013**)

$$\text{Net mass inflow rate} = \left[(\rho q_x) - \frac{\partial(\rho q_x)}{\partial x}\frac{\Delta x}{2}\right]\Delta y\Delta z - \left[(\rho q_x) + \frac{\partial(\rho q_x)}{\partial x}\frac{\Delta x}{2}\right]\Delta y\Delta z$$
$$\left[(\rho q_y) - \frac{\partial(\rho q_y)}{\partial y}\frac{\Delta y}{2}\right]\Delta x\Delta z - \left[(\rho q_y) + \frac{\partial(\rho q_y)}{\partial y}\frac{\Delta y}{2}\right]\Delta x\Delta z$$
$$\left[(\rho q_z) - \frac{\partial(\rho q_z)}{\partial z}\frac{\Delta z}{2}\right]\Delta x\Delta y - \left[(\rho q_z) + \frac{\partial(\rho q_z)}{\partial z}\frac{\Delta z}{2}\right]\Delta x\Delta y$$

……..(4.11a)

where, ρ is the density of the fluid.
Simplification of Eq. (5.26.) yields

$$\text{Net mass inflow rate} = -\left[\frac{\partial(\rho q_x)}{\partial x} + \frac{\partial(\rho q_y)}{\partial y} + \frac{\partial(\rho q_z)}{\partial z}\right]\Delta x\Delta y\Delta z \text{……..(4.12)}$$

In accordance with the law of conservation of mass, the net mass inflow rate into the control volume is equal to the rate of change of mass within the control volume, which is given by Rate of change of mass $= \frac{\partial(n\rho)}{\partial t}\Delta x\Delta y\Delta z$…….(4.12a)

where, $\boldsymbol{n}$ is the porosity of the porous medium and $\boldsymbol{t}$ is the time.

Combining Eq. (5.27.) and Eq. (5.28.) we get,

$$-\left[\frac{\partial(\rho q_x)}{\partial x}+\frac{\partial(\rho q_y)}{\partial y}+\frac{\partial(\rho q_z)}{\partial z}\right]=\frac{\partial(n\rho)}{\partial t}\text{……..(4.13)}$$

Further, if $\boldsymbol{\rho}$ is independent of space and time, reduces to

$$-\left[\frac{\partial q_x}{\partial x}+\frac{\partial q_y}{\partial y}+\frac{\partial q_z}{\partial z}\right]=\frac{\partial n}{\partial t}\text{……..(4.13a)}$$

Considering the control volume shown in Fig. the time rate of change of fluid volume within the control volume can be expressed in terms of the specific storage, S_s, by the following relation

$$\frac{\partial n}{\partial t}\Delta x\Delta y\Delta z=S_s\frac{\partial \emptyset}{\partial t}\Delta x\Delta y\Delta z\text{……(4.14)}$$

where, $\emptyset\left(=\frac{P}{\gamma}+z\right)$ is the piezometric head.

simplifies into $\frac{\partial n}{\partial t}=S_s\frac{\partial \emptyset}{\partial t}$…….(4.15)

we get,

$$-\left[\frac{\partial q_x}{\partial x}+\frac{\partial q_y}{\partial y}+\frac{\partial q_z}{\partial z}\right]=S_s\frac{\partial \emptyset}{\partial t}\text{……..(4.15a)}$$

As per Darcy's Law, the components of the specific discharge vector $\boldsymbol{q_x}, \boldsymbol{q_y}$, and $\boldsymbol{q_z}$, can be written in terms of the piezometric head gradients, where

$$q_x=-K_{xx}\frac{\partial \emptyset}{\partial x}$$
$$q_y=-K_{yy}\frac{\partial \emptyset}{\partial y}$$
$$q_z=-K_{zz}\frac{\partial \emptyset}{\partial z}$$

……..(4.15b)

Therefore,

$$\frac{\partial}{\partial x}\left(K_{xx}\frac{\partial \emptyset}{\partial x}\right)+\frac{\partial}{\partial y}\left(K_{yy}\frac{\partial \emptyset}{\partial y}\right)+\frac{\partial}{\partial z}\left(K_{zz}\frac{\partial \emptyset}{\partial z}\right)=S_s\frac{\partial \emptyset}{\partial t}\text{……..(4.16)}$$

This general equation is applicable to both non-homogenous and isotropic/ anisotropic formations.

In cases where the aquifer is homogeneous and anisotropic

$$-\left[\frac{\partial q_x}{\partial x}+\frac{\partial q_y}{\partial y}+\frac{\partial q_z}{\partial z}\right]=\frac{\partial n}{\partial t}\text{……..(4.16a)}$$

Considering the control volume shown in Fig. 5.11., the time rate of change of fluid volume within the control volume can be expressed in terms of the specific storage, S_s, by the following As per Darcy's Law, the components of the specific discharge vector $\boldsymbol{q_x}, \boldsymbol{q_y}$, and $\boldsymbol{q_z}$, can be written in terms of the piezometric head gradients, where.

$$q_x=-K_{xx}\frac{\partial \emptyset}{\partial x}$$
$$q_y=-K_{yy}\frac{\partial \emptyset}{\partial y}$$
$$q_z=-K_{zz}\frac{\partial \emptyset}{\partial z}$$

……..(4.16b)

Therefore leads to

$$\frac{\partial}{\partial x}\left(K_{xx}\frac{\partial \emptyset}{\partial x}\right)+\frac{\partial}{\partial y}\left(K_{yy}\frac{\partial \emptyset}{\partial y}\right)+\frac{\partial}{\partial z}\left(K_{zz}\frac{\partial \emptyset}{\partial z}\right)=S_s\frac{\partial \emptyset}{\partial t}\text{……(4.17)}$$

This general equation is applicable to both non-homogenous and isotropic/ anisotropic formations.

In cases where the aquifer is homogeneous and anisotropic becomes

$$\frac{\partial^2 \emptyset}{\partial x^2}+K_{yy}\frac{\partial^2 \emptyset}{\partial y^2}+K_{zz}\frac{\partial^2 \emptyset}{\partial z^2}=S_s\frac{\partial \emptyset}{\partial t}\text{……(4.18)}$$

In cases where the hydraulic conductivity is isotropic, i.e., $\boldsymbol{K_{xx}=K_{yy}=K_{zz}=K}$ (say) becomes

$$\frac{\partial^2 \emptyset}{\partial x^2}+\frac{\partial^2 \emptyset}{\partial y^2}+\frac{\partial^2 \emptyset}{\partial z^2}=\frac{s_s}{K}\frac{\partial \emptyset}{\partial t}\text{……(4.19)}$$

or in the more convenient vector form as $\nabla^2 \emptyset=\frac{s_s}{K}\frac{\partial \emptyset}{\partial t}$

where, ∇^2 is the Laplacian operator defined by $\nabla^2=\frac{\partial^2}{\partial x^2}+\frac{\partial^2}{\partial y^2}+\frac{\partial^2}{\partial z^2}$

In cylindrical coordinates $(\boldsymbol{r}, \boldsymbol{\theta}, \boldsymbol{z})$, can be written as

$$\nabla^2 \emptyset = \frac{\partial^2 \emptyset}{\partial r^2} + \frac{1}{r}\frac{\partial \emptyset}{\partial r} + \frac{1}{r^2}\frac{\partial^2 \emptyset}{\partial \theta^2} + \frac{\partial^2 \emptyset}{\partial z^2} \quad \text{.....(4.20)}$$

4.1.5 2-D Approximations in unconfined aquifers:

In case of unconfined aquifers, the general flow equation, as given by Eq. (5.35) can be simplified by using an approximation first suggested by Dupuit (1863). The Dupuit approximation is that the equipotential lines can be assumed to be vertical, making the streamlines horizontal, and the head gradients constant over the depth, in which case

$$\boldsymbol{q}_x = -\boldsymbol{K}_{xx}\frac{\partial \emptyset}{\partial x} \approx -\boldsymbol{K}_{xx}\frac{\partial h}{\partial x} \quad \text{.....(4.20a)}$$

$$\boldsymbol{q}_y = -K_{yy}\frac{\partial \emptyset}{\partial y} \approx -K_{yy}\frac{\partial h}{\partial y} \quad \text{.....(4.20b)}$$

where, $\boldsymbol{h}$ is the thickness of the saturated zone. The Dupuit approximation is equivalent to assuming that the vertical pressure distribution in the aquifer is hydrostatic, leading to twodimensional flow in the horizontal plane.

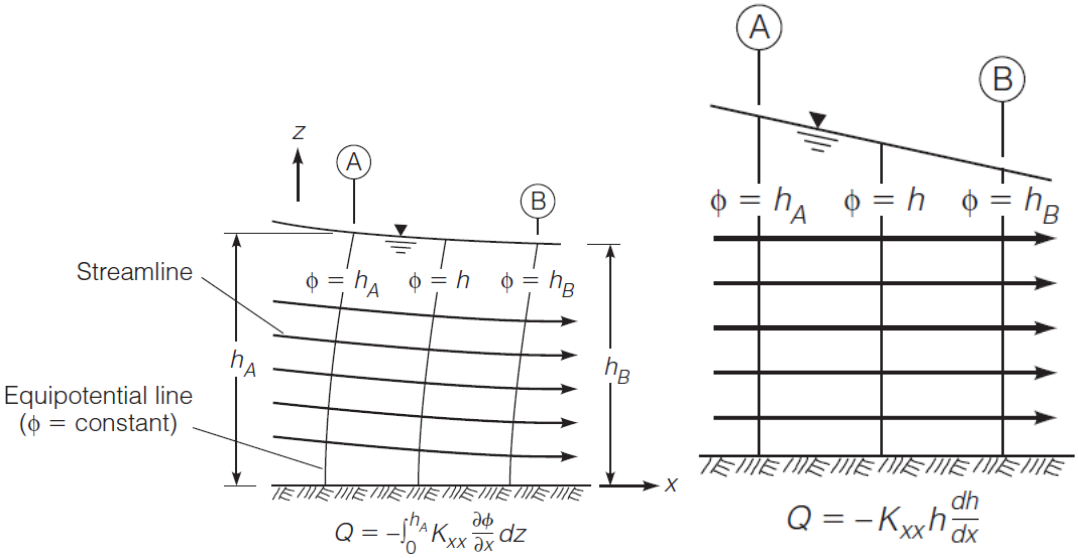


Fig. 4.10.: (a) Actual case **(b)** Dupuit approximation (**Chin, 2013**)

Consider the control volume shown in Figure 5.13., which is bounded on the bottom by the base of the aquifer and on the top by the phreatic surface. In addition to the inflows and outflows from the lateral boundaries of the control volume, there is also a surface recharge, ($\boldsymbol{x}$,), which accounts for the net inflow from above the aquifer, and is typically associated with infiltrated water from the ground surface that percolates through the vadose zone. The recharge, ($\boldsymbol{x}$,), has units of volume inflow per unit area per unit time [LT^{-1}].

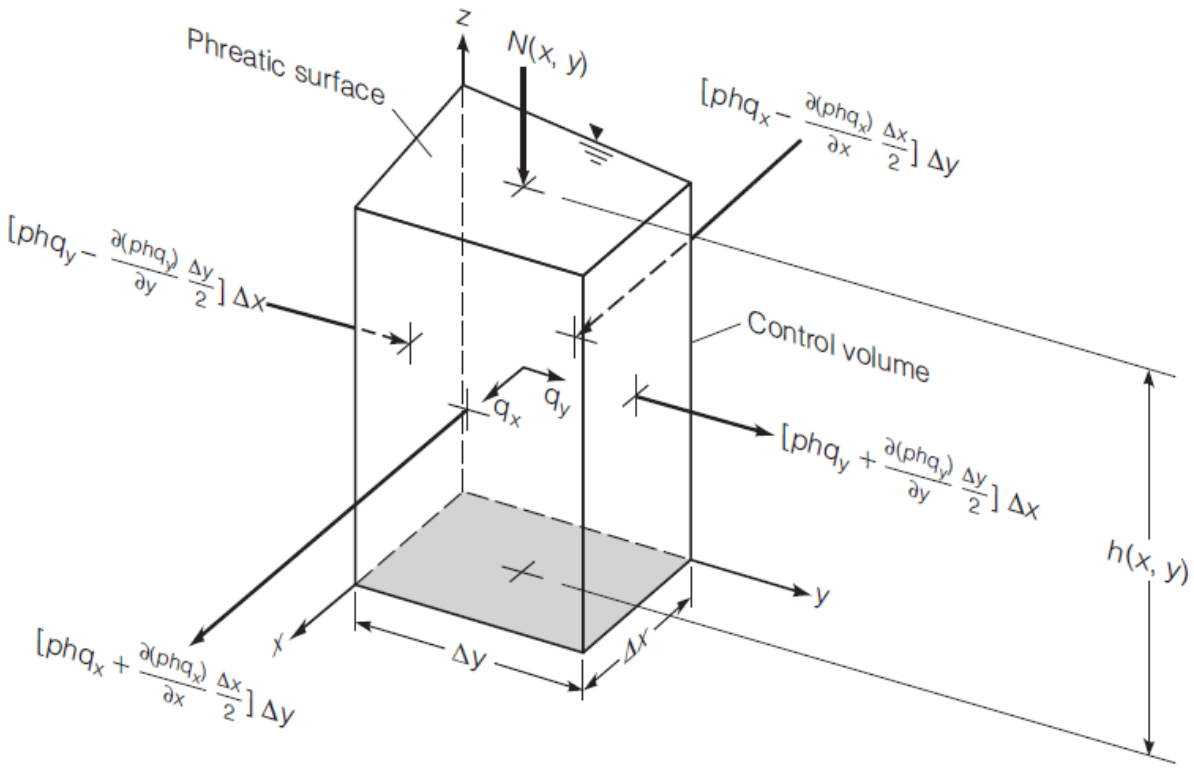


Figure. 4.11.: Control volume in an unconfined aquifer (**Chin, 2013**)

The general 2-D flow equation in an anisotropic and non-homogenous unconfined aquifer is given by

$$\frac{\partial}{\partial x}\left(K_{xx}h\frac{\partial h}{\partial x}\right)+\frac{\partial}{\partial y}\left(K_{yy}h\frac{\partial h}{\partial y}\right)+N=S_y\frac{\partial h}{\partial t} \quad \text{.....(4.21)}$$

2-D Approximations in confined aquifers: Consider the case of a confined aquifer of thickness ***b*** illustrated .

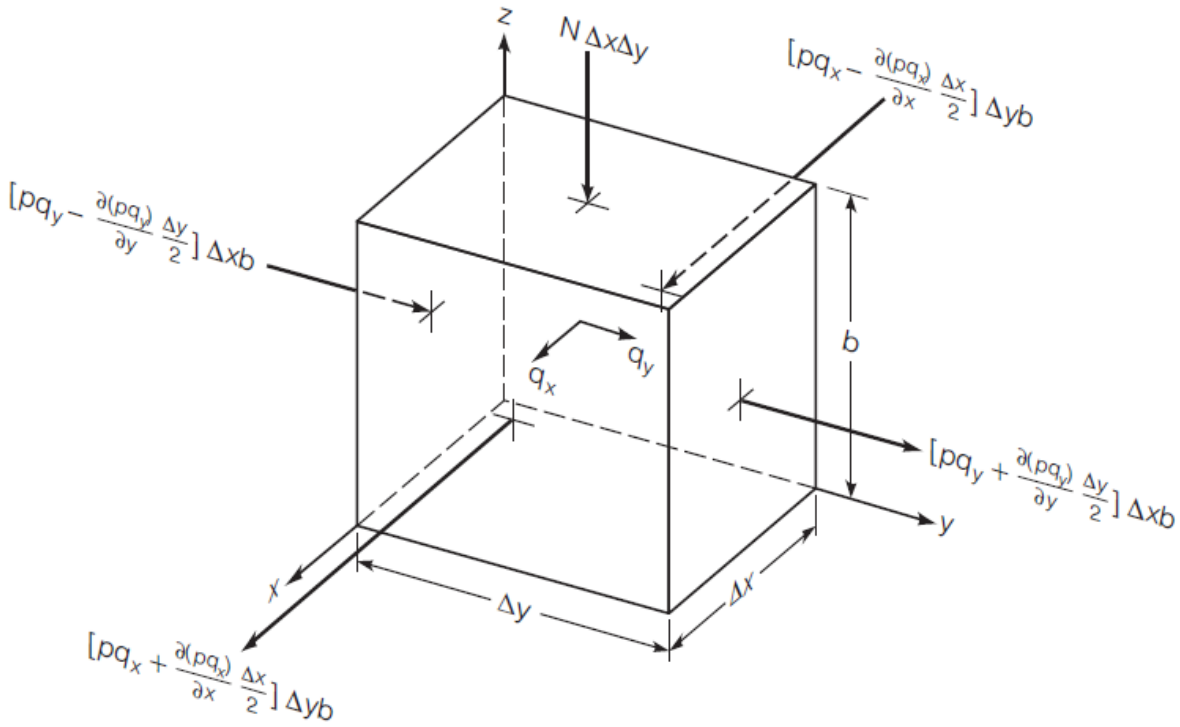


Fig. 4.12.: Control volume in a confined aquifer (Chin, 2013)

The general 2-D flow equation in an anisotropic and non-homogenous confined aquifer is given by

$$\frac{\partial}{\partial x}\left(\boldsymbol{K}_{xx}\frac{\partial \phi}{\partial x}\right)+\frac{\partial}{\partial y}\left(\boldsymbol{K}_{yy}\frac{\partial \phi}{\partial y}\right)+\frac{N}{b}=\frac{S}{b}\frac{\partial \phi}{\partial t} \quad \text{.....(4.22)}$$

4.1.6 Steady-State Well Hydraulics:

When a well is pumped, water flows into the well from the surrounding aquifer because of difference in hydraulic heads at the well and in the aquifer caused by pumping. Before pumping, water level in the well stands at a height theoretically equal to the static water pressure in the saturated layer around the well. This water level is known as ***static water level*** or ***pre-pumping water level***. When pumping starts, water is removed from the aquifer surrounding the well and the water level in the well (***piezometric level*** in case of confined aquifers and ***water table*** in case of unconfined aquifers) starts lowering. The water level in the well at any instant during pumping is known as ***pumping water level***.

The difference between the static water level and the pumping water level at any instant is called ***drawdown***, which is a function of pumping rate, pumping duration and distance from the pumping well. Drawdown is always maximum at the pumping well and it decreases with an increase in the distance from pumping well. The rate of pumping from an aquifer significantly affects the hydraulic gradient in the aquifer.

The faster the well is pumped, the steeper the hydraulic gradient will be in the vicinity of the

well. In three- dimensions, the drawdown curve takes the shape of an inverted cone centered on the pumping well, which is known as ***cone of depression***. The outer limit of the cone of depression defines the area of influence of the well. The boundary of the area of influence is called ***circle of influence*** and the radius of the circle of influence is called ***radius of influence***. Thus, the radius of influence, $\boldsymbol{R}$ is the distance from a pumping well to the edge of the cone of depression where drawdown is zero.

At constant rate of pumping, the drawdown curve develops gradually with time due to the withdrawal of water from storage. This phase is called an ***unsteady flow*** as the water table elevation at a given location near the well changes with time. On prolonged pumping, an equilibrium state is reached between the rate of pumping and the rate of inflow of groundwater from the outer edges of the zone of influence. The drawdown surface attains a constant position with respect to time when the well is known to operate under ***steady flow*** conditions.

As soon as the pumping is stopped, the depleted storage in the cone of depression is made good by groundwater inflow into the zone of influence. There is a gradual accumulation of storage till the original (static) level is reached. This stage is called ***recuperation*** or ***recovery*** and is an unsteady phenomenon, which depends upon the aquifer characteristics.

Steady-state conditions occur when all boundary conditions are constant in time. Strictly speaking, such conditions seldom occur in reality; however, in those cases where the boundary conditions change slowly in time or long-term average flow conditions are being sought, steady-state solutions can be applied as reasonable approximations.

4.1.7 Well in a confined aquifer:

In a confined aquifer, the distribution of piezometric head for 2-D flows , which can be simplified as follows considering an isotropic and homogenous state of the aquifer.

The general 2-D flow equation in an anisotropic and non-homogenous confined aquifer is given by

$$\frac{\partial}{\partial x}\left(\boldsymbol{K}_{xx}\frac{\partial \phi}{\partial x}\right)+\frac{\partial}{\partial y}\left(\boldsymbol{K}_{yy}\frac{\partial \phi}{\partial y}\right)+\frac{N}{b}=\frac{S}{b}\frac{\partial \phi}{\partial t} \quad \text{.....(4.23)}$$

When the effective hydraulic conductivity of the aquifer is homogeneous as well as isotropic in the horizontal plane ($\boldsymbol{K_{xx}=Kyy=K}$),becomes

$$\boldsymbol{K}\frac{\partial^2 \phi}{\partial x^2}+\boldsymbol{K}\frac{\partial^2 \phi}{\partial y^2}+\frac{N}{b}=\frac{s}{b}\frac{\partial \phi}{\partial t} \quad \text{.....(4.23a)}$$

or, $$\frac{\partial^2 \phi}{\partial x^2}+\frac{\partial^2 \phi}{\partial y^2}+\frac{N}{Kb}=\frac{S}{Kb}\frac{\partial \emptyset}{\partial t} \quad \text{.....(4.23b)}$$

In polar coordinate system $(\boldsymbol{r,\theta})$ can be written as

$$\frac{\partial^2 \emptyset}{\partial r^2}+\frac{1}{r}\frac{\partial \phi}{\partial r}+\frac{1}{r^2}\frac{\partial^2 \phi}{\partial \theta^2}+\frac{N}{Kb}=\frac{s}{Kb}\frac{\partial \emptyset}{\partial t} \quad \text{.....(4.24)}$$

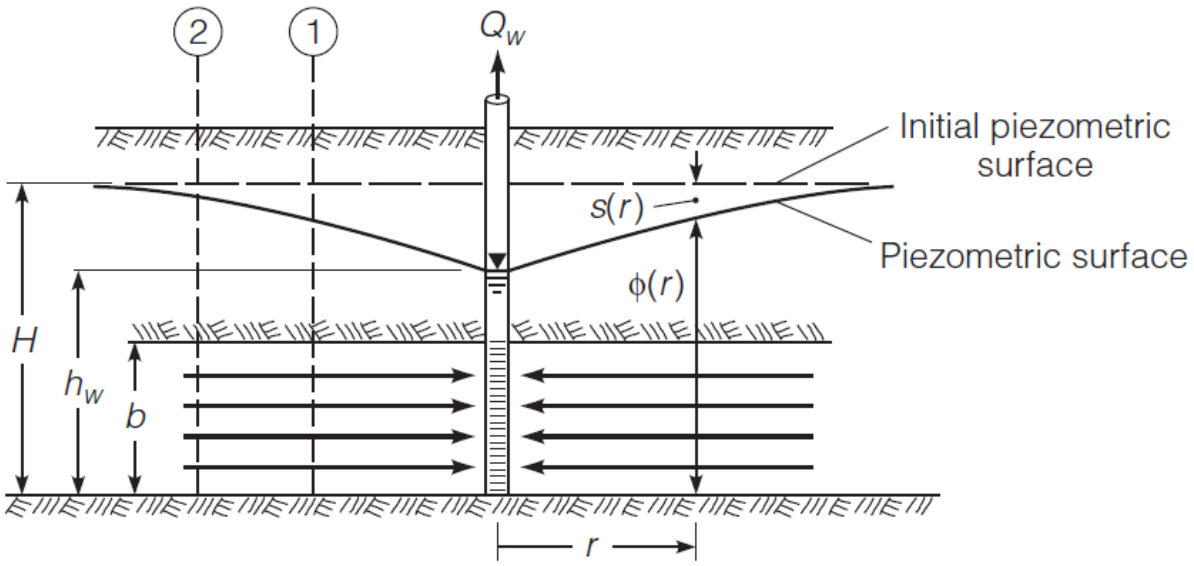


Fig.4.13: Fully penetrating well in a confined aquifer (**Chin, 2013**)

If a well fully penetrates the confined aquifer, and withdraws water at a constant rate uniformly over the aquifer thickness, $\boldsymbol{b}$, as illustrated in Fig. 5.15., then the piezometric head, $\emptyset$, is radially symmetric (independent of $\boldsymbol{\theta}$) and independent of time. Consequently, all derivatives of $\emptyset(\boldsymbol{r})$ with respect to $\boldsymbol{\theta}$ and $\boldsymbol{t}$ are zero. If there is no recharge of the confined aquifer, then $\boldsymbol{N}$ = 0 and Eq. (5.45.) reduces to

$\frac{\partial^2 \emptyset}{\partial r^2} + \frac{1}{r}\frac{\partial \emptyset}{\partial r} = 0$……(4.24a)

Since $\emptyset$ is a function of the radial distance from the well, $\boldsymbol{r}$ alone, the partial derivatives can be replaced by the total derivatives. Also, multiplying with $\boldsymbol{r}$ yields

$$\boldsymbol{r}\frac{d^2\emptyset}{dr^2} + \frac{d\emptyset}{dr} = \mathbf{0}$$

$$\text{or, } \frac{d}{dr}\left(\boldsymbol{r}\frac{d\emptyset}{dr}\right) = \mathbf{0}$$

……..(4.24b)

can be solved with the following boundary conditions.

$2\pi \mathbf{r_w b K}\frac{d\emptyset}{dr} = Q_w$ (when $r = r_w$), and,

$\emptyset(\boldsymbol{r_w}) = \boldsymbol{h_w}$……..(4.24c)

where, r_w is the radius of the well,
K is the hydraulic conductivity of the aquifer,
Q_w is the flow rate out of the well, and,
$\boldsymbol{h_w}$ is the depth of the water in the well, which is also equal to the piezometric head at the well

$(\boldsymbol{r} = \boldsymbol{r_w})$.

Integrating with respect to r yields $\boldsymbol{r}\frac{d\emptyset}{d\boldsymbol{r}} = \boldsymbol{A}$
and integrating again with respect to r yields $\emptyset = \boldsymbol{A}\,\mathbf{ln}(\boldsymbol{r}) + \boldsymbol{B}$
where, $\boldsymbol{A}$ and $\boldsymbol{B}$ are constants to be determined from the boundary conditions,

Applying the boundary conditions yields

$\boldsymbol{A} = \frac{Q_w}{2\pi b\mathbf{K}}$ and $B = h_w - A\ln(r_w)$……(4.25)

yields the following expression for the piezometric head distribution induced by a fully penetrating pumping well in a confined aquifer

$\emptyset(\boldsymbol{r}) = \boldsymbol{h_w} + \frac{Q_w}{2\pi\mathrm{bK}}\ln\left(\frac{\boldsymbol{r}}{r_w}\right)$……(4.26)

provides a reasonably accurate description of the piezometric surface, as long as $\emptyset < \boldsymbol{H}$, where $\boldsymbol{H}$ is the elevation of the piezometric surface in the absence of pumping.

This limitation in applying is frequently made explicit by defining the boundary condition
$\emptyset(\boldsymbol{R}) = \boldsymbol{H}$
where $\boldsymbol{R}$ is referred to as the radius of influence of the well. as a boundary condition, the head distribution is given by

$\emptyset(\boldsymbol{R}) = \boldsymbol{H} - \frac{Q_w}{2\pi\mathrm{bK}}\mathbf{l\,n}\left(\frac{\boldsymbol{R}}{\boldsymbol{r}}\right)$……(4.27)

was originally derived by Dupuit (1857) and subsequently by Thiem (1906), and is commonly known as the Thiem equation.

. Well in an unconfined aquifer: In an unconfined aquifer, the distribution of piezometric head for 2-D flows by Dupuit approximation is given by which can be simplified as follows considering an isotropic and homogenous state of the aquifer.

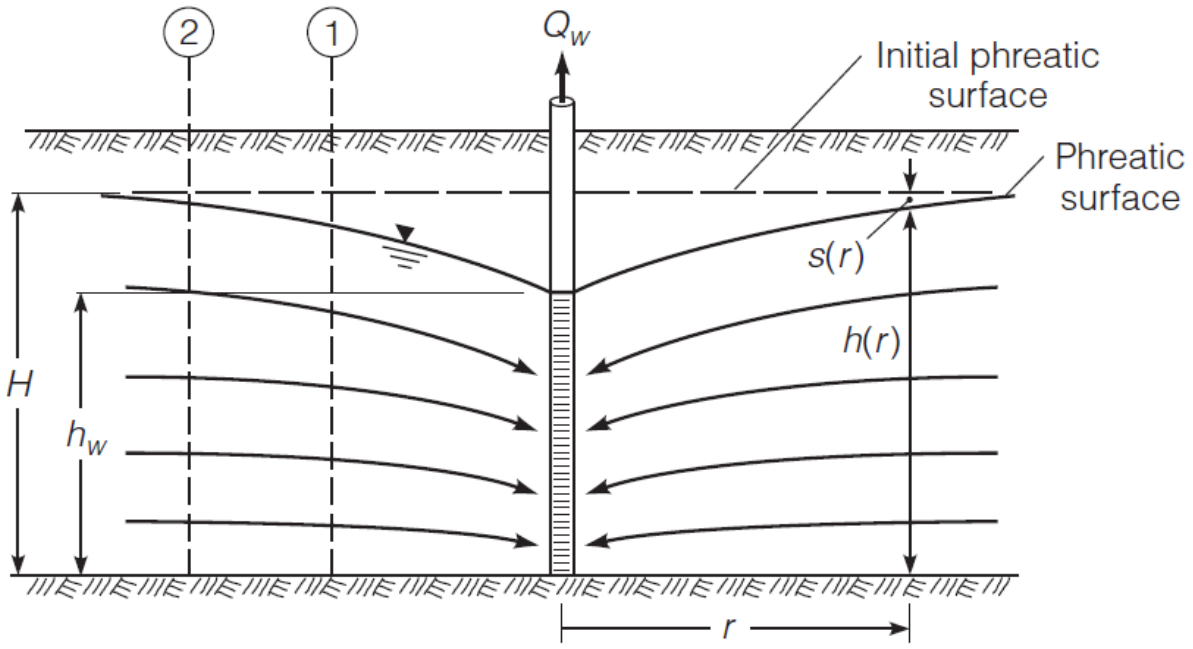


Fig. 4.14: Fully penetrating well in an unconfined aquifer (**Chin, 2013**)

The general 2-D flow equation in an anisotropic and non-homogenous confined aquifer is given by

$$\frac{\partial}{\partial x}\left(K_{xx}h\frac{\partial h}{\partial x}\right)+\frac{\partial}{\partial y}\left(K_{yy}h\frac{\partial h}{\partial y}\right)+N=S_y\frac{\partial h}{\partial t} \quad \text{.....(4.28)}$$

In cases where the hydraulic conductivity of the aquifer is homogeneous, describes the distribution of saturated thickness, $\boldsymbol{h}$, by

$$K_{xx}\frac{\partial}{\partial x}\left(h\frac{\partial h}{\partial x}\right)+K_{yy}\frac{\partial}{\partial y}\left(h\frac{\partial h}{\partial y}\right)+N=S_y\frac{\partial h}{\partial t} \quad \text{.....(4.29)}$$

From the identities already established, $h\frac{\partial h}{\partial x}=\frac{1}{2}\frac{\partial h^2}{\partial x}$ and $h\frac{\partial h}{\partial y}=\frac{1}{2}\frac{\partial h^2}{\partial y}$

Therefore, Eq. (5.56.) simplifies to

$$K_{xx}\frac{\partial^2 h^2}{\partial x^2}+K_{yy}\frac{\partial^2 \hbar^2}{\partial y^2}+2N=2S_y\frac{\partial h}{\partial t} \quad \text{.....(4.30)}$$

Now, if the hydraulic conductivity is isotropic in the horizontal plane ($\boldsymbol{K_{xx}=K_{yy}=K}$), becomes

$$K\frac{\partial^2 \hbar^2}{\partial x^2}+K\frac{\partial^2 \hbar^2}{\partial y^2}+2N=2S_y\frac{\partial h}{\partial t} \quad \text{.....(4.31)}$$

In polar coordinate system (r, θ), Eq. can be written as

$$\frac{\partial^2(h^2)}{\partial r^2} + \frac{1}{r}\frac{\partial(h^2)}{\partial r} + \frac{1}{r^2}\frac{\partial^2(h^2)}{\partial \theta^2} + \frac{2N}{K} = \frac{2S_y}{K}\frac{\partial h}{\partial t} \quad \text{.....(4.32)}$$

The case of a fully penetrating pumping well in an unconfined aquifer is illustrated in Fig. 5.16. Since the aquifer response to pumping is radially symmetric around the well, derivatives with respect to θ are equal to zero

$$\frac{\partial^2(h^2)}{\partial r^2} + \frac{1}{r}\frac{\partial(h^2)}{\partial r} = 0 \quad \text{.....(4.33)}$$

Since $\boldsymbol{h}$ is a function of the radial distance from the well, $\boldsymbol{r}$ alone, the partial derivatives can be replaced by the total derivatives. Also, multiplying Eq. (5.46.) with r yields

$$r\frac{d^2(h^2)}{dr^2} + \frac{d(h^2)}{dr} = 0$$
$$\text{or, } \frac{d}{dr}\left(r\frac{d(h^2)}{dr}\right) = 0 \quad \text{.....(4.34)}$$

Eq. (5.63.) can be solved with the following boundary conditions.

$2\pi \mathbf{r}_w \mathbf{h} K \frac{dh}{dr} = Q_w$ (when $r = r_w$), and,

$\boldsymbol{h}(\boldsymbol{r}_w) = \boldsymbol{h}_w$

where, r_w is the radius of the well,

K is the hydraulic conductivity of the aquifer,

Q_w is the flow rate out of the well, and,

$\boldsymbol{h}_w$ is the depth of the water in the well.

Integrating Eq.with respect to r yields $r\frac{d(h^2)}{dr} = A$

and integrating again with respect to r yields $h^2 = A\ln(\boldsymbol{r}) + B$

where, A and B are constants to be determined from the boundary conditions, Eq. (5.64a) and Eq. $(5.64b.)$.

Applying the boundary conditions yields $A = \frac{Q_w}{\pi K}$ and $B = h_w^2 - A\ln(r_w)$ .....(4.35)

Substituting yields the following expression for the head distribution induced by a fully penetrating pumping well in an unconfined aquifer

$$h(r) = \sqrt{h_w^2 + \underbrace{\frac{Q_w}{\pi K}}_{\equiv K}\ln\left(\frac{r}{r_w}\right)} \quad \text{.....(4.36)}$$

Eq. (5.68.) provides a reasonably accurate description of the phreatic surface, as long as $\boldsymbol{h} < \boldsymbol{H}$, where $\boldsymbol{H}$ is the saturated thickness in the absence of pumping. This limitation can be circumvented by using the following boundary conditions in Eq. (5.66.)

$\boldsymbol{h}(\boldsymbol{r}_w) = \boldsymbol{h}_w$ and $\boldsymbol{h}(\boldsymbol{R}) = H$

Using Eq. (5.69.) as a boundary condition, the head distribution is given by

$$h(r) = \sqrt{h_w^2 + (H - h_w)^2 \frac{\ln\left(\frac{r}{r_w}\right)}{\ln\left(\frac{H}{r_w}\right)}} \text{.....(4.37)}$$

4.1.8 Well in a leaky confined aquifer:

In isotropic and homogeneous semiconfined (leaky) aquifers, the distribution of piezometric head for 2-D flows is given by

$$\frac{\partial^2\theta}{\partial r^2} + \frac{1}{r}\frac{\partial\theta}{\partial r} + \frac{1}{r^2}\frac{\partial^2\theta}{\partial\theta^2} + \frac{N}{Kb} = \frac{s}{Kb}\frac{\partial\phi}{\partial t} \text{.....(4.38)}$$

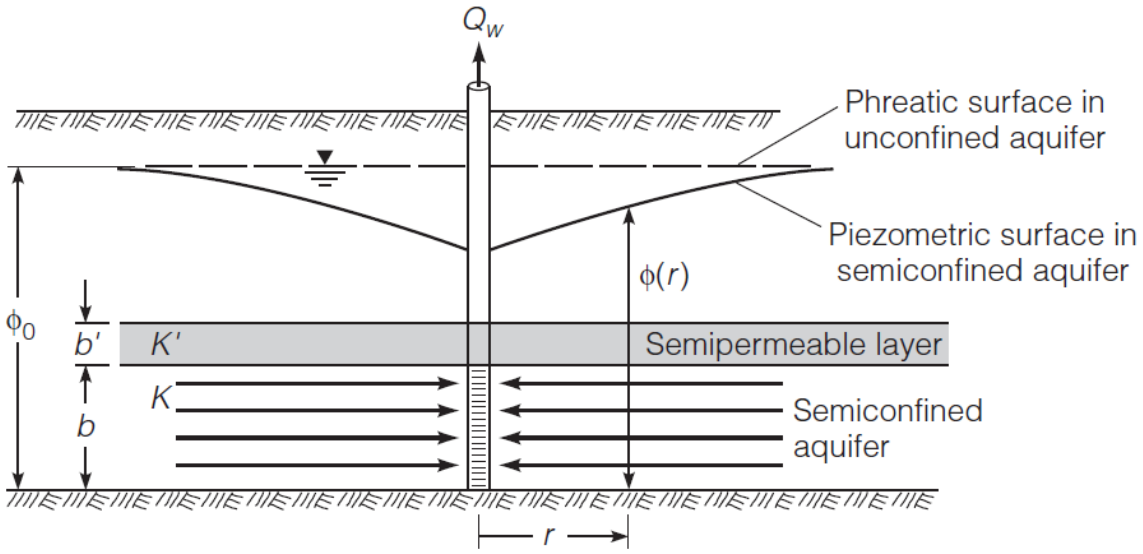


Fig. 4.15.: Fully penetrating well in a semi-confined aquifer (**Chin, 2013**)

If a well fully penetrates the semiconfined aquifer and withdraws water at a constant rate uniformly over the aquifer thickness, ***b***, as illustrated in Fig. 5.17., then the piezometric head, ∅, is radially symmetric (independent of ***θ***) and, under steady-state conditions, is independent of time.

Therefore, all derivatives with respect to ***θ*** and ***t*** are zero, and Eq. (5.45.) can be written in the form

$$\frac{d^2\emptyset}{dr^2} + \frac{1d\emptyset}{rdr} + \frac{N}{Kb} = 0 \text{.....(4.39)}$$

where partial derivatives have replaced total derivatives, since ∅ depends only on r.

Leakage into the semiconfined aquifer can be calculated by applying Darcy's law across the

semipermeable layer, in which case

$N = -K' \frac{\emptyset - \emptyset_0}{b'}$.....(4.40)

where, $\mathbf{K}'$ is the hydraulic conductivity of the semipermeable layer, $\mathbf{b}'$ is the thickness of the semipermeable layer, and,
$\emptyset_0$ is the piezometric head above the semipermeable layer, assumed to be constant.
Combining, we get $\frac{d^2\theta}{dr^2} + \frac{1}{r}\frac{d\rho}{dr} + \frac{K'(\varphi_0 - \varphi)}{K\Delta v'} = 0$.....(4.41)
Defining the parameter λ by the expression $\lambda^2 = \frac{K\Delta v'}{K'}$
Therefore, can be written as $\frac{d^2\theta}{dr^2} + \frac{1}{r}\frac{d\theta}{dr} + \frac{\phi_0 - \phi}{\lambda^2} = 0$.....(4.42)
The quantity λ defined by Eq. (5.74.) is commonly used to parameterize the leakage in semiconfined aquifers, and is called the leakage factor.

Defining new variables $\emptyset'$ and $\mathbf{r}'$ by

$\emptyset' = \emptyset_0 - \emptyset$ and $\mathbf{r}' = \frac{r}{2}$.....(4.43)

can be written as $r'^2 \frac{d^2\varphi'}{dr'^2} + r' \frac{d\varphi'}{dr'} - \mathbf{r}'^2\emptyset' = 0$.....(4.44)
This equation is a modified Bessel's equation of order zero, and has the solution $\emptyset' = AI_0(r') + BK_0(r')$
or, $\emptyset_0 - \emptyset(r) = AI_0\left(\frac{r}{2}\right) + BK_0\left(\frac{r}{2}\right)$.....(4.45)
where, $I_0(x)$ and $K_0(x)$ are modified Bessel functions of the first and second kind, respectively, of order zero, and A and B are constants to be determined from the boundary conditions.

In this case, the boundary conditions are
$2\pi r_w b\, K \frac{d\rho}{dr} = Q_w$ (when $r = r_w$), and, $\emptyset(\infty) = \emptyset_0$

Noting the following Bessel function properties

$$\boldsymbol{I}_0(\infty) = \infty \text{ and } \boldsymbol{K}_0(\infty) = 0$$

the boundary condition given by Eq. (1.80b.) requires that $A = 0$ in Eq. (5.79.), which now becomes

$$\emptyset_0 - \emptyset(\boldsymbol{r}) = \boldsymbol{B}\boldsymbol{K}_0\left(\frac{r}{2}\right)$$

Application of the other boundary condition, Eq. (5.80b.), requires using the Bessel function identity

$$\frac{d}{dr'}\boldsymbol{K}_0(\boldsymbol{r}') = -\boldsymbol{K}_1(\boldsymbol{r}')$$

where, $\boldsymbol{K}_1(\boldsymbol{r}')$ is the modified Bessel function of the second kind of order one.
Differentiating Eq. (5.82.) and applying the boundary condition given by Eq. (5.80a.) leads to

the following expression for :

$$B = \frac{Q_w}{2\pi T\left(\frac{T_w}{\lambda}\right)K_1\left(\frac{r_\mu}{1}\right)} \text{.....(4.46)}$$

where, $\boldsymbol{T}(= \boldsymbol{Kb})$ is the transmissivity of the semiconfined aquifer.
Substituting yields the following expression for the piezometric head distribution

$$\emptyset_0 - \emptyset(\boldsymbol{r}) = \frac{\vartheta_w}{2\pi\tau}\frac{\kappa_0\left(\frac{\tau}{2}\right)}{\left(\frac{\tau_w}{2}\right)K_1\left(\frac{r_\pi}{\lambda}\right)} \text{.....(4.46b)}$$

Defining the drawdown, $s(r) = \emptyset_0 - \emptyset(\boldsymbol{r})$
yield the following expression for the drawdown

$$s(r) = \frac{Q_w}{2\pi T}\frac{\kappa_0\left(\frac{r}{2}\right)}{\left(\frac{N_\psi}{2}\right)\kappa_1\left(\frac{r_w}{2}\right)} \text{.....(4.47)}$$

In this case, there are two aquifer properties: transmissivity, $\boldsymbol{T}$, and leakage factor, λ. These aquifer properties can be estimated using Eq. (5.87.) with drawdown measurements at two locations.

Denoting the drawdown measurements by s_1 and s_2, at r_1 and r_2, respectively, Eq. (1.87.) yields

$$\frac{K_0\left(\frac{r_1}{\lambda}\right)}{K_0\left(\frac{r_2}{\lambda}\right)} = \frac{s_1}{s_2} \text{.....(4.47a)}$$

$$\mathrm{T} = \frac{\mathrm{Q_w}}{2\pi \mathrm{s_1}}\frac{\mathrm{K_0}\left(\frac{\mathrm{r_1}}{\lambda}\right)}{\left(\frac{\mathrm{r_w}}{\lambda}\right)\mathrm{K_1}\left(\frac{\mathrm{r_w}}{\lambda}\right)} \text{.....(4.48)}$$

can be used to estimate the leakage factor from the drawdown measurements. This leakage factor can subsequently be used in to calculate the transmissivity of the semiconfined aquifer.

The derived leakage factor can be used to classify the leakiness of the semi-confining layer using the classification system in Fig.5.18. that was originally suggested by Sen (1995). Aquifers with leakage factors exceeding 10,000 m can be treated as confined aquifers.

The equations derived in this section assume that the flow is horizontal in the aquifer and vertical in the semi-confining (leaky) layer. Errors introduced by these assumptions are generally less than 5%, provided that the hydraulic conductivity of the aquifer is more than two orders of magnitude greater than that of the semi-confining layer **(Neuman and Witherspoon, 1969).**

4.1.9 Thiem's Method For Steady-State Flow In A Confined Aquifer:

Historically, one of the first quantitative approaches for looking at flow in a confined aquifer was that of Thiem (1906). This theory applies to a homogeneous and isotropic aquifer that is infinite in extent. The analysis also assumes that there has been sufficient pumping to allow the ground-water system to achieve steady state. In other words, water levels in the wells do not change with time (Figure 9.2a). The map view in Figure 9.2b shows that the flow in this case is radial, toward the well, with hydraulic heads increasing away from the pumping well.

The hydraulic head in the aquifer can be determined as a solution to a ground-water flow equation, like those we presented in Chapter 3. However, in this case, it is beneficial to use radial coordinates, where distances (r) are measured from the well to some point of interest. A solution to the flow equation with appropriate boundary conditions is

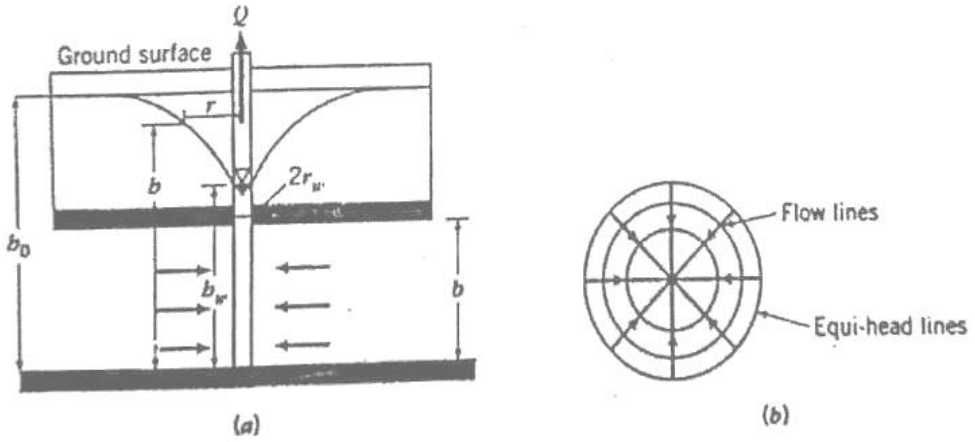


Figure 4.16: Steady-state cone of depression in a confined aquifer, (a) sectional view, (b) map view

$$h = ho + \frac{Q}{2\pi T} ln \frac{r}{R} \text{.....(4.49)}$$

where h is the hydraulic head at a distance r from a pumped well, ho is the pre pumping hydraulic head, Q is the pumping rate of the well (positive for withdrawal and negative for injection), T is the transmissivity of the aquifer, and R is the radius of influence of the pumped well. You can determine the hydraulic head in the actual pumping well by assuming that the radius to the observation point is equal to the radius of the pumped well, as

$$h_w = ho + \frac{Q}{2\pi T} ln \frac{r_w}{R} \text{.....(4.50)}$$

where r_w is the radius of the pumped well. In a situation with two observation wells, the hydraulic heads in the wells are related by

$$h_2 = h_1 + \frac{Q}{2\pi T} ln \frac{r_2}{r_1} \text{.....(4.51)}$$

Remember Eq. (9.7) because it will be used as the basis for a field test to estimate transmissivity. The radius of influence can be estimated from the hydraulic-head measurements.

$$\ln R = \frac{h_o - h_1}{h_2 - h_1} \ln r_2 - \frac{h_o - h_1}{h_2 - h_1} \ln r_1 \text{.....(4.52)}$$

4.1.10 Theis Solution For Transient Flow In A Fully Penetrating, Confined Aquifer:

Theis theory lets us evaluate the behavior of a well pumping in a confined aquifer that is under transient (that is, nonsteady-state) conditions. The flow equation describing hydraulic head in a confined aquifer (Figure 9.4) can be written in polar coordinates as

$$\frac{\delta^2 h}{\delta^2 r} + \frac{1}{r}\frac{\delta h}{\delta r} = \frac{S}{T}\frac{\delta h}{\delta t} \text{.....(4.53).}$$

where 'h' is the hydraulic head, 'r' is the radial distance from a pumped well to an observation well, 't' is time since the pumping started, S is the storativity of the aquifer, and T is the transmissivity of the aquifer. The following initial and two boundary conditions apply to this problem

$h(r, 0) = h_0$ & $h(\infty, t) = h_0$

$$\lim_{r \to 0} \left(r \frac{\partial h}{\partial r} \right) = \frac{Q}{2\pi T} \text{.....(4.53a)}$$

In words, the first condition means that at time zero and any distance from the well, the head is equal to the initial head, h_o. The second condition means that at an infinite radius (one boundary) for all time the hydraulic head is fixed at ho. The third condition provides a constant withdrawal rate at the pumping well (another boundary).

The solution of Eq. (9.12) was first derived by Theis (1935) and is expressed as

$$h_0 - h = s = \frac{Q}{4\pi T} W(u) \text{.....(4.54)}$$

Where Q is the pumping rate and T is the transmissivity of the aquifer. The well function W(u) and the dimensionless variable u are expressed as:

$$W(u) = \int_x^\infty \frac{e^{-\gamma}}{y} dy = -0.577216 - \ln(u) + u - \frac{u^2}{2!2} + \frac{u^3}{3!3} - \frac{u^4}{4!4} + \cdots \text{.....(4.55)}$$

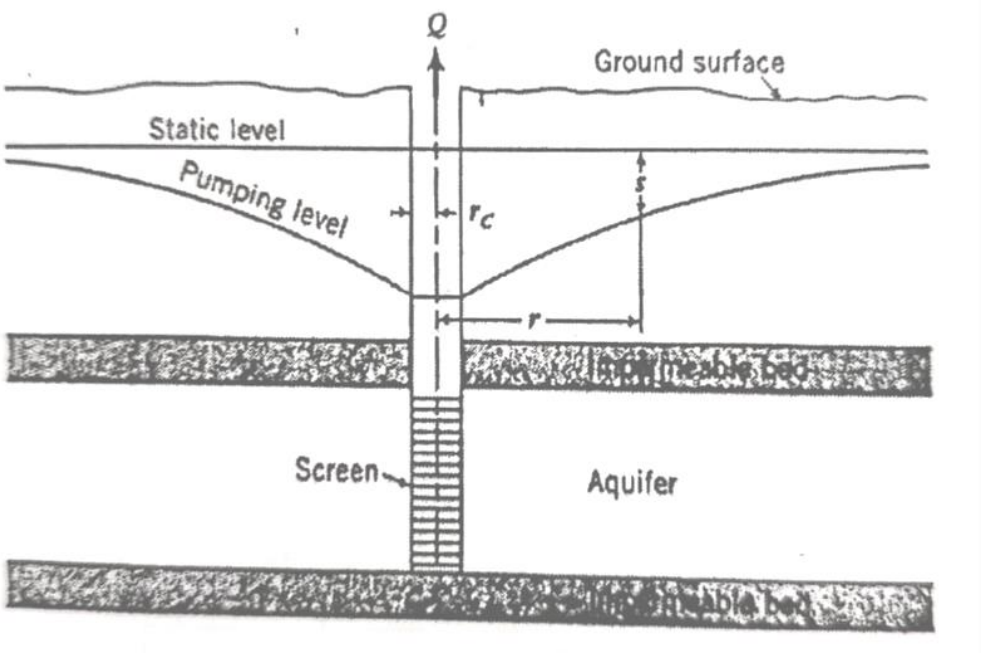


Figure 4.17 Ullastration of a nonleaky, confined aquifer being pumped by a fully penetratintg well (from Reed, 1980).

and

$u = \frac{r^2 S}{4Tt}$……..(4.56)

Even though $W(u)$ is a complicated function, it can be evaluated by using well function tables (Table 9.2) or by approximating computer programs.

Table 4.4.: Values of ($\boldsymbol{u}$) for the different values of $\boldsymbol{u}$

$\boldsymbol{u}$	**1.0**	**2.0**	**3.0**	**4.0**	**5.0**	**6.0**	**7.0**	**8.0**	**9.0**
× **1**	0.2194	0.1489	0.0130	0.0038	0.0011	0.0004	0.0001	0.0000	0.0000
× 10^{-1}	1.8229	1.2227	0.9057	0.7024	0.5598	0.4544	0.3738	0.3106	0.2602
× **10^{-2}**	4.0379	3.3547	2.9591	2.6813	2.4679	2.2953	2.1508	2.0269	1.9187
× 10^{-3}	6.3315	5.6394	5.2349	4.9482	4.7261	4.5448	4.3916	4.2591	4.1423
× **10^{-4}**	8.6332	7.9401	7.5348	7.2472	7.0242	6.8420	6.6879	6.5545	6.4368
× 10^{-5}	10.9357	10.2428	9.8372	9.5494	9.3264	9.1440	8.9899	8.8564	8.7386

Source: From Wenzel(1942)

The Theis solution is based on the following assumptions:

- The pumping well is fully penetrating, with a constant discharge rate. intinitesimal diameter, and negligible storage.

- The aquifer is confined, infinite in extent, homogencous, and isotropic.
- All water pumped by the well comes from the storage and is discharged instantaneously with the decline in head.

Prediction of Drawdown and Pumping Rate Using the Theis Solution:

The drawdown in an observation well at some future time can be calculated directly using Eq. (9.13) for known hydraulic parameters. For other problems, we might need to know what pumping rate provides a specificd drawdown at a fixed place and time in the future. This calculation requires transforming the Theis equation into the following form.

$Q = \frac{4\pi Ts}{W(u)}$.....(4.57)

4.1.11 Theis Type-Curve Method:

Another important use of the Theis solution is in determinating the transmissivity and storativity from data collected from an aquifer test. A variety of aquifer testing approaches are available. We begin here with the so-called type-curve matching technique, which is widely used. The test data are a series of drawdown values in an observation well, each matched with a time since pumping began. The approach involves plotting the field data on one graph, which is overlain on a type curve plotted at the same scale. Here are the details:

1 Create the type curve by plotting the well function $W(u)$ versus $1/u$ on $\log - \log$ graph paper (Figure 9.5). Usully, you can buy a copy of this curve.

2 Define a match point on the type carve. This match point only serves as a reference and cas be located anywhere on the graph. However, the math works oat best if you choose a match point with "simple" coordinates like $W(u) = 1$ and $1/u = 10^5$, 10^2, or 10 .

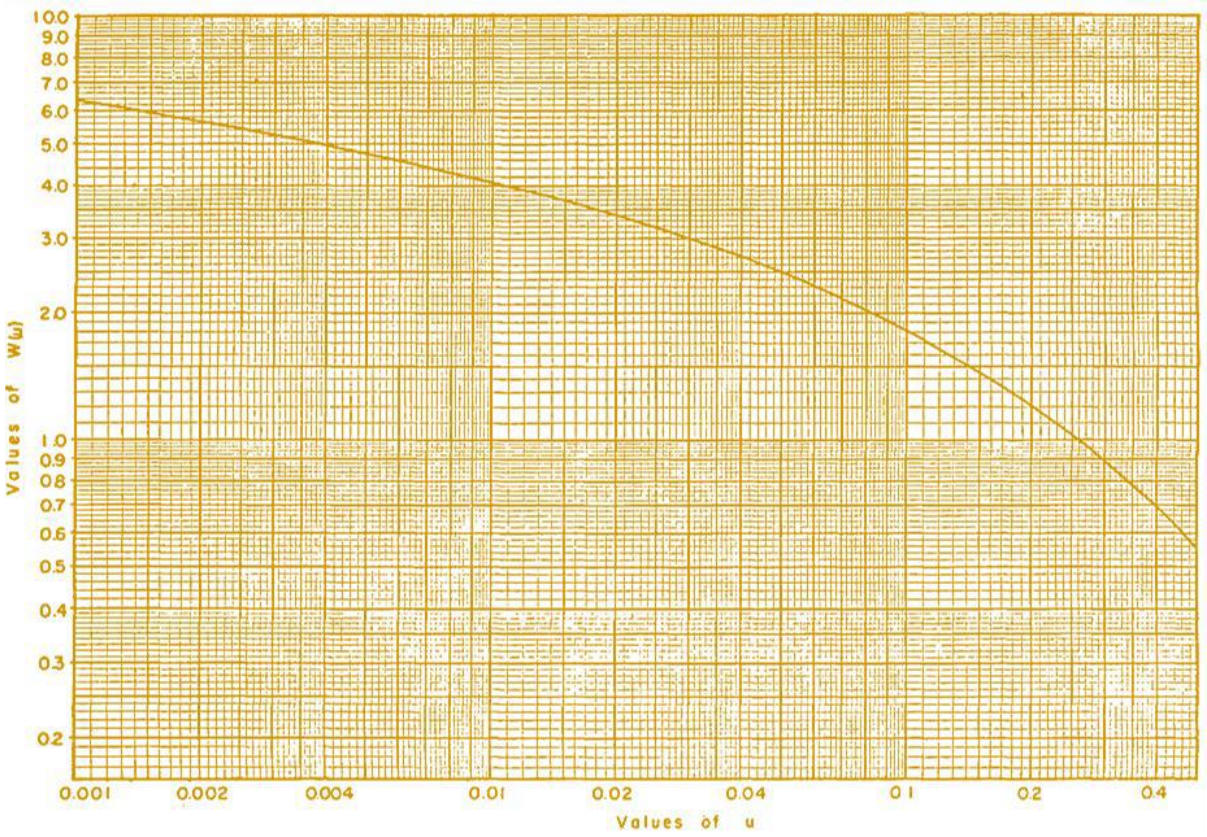


Fig. 4.18.: Plot of ($\boldsymbol{u}$) versus $\boldsymbol{u}$, known as a **type curve** (Bruin & Hudson Jr., 1961)

3.Prepare a transparent overlay with drawdown (s) plotted versus time (t) on log-log graph paper. This graph paper must be the same as the type carve. This step is where you use the set of field data from the observation well.

4. Superimpose the transparent graph of the field data on the type curve. Adjust the field curve until the collection of field points appears to fall along the type curve underneath. You must keep the axes of the two graphs parallel to each other.

5. Mark the point on the field curve that exactly corresponds with the match print on the type curve underneath. Now you will have points marked on both graphs with coordinate W(u),1/u,and s(t),t.

These pairs of values will be substituted in step 5.

6. Calculate T and S using the following equations.

$T = \frac{Q}{4\pi s} W(u)$……..(4.58)

And

$S = \frac{4Ttu}{r^2}$.....(4.59)

La the case of Eq. (9.17). Q is known from the purup-test dala, W(1) is the conrdintahe vatoc of the match point on the type curve. and s is the coordinate value for the match point on the carve of the field data. In the case of Eq. (9.18), T is known from the previous calculation. r is known from the setup of the aquifer test, and $l/$u and t are the match-point coordinates obtained via curve matching. Here is an example that illustrates these steps.

COOPER-JACOB STRAIGHT-LINE METHOD

Using the Theis solution (Eq, 9,13) is complicated by the fact that it contains the function using the Theis solution $W(u)$. which is an exponential integral. The value of $W(u)$ is the sum of an infinite series (see Eq 9.14) which we normally evaluate using the table of the well functions .However, when the values of u are small, less than 0.01 the higher order terms of the infinite series are negligible and can be ignored Cooper-Jacob's assumption, drawdown is calculated as

$s(t) = \frac{Q}{4\pi T}(-0.577216 - \mathrm{lm}(w)) = \frac{2.30}{4\pi T}\log\frac{2.25Tt}{r^2S}$.....(4.60)

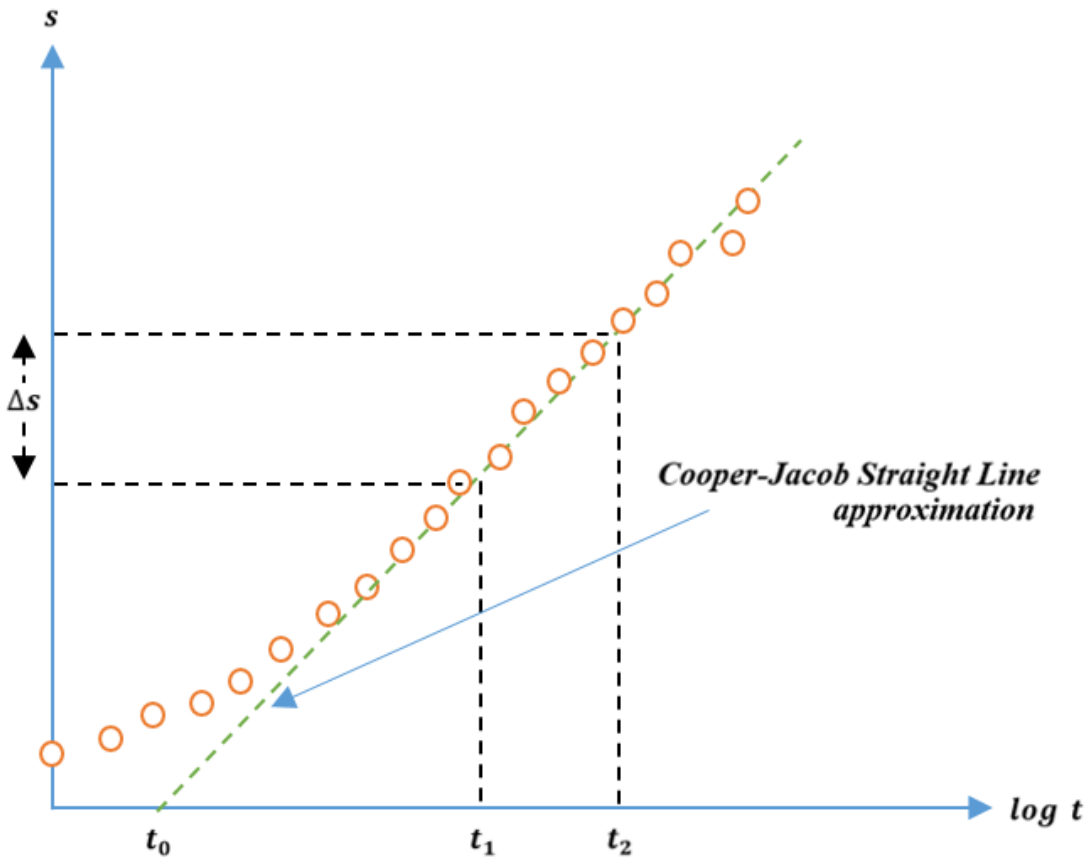


Fig. 4.19.: Cooper-Jacob Approximation using Time-Drawdown Method

The by a result of this simplification is that integral expression in the Theis solution is replaced much simpler function. It can be evaluated using a calculator without the need for the table of well function.

Another benefit of the Cooper and Jacob (1946) modification of the Theis equation is that it leads to a simple, graphical approach to evaluating aquifer test data. If drawdown/time data are plotted as drawdown versus the logarithm of time, the Cooper-Jacob theory predicts that the data will fall along a straight line. By extracting two numbers from the graph, we can solve equations to determine transmissivity and storativity. Here is a summary of the steps involved, followed by an example.

1. Plot drawdown versus time on semi-log graph paper, with time on the x-axis as a logarithmic scale and drawdown on the y-axis as an arithmetic scale. Often, zero drawdown is at the top of the y-axis.

2. Fit a straight line through the data points. If there is difficulty, use the later-time points.

3. Select two points (t_1, s_1 and t_2, s_2) on the line. The equation that is needed can be derived from Eq. (9.19) by writing one equation in terms of s2 and one equation in terms of s_1 and subtracting them from each other. After some manipulation, the resulting equation is

$$\Delta s = s_2 - s_1 = \frac{2.3Q}{4\pi}\log\frac{t_2}{t_1} \text{.....(4.61)}$$

4 . Choose t_1, and t_2, one log cycle apart, for example t_1 = 10 minutes and t_2= 100 minutes, to give As or drawdown per log cycle. This choice simplifies the math. For example, with t_1= 10 minutes and t_2 = 100 minutes, $log\frac{t_2}{t_1}$= log(100/10) = 1. The log term in Eq. (9.20) becomes one, and the equation simplifies to

$$T = \frac{2.3Q}{4\pi\Delta s} \text{.....(4.62)}$$

where Δs is the drawdown per log cycle. All the terms on the RHS of Eq. (9.21) are known, so it is a simple matter to calculate transmissivity.

5. Find the value of to on the graph by extending the straight line to intersect the line of zero drawdown (s = 0) The corresponding time (t_0) is in effect the time that it takes for the cone of depression to reach the observation well. With this value of to, all values on the RHS of Eq. (9.21) are known, and storativity can be calculated as

$S = \frac{2.25Tt_0}{r^2}$……(4.63)

You can derive Eq. (9.22) by setting the drawdown in Eq. (9.19) to zero and rearranging terms.

6. The final step is a final check to make sure that the Cooper-Jacob simplification applies to this problem or in other words whether u = r ^ 2 * S / (4Tt) < 0.01 . Hopefully, the check will be successful and the problem solved.

DISTANCE-DRAWDOWN METHOD

he Cooper-Jacob simplification is also useful in determining transmissivity and storativity values in aquifer tests if water levels are measured in two or more observation wells at the same time. For example, assume that two observation wells are located at distances r_1 and r_2 from the pumping well. Knowing the drawdowns at these two wells are s_1 and$s_2$respectively, at some time t, we can write this equation based on Eq. (9.19):

$s_1 = \frac{2.3\mathrm{Q}}{4\pi T}\log\frac{2.25\mathrm{T}t}{r_1^2 S}$……(4.64)

and

$s_2 = \frac{2.3Q}{4\pi T}\log\frac{2.25Tt}{r_2^2 S}$…….(4.65)

The combination of Eqs. (9.23) and (9.24) yields

$s_1 - s_2 = \frac{2.3\mathrm{Q}}{2\pi T}\log\frac{r_2}{r_1}$……(4.66)

The procedures for determining the transmissivity the distance-drawdown method are as follows: and storativity for an aquifer using the distance-drawdown method are as follows:

1. For a selected time, plot the drawdown and distance information for the observation wells on semi-log graph paper. Distance is plotted as a logarithmic scale on the x-axis, and drawdown is plotted on a linear scale on the y-axis.

2. Fit a straight line through the data points.

3. Select two points (r_1, r_2) on the line, one log cycle apart, and determine the drawdown Δs. The transmissivity is calculated by

$T = \frac{2.3Q}{2\pi(\Delta s)}$…….(4.67)

4. Extend the straight line to s = 0 and determine the distance r_0. The storativity is calculated by

$$S = \frac{2.25Tt}{r_0^2} \text{.....(4.68)}$$

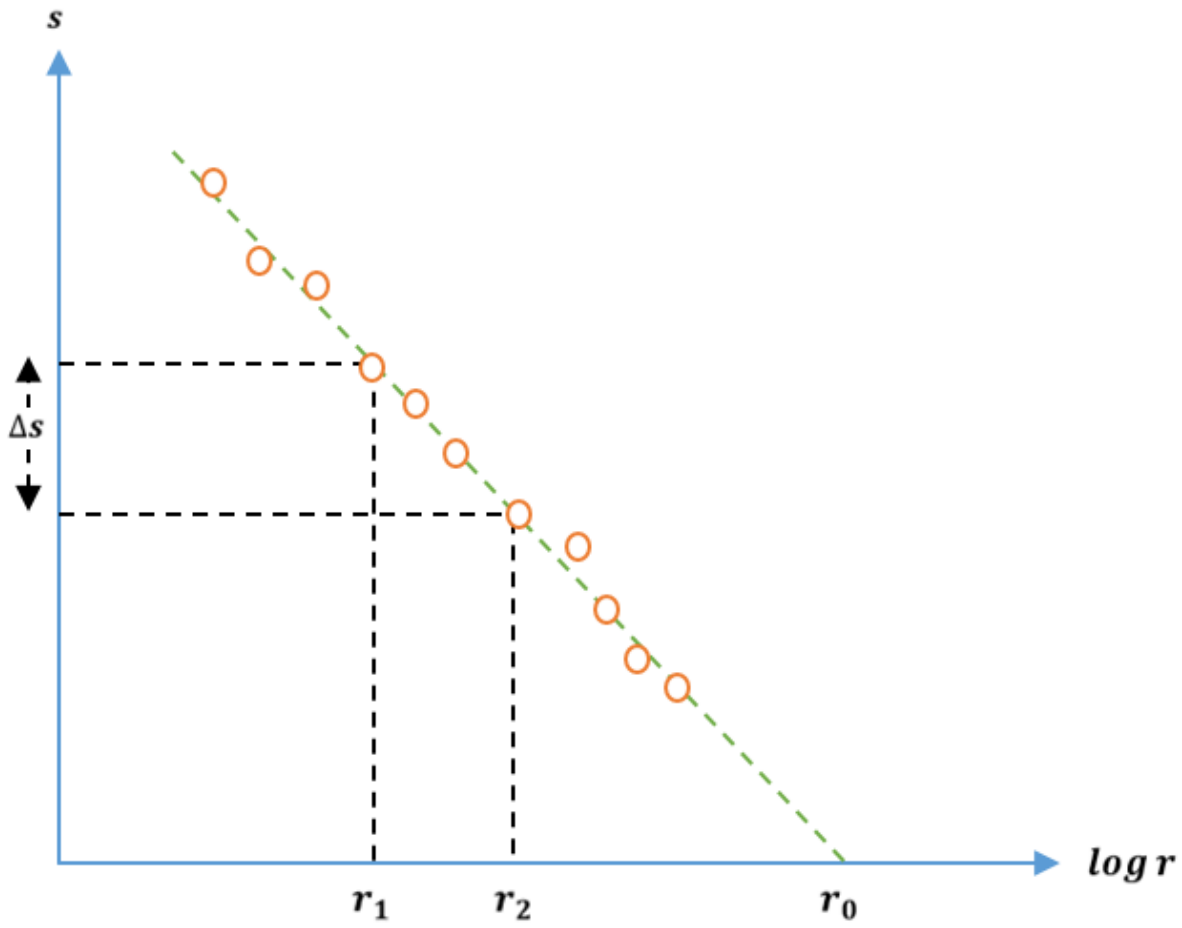


Fig. 4.20.: Cooper-Jacob Approximation using Distance-Drawdown Method

4.1.12 Estimating "T" And "S" Using Recovery Data (Theis, 1935)

If pumping of a well is halted, theory predicts that the water level in the aquifer will return to its prepumping level, h_o. Water-level data obtained during this recovery phase of a test provides a basis for determining the transmissivity of the aquifer. The residual drawdown during the recovery period for a confined aquifer is expressed as

$$s' = \frac{Q}{4\pi T}\left[\int_u^\infty \frac{e^{-u}}{u}du - \int_u^\infty \frac{e^{-u'}}{u'}du'\right] \text{.....(4.69)}$$

Where

$$u = \frac{r^2 S}{4Tt} \text{.....(4.70)}$$

and

$$u' = \frac{r^2 S}{4Tu'} \text{.....(4.71)}$$

Where t is the time since pumping starts, r' is time since pumping stops, and s' is the residual drawdown. Because recovery measurements are made in the pumped well or in a nearby observation well, the radius to the measurement point, r, is typically small. A small r usually leads to a small value w', which enables us to take advantage of the Cooper-Jacob simplification. Under the Cooper-Jacob assumption, Eq. (9.28) reduces to

$$s' = \frac{2.3Q}{4\pi T} \log\left(\frac{t}{t'}\right) \text{.....(4.72)}$$

and transmissivity can be determined as

$$T = \frac{2.3Q}{4\pi s'} \log\left(\frac{t}{t'}\right) \text{.....(4.73)}$$

The procedure for determining transmissivity using recovery data is as follows:

1. Plot the residual drawdown (s') on an arithimetic scale versus the time ratio (t/t') on a logarithmic scale.

2. Choose two points on the graph. Again it helps to select the two points one log cycle apart.

The transmissivity is obtained by

$$T = \frac{2.3Q}{4\pi \Delta s'} \text{.....(4.74)}$$

where $\Delta s'$ is the change in residual drawdown over one log cycle (t / (t'))

Storativity can be calculated if the recovery data are collected in an observation well rather than the pumping well. The drawdown (s_p) when the pump is turned off at time (t_p) is expressed as

$$sp = \frac{2.3Q}{4\pi T} \log \frac{2.25T\text{tp}}{r^2 S} \text{.....(4.75)}$$

Once T is known, the storativity is obtained by

$$S = \frac{2.25Tt_p}{r^2} 10^{-\frac{4\pi Tsp}{2.30}} \text{.....(4.76)}$$

4.1.13 Response Of An Unconfined Aquifer To Pumping:

The response of an unconfined aquifer to pumping is complicated. Once a cone of depres sion forms, it naturally decreases the aquifer thickness and transmissivity because the upper boundary of the aquifer is the water table. Also, the way in which water comes out of storage in the aquifer changes with time. At early time, when the well is first turned on, water is released from storage due to compression of the matrix and expansion of the water. This response is the same Theis behavior that applies to confined aquifers (Chapter 9). Thus, early-time/drawdown data, plotted on log-log graph paper, follow the Theis-type curve . Storativity values would be comparable to those for confined aquifers, 10^{-4} or 10^{-5}

As pumping continues, water comes from the slow gravity drainage of water from pores as the water table falls near the well. The pattern of drawdown depends on the vertical and horizontal hydraulic conductivity and the thickness of the aquifer. Once this delayed drainage begins, drawdown data deviate from the Theis curve. The drawdown is less than expected, resembling the pattern of drawdown in a leaky aquifer . Eventually, the contribution of water from delayed drainage ceases. Flow in the aquifer is mainly radial, and drawdown/time data again fall on a Theis-type curve . The storativity of the aquifer now is the same as the specific yield (Sy). The specific yield is the ratio of the volume of water that drains from a rock or sediment by gravity to the volume of the rock or soil. The curve-fitting approach developed in this chapter for interpreting aquifer test data requires the ability to recognize these differing aquifer responses

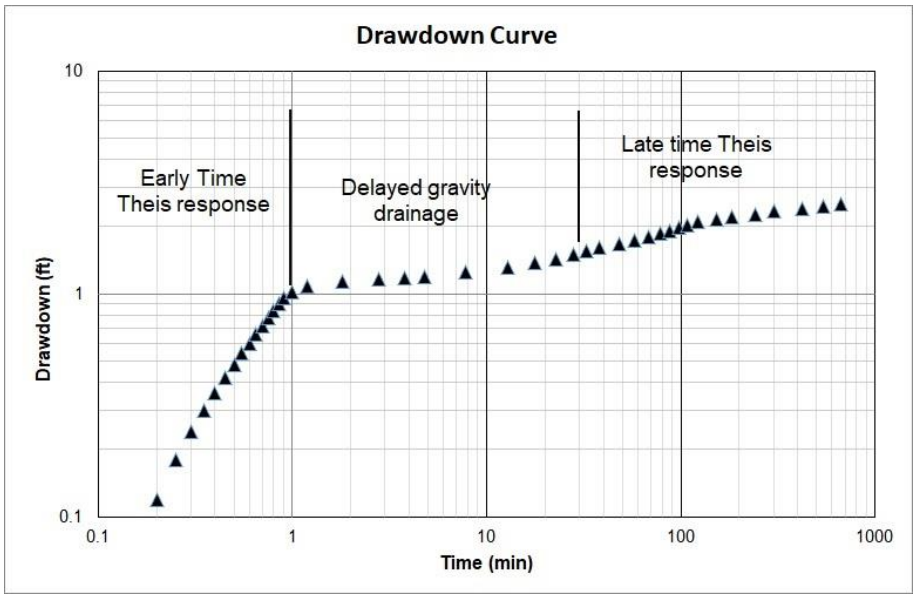


Figure. 4.21.: An example of the characteristic S shaped drawdown curve obtained from a test wth an unconfined aquifer

4.1.14 Calculation Of Drawdowns By Correcting Estimates For A Confined Aquifer:

Because of the intricacies in the response of an unconfined aquifer to pamping, the theory developed for confined aquifers is not generally transferable. However, if the point of interest is far away from the pumped well, one can simply apply confired-aquifer theory without too much error. A slightly more sophisticated approach is to e. culate drawdown assuming the aquifer to be confined and correcting the drawdown value with the following equation:

$S=b-(b-2s'b)^{1/2}$ ……(4.77)

where s is the drawdown for the unconfined aquifer, s' is the drawdown for the equivalent confined aquifer, and b is the original thickness of the aquifer.

Calculation of drawdown by correcting the estimate for a confined aquifer was done using equation 1.

$$s' = s - \frac{s^2}{2b} \quad \text{……..(4.78)}$$

Where, *s* is the drawdown for the unconfined aquifer and s' is the drawdown for the equivalent confined aquifer.

4.1.15 Determination Of Hydraulic Parameters Using Distance- Drawdown Data:

The following methodology has been adopted to determine the hydraulic parameters using the Distance Drawdown Method by taking the following steps:

- Calculate the corrected drawdown using equation (1)
- Plot corrected drawdowns against *r* on semi-log graph paper
- Approximate the curves versus log(*t*) with a straight line
- Determine the hydraulic parameters using the following equations (2-4):

a) Transmissivity (*T*)

$$T = \frac{2.3Q}{4\pi\Delta s} \text{……(4.79)}$$

b) Specific Yield /Storativity (*S*)

$$S_y = \frac{2.25Tt_{0y}}{r^2} \quad \text{.....(4.80)}$$

c) **Radius of Influence** $Q = \frac{2\pi T s_d}{ln\left(\frac{R}{r}\right)}$.....(4.81)

4.2 VERTICAL ELECTRICAL SOUNDING (VES) SURVEY

VES: Vertical Electrical Resistivity (VES) survey was used to find out the soil profile and depth of water tables/piezometer by using SSR-MP-ATS Resistivity Meter which gives resistance dataset. The type of soil, depth of aquifers and sand layers were also obtained by VES survey. For analysis of resistivity data Schlumberger array was used for analysis of depth variation of soil strata. The resistivity data is analyzed using ZONDIP1D software to find out the true resistivity of each layer and the layer thickness to determine the soil characteristics.

Schlumberger Configuration: In Schlumberger configuration, four electrodes are used and kept in a similar line to Wenner but the spacing between outer electrodes has been kept large compared to inner electrodes spacing (usually more than four to five times). For each measurement, the current electrodes are moved but potential electrodes are kept at the same locations. The apparent resistivity for this configuration is computed with the formula [Ahilan et al., 2011] and shown in Figure.

$$K = \frac{\pi}{a}\left[\left(\frac{L}{2}\right)^2 - \left(\frac{a}{2}\right)^2\right] \text{.....(4.82)}$$

Apparent Resistivity (ρ) = K × resistance (R)..... (4.83)

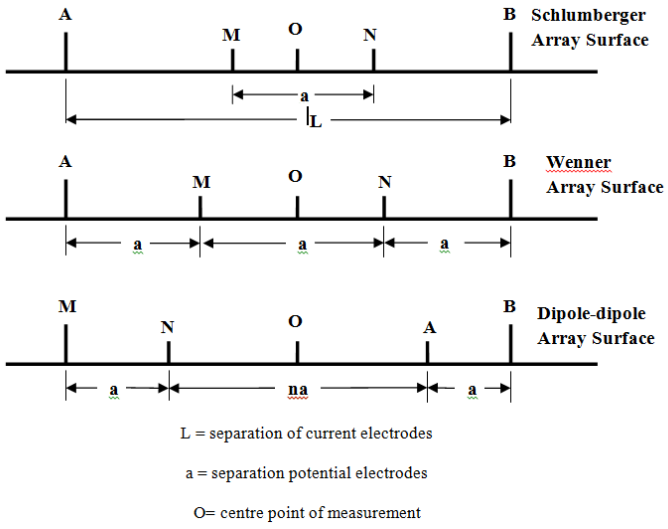


Figure 4.22: Different types of arrays used in resistivity sounding

The interpretation of the VES data was conducted using the Resistivity software ZONDIP1D which produces the resistivity model (resistivity, thickness and depth) by fitting the aquifer data collected from the field with the least RMS-error between the observed and calculated resistivity. The variation of resistivity of the observed and the modelled resistive layer with depth at each point is plotted and shown below.

For each VES Sounding, the distance between potential electrodes MN was kept fixed at 2 m and the distance between current electrodes was increased gradually from 1 m to 52 m (AB/2) with a step increase different distance. The output resistivity data for each AB/2 distance was collected. Analysis of collected resistance was done by using ZOND1D software and generated a tabular form of apparent resistivity and depth.

Total transverse resistance and total longitudinal conductance:

The total transverse resistance (T) and the total longitudinal conductance (S) are used to acknowledge the projected areas of well groundwater potential. It has a direct relationship with transmissivity where high T values show the high transmissivity values of the aquifer zones. High S values usually indicate the thick succession and it has importance in groundwater potential.

The total transverse resistance (T) for each geo-electric sounding (VES) station is computed below in tabular form from the relation:

$$T = \Sigma\, h_i\rho_i = h_1\,\rho_1 + h_2\,\rho_2 + \ldots + h_n\rho_n \quad (4.84)$$

where T is the total transverse resistance, h_i is the thickness of the ith layer and $\rho_i$is the resistivity of the ith layer.

The total longitudinal conductance (S) for each of geo-electric sounding (VES) stations is computed below in tabular form from the relation.)

$$S = \Sigma\,(h_i / \rho_i) = h_1 / \rho_1 + h_2 / \rho_2 + \ldots + h_n / \rho_n \quad (4.85)$$

where S is the total longitudinal conductance, h_i is the thickness of the i^{th} layer and ρ_i is the resistivity of the i^{th} layer.

4.3 THEORY OF PUMPING TEST:

The basic concept of a pumping test is very simple: water is abstracted (removed by pumping or bailing) from a well or borehole, thus lowering the water level. The water level in the abstraction borehole and the pumping rate are monitored over time, along with various other parameters if possible (such as water levels in observation boreholes). The way in which the water levels respond to the pumping is then analysed to derive information about the performance characteristics of the borehole and the hydraulic properties of the aquifer.

A pumping test consists of pumping groundwater from a well, usually at a constant rate, and measuring the change in water level (drawdown) in the pumping well and any nearby wells

(observation wells) or surface water bodies during and after pumping (see Figure 1). Pumping tests can last from hours to days or even weeks, depending on the purpose of the pumping test, but traditional pumping tests typically last for 24 to 72 hours.

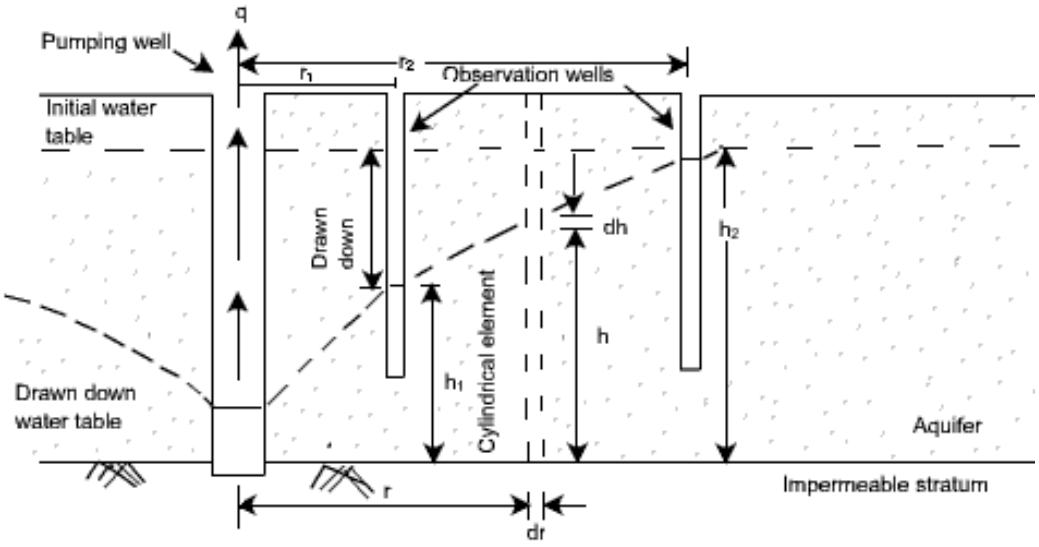


Figure 4.23 : This figure shows the impact of a pumping well on the water table and a neighbouring well (observation well) in an unconfined aquifer

Why do we undertake pumping tests?

Pumping tests can be undertaken for a wide variety of reasons, including the following:

- To determine the reliable long-term yield (or 'safe' yield) of a borehole, and therefore whether or not the borehole can be regarded as a 'success,' and how many people it will be able to supply.
- To assess the hydraulic performance of a borehole, usually in terms of its yield-drawdown characteristics. How much drawdown does it take to yield a certain amount of water?
- To derive the hydraulic properties of the aquifer. Pumping tests are the classic (and perhaps the only) way to derive in situ aquifer hydraulic properties, such as transmissivity and the storage coefficient, or to reveal the presence of any hydraulic boundaries.
- To test the operation of the pumping and monitoring equipment, to make sure that everything is working safely and efficiently, and if applicable, to confirm that the contractors have done their job properly.
- To provide information on water quality. Is the water quality suitable for the intended use? Is it stable in the long term? Are there likely to be any problems such as drawing in saline or polluted water after extended periods of pumping?

- To optimize operational pumping regimes (especially from multiple-borehole sources), including selecting the most suitable pumping plant for long-term use, and estimating probable pumping and/or treatment costs.

The goal of a pumping test, as in any aquifer test, is to estimate hydraulic properties of an aquifer system. For the pumped aquifer, one seeks to determine transmissivity, hydraulic conductivity (horizontal and vertical) and storativity (storage coefficient). In layered systems, one also uses pumping tests to estimate the properties of aquitards (vertical hydraulic conductivity and specific storage). Pumping tests can identify and locate recharge and no-flow boundaries that may limit the lateral extent of aquifers as well.

Types of pumping test:

There are many different types of pumping test from which to choose. The main types that are applicable to the situations faced by WatHab engineers are as follows:

1. step test: Designed to establish the short-term relationship between yield and drawdown for the borehole being tested. It consists of pumping the borehole in a series of steps, each at a different discharge rate, usually with the rate increasing with each step. The final step should approach the estimated maximum yield of the borehole.

2. Constant-rate test: Carried out by pumping at a constant rate for a much longer period of time than the step test, and primarily designed to provide information on the hydraulic characteristics of the aquifer. Information on the aquifer storage coefficient can be deduced only if data are available from suitable observation boreholes.

3. Recovery test: Carried out by monitoring the recovery of water levels on cessation of pumping at the end of a constant-rate test (and sometimes after a step test). It provides a useful check on the aquifer characteristics derived from the other tests but is valid only if a foot-valve is fitted to the rising main; otherwise water surges back into the borehole.

Preparations for test pumping

Introduction Before commencing any pumping test, there are certain basic preparations that should be made. These include gathering information about the borehole or well that is about to be tested. The outcome of the preparations may influence the choice of test and will certainly increase the value of the results obtained from the test.

Basic monitoring equipment:

The two parameters that must be measured in any pumping test are the water level in the pumped borehole and the rate at which water is being abstracted (pumped or bailed). The basic equipment necessary for monitoring these two parameters is as follows

Monitoring water levels :

The hand-held water-level monitor, commonly known as a “dipper,” is the most practical, robust and easily available method of monitoring water levels in boreholes and wells. The dipper probe is lowered down the borehole, and when it reaches the water surface, an electrical circuit is completed and a ‘bleep’ is heard. The water level is then read off a graduated tape, usually to a resolution of the nearest centimetre. The water level is typically recorded in metres below a local measuring datum, such as the lip of the borehole casing. Manual dipping is widely trusted as a reliable and relatively trouble-free way of obtaining water-level data, but it is not without its problems, for instance.

- Different people visiting the same site can inadvertently use different local datums for taking the reading. If they do not record this fact, there may be confusion when comparing readings in the future
- The graduated dipper tape can suffer from stretch due to age, temperature or misuse, introducing a systematic inaccuracy, especially if different dippers are use
- . If the water level is falling or rising quickly, as during the early stages of a pumping test, it can be difficult to take manual readings fast enough, although this problem improves with practice.
- It can be difficult to get a ‘clean’ water-level reading from the borehole, especially if there is water cascading down the side of the borehole, or there is turbulence at the water surface
- .The dipper can become stuck, entangled or wrapped around the pump, rising main, electrical cables, or other items down the borehole. This can be avoided by the use of a dip tube (an open-ended plastic tube installed in the borehole specifically for the dipper to go down), which also solves the problem of cascading water and turbulence. Picture 3: Pressure-transducer installation Richard Boak The main alternative to manual dipping is to install a pressure transducer in the borehole. The transducer is placed in a known position down the borehole (below the water level) and it measures the pressure at that point. This information can be used to deduce the height of the water above that point, and therefore the water level in the borehole. Transducers (with built-in dataloggers) have an obvious advantage: they can be left unattended for long periods, while still taking frequent water-level readings. In practice, however, they can pose the following problems:
- Transducers are expensive compared to manual dipping, and they cannot always cope with rough field conditions and high temperatures.
- Transducers are manufactured to cope with different pressure ranges, and if the wrong type of transducer is used, it may be damaged and the data corrupted.
- If the transducer or datalogger malfunctions, or the battery runs out, the data obtained since the last download may be lost, and the test may have to be repeated.

Monitoring pumping rates:

There are many methods of measuring pumping rates, of which the most common, or the ones most likely to be of uses are as follows:

Bucket and stopwatch: The simplest method of measuring relatively low pumping rates is to use a bucket and a stopwatch. Arrangements are made for the discharge from the pump to flow freely into a bucket of known volume, and the time taken for the bucket to fill is recorded. The flow rate is then calculated by dividing the volume of the bucket by the time taken to fill it. For this method to be precise, it should take a minimum time of about 100 seconds to fill the bucket. If necessary, use a larger container of known volume, such as an oil drum.

Flow meters: Where more sophisticated equipment is available, pumping rates can be measured using flow meters, of which there are various types. Shown on the right is the flow meter supplied with the ICRC's standard test-pumping kit. This uses spring-loaded pistons that are deflected by the flow of water, and the flow rate is read off the graduated scales. It is important to double-check the flow rate by using another method, to operate the gauge correctly, and to keep the equipment in good condition.

Other equipment available

Before choosing the type of test to conduct, WatHab engineers should establish what equipment is available, practicable or affordable. In addition to the water-level and flow-monitoring equipment described above, potential equipment includes the following:

- Motorized pump: Commonly an electrical submersible pump. Check whether or not a suitable power supply is available; many submersible pumps require a threephase power supply, so ordinary mains electricity is not always suitable.
- Generator: Necessary if a motorized pump is being used in remote locations, or if the local electricity supply is unsuitable or unreliable. Make sure that there is sufficient fuel available for the planned length of the test.
- Rising main: To carry the water up the borehole from a submersible pump; it can be made of flexible tubing or lengths of rigid pipe connected together.
- Manually-operated valves: Installed between the rising main and the discharge pipes, to control the pumping rate if the pump is operated at a fixed speed.
- Discharge pipes: To carry the water far enough away from the borehole so that it does not recirculate (that is, flow back down into the borehole, or quickly soak into the ground and affect the groundwater levels close to the borehole being tested).
- Water-quality monitoring equipment: See separate discussion below about water-quality monitoring.
- Surface water flow-gauging equipment: It is sometimes necessary to monitor the flow in a nearby river or stream to establish whether or not the groundwater abstraction is

affecting the flow or causing infiltration from the river (which may represent a health risk because of poor surface-water quality).

4.4 RECOVERY TEST:

The recovery test is not strictly a pumping test, because it involves monitoring the recovery of the water level after the pump has been switched off. We have already come across it in the final stages of the procedures for undertaking step tests and constant-rate tests. Recovery tests are valuable for several reasons:

- They provide a useful check on the aquifer characteristics derived from pumping tests, for very little extra effort – just extending the monitoring period after the pump has been switched off.
- The start of the test is relatively 'clean.' In practice, the start of a constant-rate test, for example, rarely achieves a clean jump from no pumping to the chosen pumping rate. Switching a pump off is usually much easier than starting a pump, and the jump from a constant pumping rate to no pumping can be achieved fairly cleanly.
- Similarly, recovery smoothes out small changes in the pumping rate that occurred during the pumping phase, and there is no problem with well losses from turbulent flow. This results in more reliable estimates of aquifer properties when the recovery data are analysed.
- The water levels in the borehole are easier to measure accurately in the absence of turbulence caused by the pumping (especially in the early stages of the test, when water levels are changing quickly). Some people find that it is easier to take readings quickly with a dipper when the water level is rising than when it is falling.
- Recovery tests represent a good option for testing operational boreholes that have already been pumping at a constant rate for extended periods. In these cases, the recovery test can be performed when the pumps are first switched off, followed by a constant discharge test when the pumps are switched back on again.

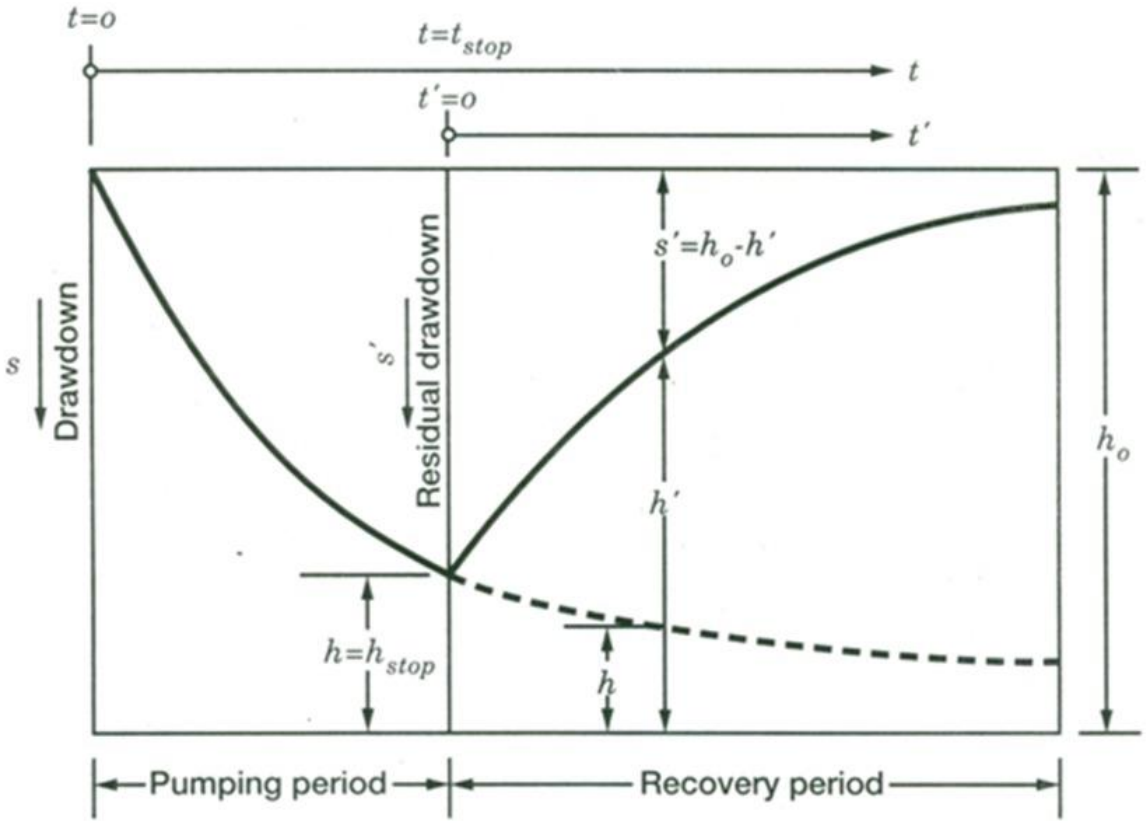


Figure 4.24: Drawdown and recovery curves in a pumping well.

Recovery-test procedure

The procedure for undertaking a recovery test is as follows:

1. Switch the pump off and start the stopwatch at the same time.

2. Measure the water level in the borehole in the same way as for the start of the pumping test, that is, every 1 minute for the first 10 minutes, then every 2 minute until 30 minutes have elapsed, then every 5 minutes until 2 hours have elapsed. After 2 hours, observe how quickly the water level is still rising, and decide an appropriate frequency for water-level readings until the end of the test. If the water level is rising very slowly, then a reading every 30 minutes or even every hour may be sufficient. If you miss the planned time for a water-level reading, write down the actual time the reading was taken. Record all the readings on the standard form. Make sure the same datum is used for measuring water levels as for the pumping phase.

4.5 Water GEMS -WATER DISTRIBUTION NETWORK TOOL:

Water GEMS from Bentley Systems helps engineers to model, design and analyze complex pressurized piping systems. This software has a powerful graphical interface (both in Stand-Alone complex and AutoCAD mode) makes it easy to quickly layout network of pipes, tanks, pumps, and more.In industries, this network simulation software is used to

- perform steady-state analyses of water distribution systems with pumps, tanks, and control valves.
- perform extended period simulations to determine the piping system's response in varying supply and demand schedules.
- perform water quality simulations to determine the water source and age, or track the growth or decay of a chemical constituent throughout the network.
- perform Fire Flow Analysis on the system to determine how your system will behave under extreme conditions.
- Create multiple sets of hydraulic, physical property, operational, initial setting, fire flow, cost, and water quality alternatives.
- Calibrate our design manually or with the assistance of the Darwin Calibrator, which utilizes the power of Genetic Algorithms.

Water GEMS is a super-set of Water CAD. Water GEMS is an efficient and versatile modeling software which helps to improve comprehension of system behavior, system reaction to operational strategies and system ability to meet future demands. Its flexible multi-platform workspace allows fire flow and water quality simulation, pipe flow and pressure analysis and energy cost analysis. Water GEMS capabilities include intelligent system management and planning for system reliability, optimization of operation (pumping strategies, system shutdowns and preventive maintenance to minimize disruptions) for efficiency of system and asset renewal or renovation support to ensure sustainability. Its features include prefixed model building, integration with multiple platforms, design and other operations. The unique aspect of Water GEMS is the data presentation mode which is highly appealing and comprehensible. Its versatility also allows presentation with variety of graphical tools. Water GEMS is not an open source software but is commercially available. Water GEMS software was built with a strong design algorithm to meet the criteria of precision in modelling, analysis and design of WDSs

WaterGEMS provide different software tool for-

- **Intelligent planning for system reliability:** The capability of water distribution network to adequately serve water to the consumers must be evaluated whenever system growth is predicted. WaterGEMS also identified problem area and plan capital investments.
- **Optimised operation for system efficiency:** Pragmatic modelling of complex operation of water distribution network is very difficult. But with help of WaterGEMS optimise pumping strategies, and plan shutdowns and routine operations to minimise disruption.
- **Reliable asset renewal decision support for system sustainability:** In a water distribution network, when we renew or replace water infrastructure, a lot of information regarding network we required and analysis is very complex and tedious. WaterGEMS tool is used as Pipe Renewal Planner makes very easier and fast by analysing and comparing a broad range of prioritise the renewal approach.

In our analysis we uses WaterGEMS V8i series for our case study area. The results obtained from WaterGEMS are used to compare the performance of water distribution network based on its consistency.

WaterGEMS uses the “Gradient Method” for solving the water distribution network. The solutions obtained from the WaterGEMS software are matched with the actual performance of the system. Cast Iron pipes are used in our water distribution network, hence C = 100 is adopted for the pipes.

4.6. DESIGN OF GROUNDWATER SYSTEMS

Introduction

In areas where groundwater is a source of public water supply, wellfields must be designed with a variety of constraints, such as pumpage from individual wells must not produce excessive drawdowns, the rates of pumpage must be sustainable, and the wellfield must be adequately protected from contaminants released into the groundwater from surrounding areas. The impacts of wellfields on the environment, such as reduced water availability to plants caused by lower water tables and decreased surface-water flows caused by well capture must generally be assessed. Many surface water management systems and water-treatment effluent-discharge systems can also be considered as groundwater systems since they are designed to provide groundwater recharge via infiltration (e.g., infiltration basins), and the performance of such systems must typically be assessed in terms of the capacity of the sub- surface matrix to percolate the design infiltration amounts, and the effect that the induced groundwater mounding will have on the performance of these systems.

Design of Wellfields

The objective of wellfield design is to determine the number and locations of production wells required to supply water at a specified rate. For large municipal and agricultural production wells, pumping-rate requirements are typically in the range of 30-250 L/s (500-4000 gpm). Small- and medium-size community water systems may depend on water wells that produce 5-30 1/s (100-500 gpm). Individual homes' domestic wells usually meet their needs with as few as 0.07-0.3 1/s (1-5 gpm), depending on local regulations.

A primary constraint in wellfield design is the maximum allowable drawdown in the aquifer caused by wellfield operation. To accommodate this constraint, the following design procedure is recommended:

Step1:

It Assume that each well in the wellfield causes a drawdown (at the well) equal to one- half the allowable drawdown, with the other half of the allowable drawdown caused by interference from other wells, boundary effects, and well losses. Determine the pumping rate, Qw, at each well that would cause a drawdown (at the well) equal to one-half the allowable drawdown. This can be done using the Theis equation, with a pumping time equal to 1 year.

Step:2

The number of wells required in the wellfield is equal to the required water-supply rate, Q,

divided by the pumping rate from each well, Q. This ratio is rounded upward to the nearest integer.

Step 3: Arrange the wells such that the total drawdown at each well does not exceed the allowable drawdown. Selecting the relative locations of the wells will depend on the individual site characteristics, such as property boundaries and existing pipe net- works, but the wells should generally be aligned parallel to and as close as possible to surface-water recharge boundaries, such as rivers and canals, and as far away as possible from impermeable boundaries. Typically, production wells are spaced at least 75 m (250 ft) apart (Walton, 1991).

4.7 MECHANICAL ANALYSIS OF SOIL

Introduction:

The properties of an aquifer material related to its storage function are its porosity and specific yield. Porosity is the ratio of the volume of voids or pores in a soil mass to its total volume. Shape, size and packing of the grains affect the porosity of granular material. The grain size distribution of the formation or aquifer material can be determined by conducting a mechanical analysis test in a nest of standard sieves with the coarsest on top and finest at the bottom, covered with lid on the top and bottom pan as receiver.

A representative sample, about 500-1000 gm, is taken in the laboratory by quartering, oven dried and an exact weight poured into the top sieve and covered with lid. The whole nest is shaken through a mechanical sieve shaker (hand operated /electrical) for about 5 minutes and the material retained on each sieve and bottom pan is accurately weighed. Percentage of material passing through each sieve gives a point on the grading curve.

Description:

Sieve diameter (d): In most cases a series of sieves is used for separation of sediment into various size grades provided particles are larger than 0.0625 (= 1/16) mm in diameter. Sieve openings are square in shape. Since a long particle with a very small cross sectional area can pass through a sieve, sieves classify particles on the basis of their least cross sectional area and thus this classification is not based purely on size. Sieve diameter “d” of a particle is the size of the sieve opening through which a given particle will just pass.

Size terms for particles: It is essential to standardize the terms related to particle size so that they could be used to convey definite ideas regarding the size. The sizes given in Table 1 are in terms of triaxial size (b) for boulders, cobbles and upto coarse gravel, and in terms of sieve diameters (d) for medium gravel to very fine sand; for the finer material sedimentation diameter is recommended.

Table 4.5: Grade Scale for Size Terms

Range in mm	Class name	Range in mm	Class name	Range in mm
4096-2048	Very Large Boulders	**1½**	**Coarse Sand**	**1– 0.5**
2048-1024	Large Boulders	**½¼**	**Medium Sand**	**0.5–0.25**
1024-512	Medium Boulders	**¼1/8**	**Fine Sand**	**0.25–0.125**
512-256	Small Boulders	**1/8–1/16**	**Very Fine Sand**	**0.125–0.0625**
256-128	Large Cobbles	1/16–1/32	Coarse Silt	0.0625–0.03125
128-64	Small Cobbles	1/32–1/64	Medium Silt	0.03125–0.015625
64-32	Very Coarse Gravel	1/64–1/128	Fine Silt	0.015625-0.007813
32-16	Coarse Gravel	1/128–1/256	Very Fine Silt	0.007813-0.003906
168	**Medium Gravel**	1/256–1/512	Coarse Clay	0.003906-0.001953
84	**Fine Gravel**	1/512–1/1024	Medium Clay	0.001953-0.000977
42	**Very Fine Gravel**	1/1024–1/2048	Fine Clay	0.000488-0.000224
21	**Very Coarse Sand**	1/2048–1/4096	Very Fine Clay	0.000224-0.000112

The **effective size** (***d_{10}***)isthesizecorrespondingto10%ofthematerialbeingfiner and 90%coarser(i.e., the size corresponding to p = 10%) and an index of fineness of the soil.

The ***uniformity coefficient*(*C_u*)** is the average slope of the grade curve between10% and 60% size sand is given by

$$Cu=\frac{d_{60}}{d_{10}} \quad \text{.....(4.86)}$$

And gives an idea of the grading or particle size distribution in the material. Lower values C_u<2 indicate more uniform material or poor grading and higher values indicate well graded material.

Another term to indicate the effective distribution of grain size is the '**range sizes' C_r** defined on the basis of the mean slope of the grain size curve. And gives an idea of the grading or particle size distribution in the material. Lower values C_u<2 indicate more uniform material or poor grading and higher values indicate well graded material. Another term to indicate the effective distribution of grain size is the '***range sizes' C_r*** defined on the basis of the mean slope of the grain size curve. A uniformly graded sand has a higher porosity than a less uniform, fine and coarse mixture because in the latter the fines occupy

the voids in the coarse material. Wider the range in size, lower the porosity.

Instruments/Apparatus required:

- **Mechanical/Vibrating Sieve Shaker** (Carries upto 7 sieves, driven by 1/4thH.P. Motor. A pair of rods and a holder are supplied, operation on 230 Volts)
- **Test Sieves** (IS460) Brass Frame,diameter 200 mm with a stainless steel wire machine made:33 numbers

  Available sizes of the sieves are 11.2 mm,5.60 mm,4.75 mm,,3.35 mm, 2.3 mm,1.70 mm,850 micron,500 micron,300 micron,250 micron,120 micron, 90 micron, **Lid** (top cover) and **Pan** (Receiver).*(1 micron = 1 µm = 1/1000 mm)*

- Hot Air Oven

- **Rubber pestle and Mortar**(for crushing the soil if lumped or conglomerated)
- **Electronic Digital Balance** (The balance, to be used, should be sensitive to the extent of 0.1% of total weight of sample taken).

CHAPTER 5- METHODOLOGY

5.1Overall Methodology Flow Chart

The overall methodology flow chart adopted for the present work is depicted by the flowchart given Fig. 5.1

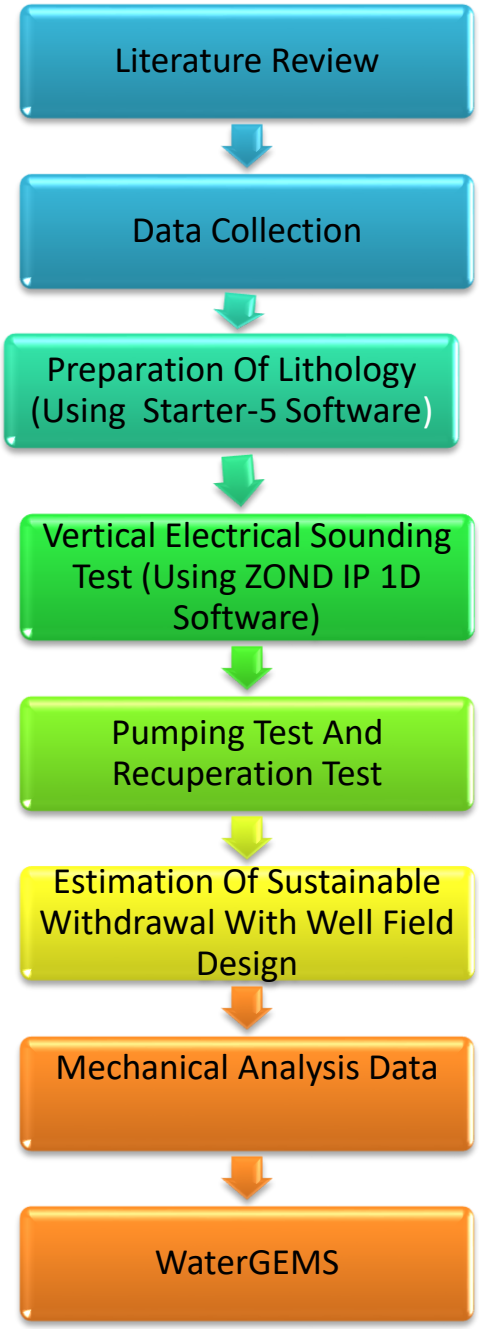


Figure 5.1.: *Flowchart for the overall methodology*

5.2. Literature Review

At the initial stage, a comprehensive review of the literature already available in the form of scientific publications/ case studies/ review works/ reports/ book chapters etc., have been accomplished, to have an overview of the basics of the works that have already carried out related to the present research study.

Proceeding further, the pumping test data,vertical electrical sounding(VES) data (*SWRE, 2024*) has been collected to determine and characterise the important hydraulic parameters of the aquifer for the study area. A combination of the above data forms the secondary dataset for this present study, and is crucial for the initial development of a groundwater model, which will actually approximate and conceptualize the groundwater flow of the study area to carry out future predictions with an acceptable range of accuracy. Moreover, the rainfall distribution, temperature, evapotranspiration etc. data have also been obtained for the study area for the complete simulation of the groundwater flow in the region.

Water distribution networks are designed after recognizing the consumption of water that changes according with the summer and winter season, monthly basis, daily and hourly requirement. For designing of water distribution network, we considers the fluctuation that can be occurs during the supply period. Hourly fluctuation are concern for the designing water distribution network because fluctuation are accounted for peak demand of water supply. Hourly fluctuation has higher value than other fluctuations, excluding fire demand fluctuation. The design discharge for water distribution network is calculated by average water supply rate multiplied by peak factor.

The fluctuation in water supply also occurs due to type of gentry, type of supply pattern i.e. continuous or intermittent water supply and local area i.e. residential, educational and industrial area. Water demand will be more in small population area as compared with large population area because in case of large population area demand increases very gradually due to different customs and religions, and different habits of people. All these factors leads to minimizing the variation in water demand pattern.

5.2.1 Data Collection:

The necessary investigation required for design of water supply distribution network shall relate to carrying out the property survey data for all habitations within the project area including –

5.2.2.Reconnaissance Survey:

Initially, a reconnaissance survey was done to examine the general character of the area to determine the most feasible preliminary water intake location, and this was followed by the collection of necessary information from different sources. The reconnaissance survey was conducted to cover the following aspects.

- Identification of study locations
- Assessment of field condition for the detailed hydrogeological investigation
- Study of topographical survey sheets,
- GPS data collection for GIS based map preparation.

5.3. Preparation of lithology of borehole:

In this section, an important geophysical investigation has been carried out to ascertain the subsurface strata in the study location. Along the bank of River Damodar, slim bores of 50 mm diameter up to 45 m depth were targeted to drill in the selected locations. The borehole module of Starter 5.0 software has been used to visualise the borehole lithology created from drilling logs. The depth of the drilled slim bores ranges from 5 to 45 m. Lithologs obtained in **slim bores** to show vertical transitions for the present study along with their lateral persistence are given below (Figure and Figure reveal the locations of the lithologs and their geological details).

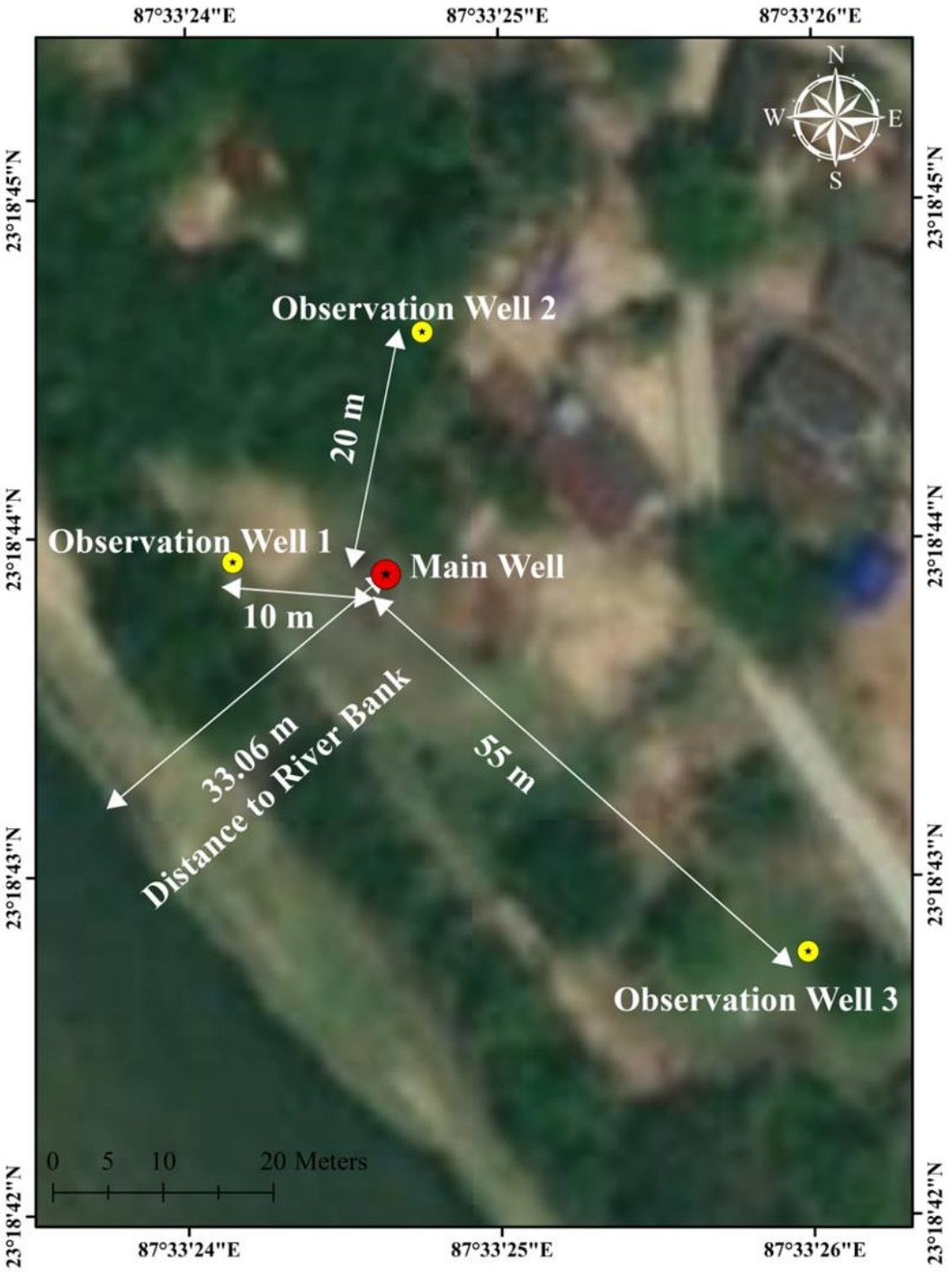


Figure 5.2 : Location of the slim bores and pumping well/main well and three observation wells.



Photograph 5.1 : Insitu Main well, Obs-1, Obs-3,Obs-3 lithological Sample inspection

The lithological borehole data (**SWRE, 2024**) has been obtained to analyse the sub-surface soil characteristics of the study area using **STRATER** software (developed by **Golden Software**) to further obtain the most approximate locations of the water bearing aquifer layers at different depths.

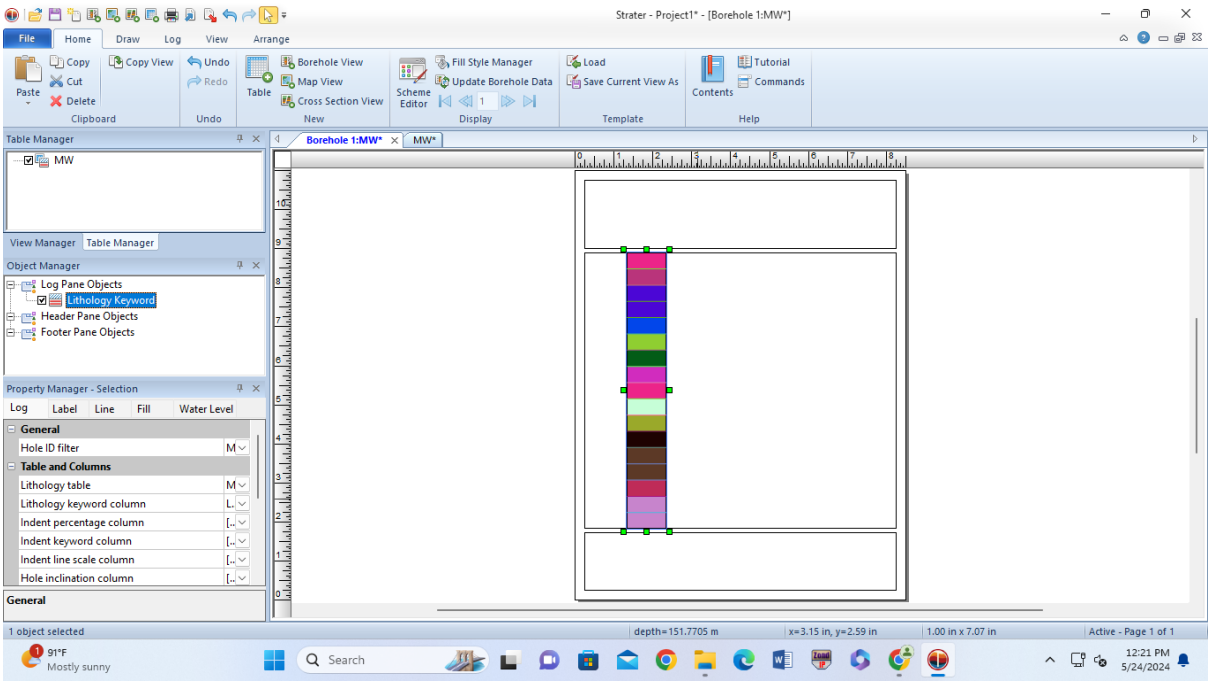


Figure 5.3.: Preparation of lithology of borehole using **STRATER** software

5.4. Ves Test:

The electrical resistivity survey involved vertical electrical sounding (VES) is based on measuring the potentials between one pair of electrodes while transmitting a direct current between another pair of electrodes. Depth of current penetration is proportional to the spacing between the electrodes in homogeneous ground, and varying the electrode separation provides information about the stratification of the ground (Koefoed 1979).

VES survey was carried out in the study area with an MODEL-SSR-MP1 RESISTIVITY METER for measuring the earth resistance, four one-metre length of 1.5 cm diameter cylindrical steel stakes as electrodes, and wire to connect the electrodes to the Resitivity meter. The wire is coiled around reels for ease in winding and unwinding as electrode spreads are increased. The length of wire on reels connecting the resistivity meter to the current electrodes is 300 m while the length of wire for connecting the potential electrodes is 50 m. MODEL-SSR-MP1 equipment is light and powerful for deep current penetration.



Photograph 5.4.VES survey at the study area

The electrical sounding in this study was conducted by using the Schlumberger array (Koefoed 1979). This array is a popular method, which is rather time consuming.

The Schlumberger soundings were carried out with current electrode spacing (AB) ranging from 2 to 210 m (AB/2 = 1 m to 105 m). The distance used for potential electrode spacing (MN) ranged from 1 m to 10 m (MN/2 = 0.5 m to 5 m). The field data acquisition was generally carried out by moving two or four of the electrodes used, between each measurement.

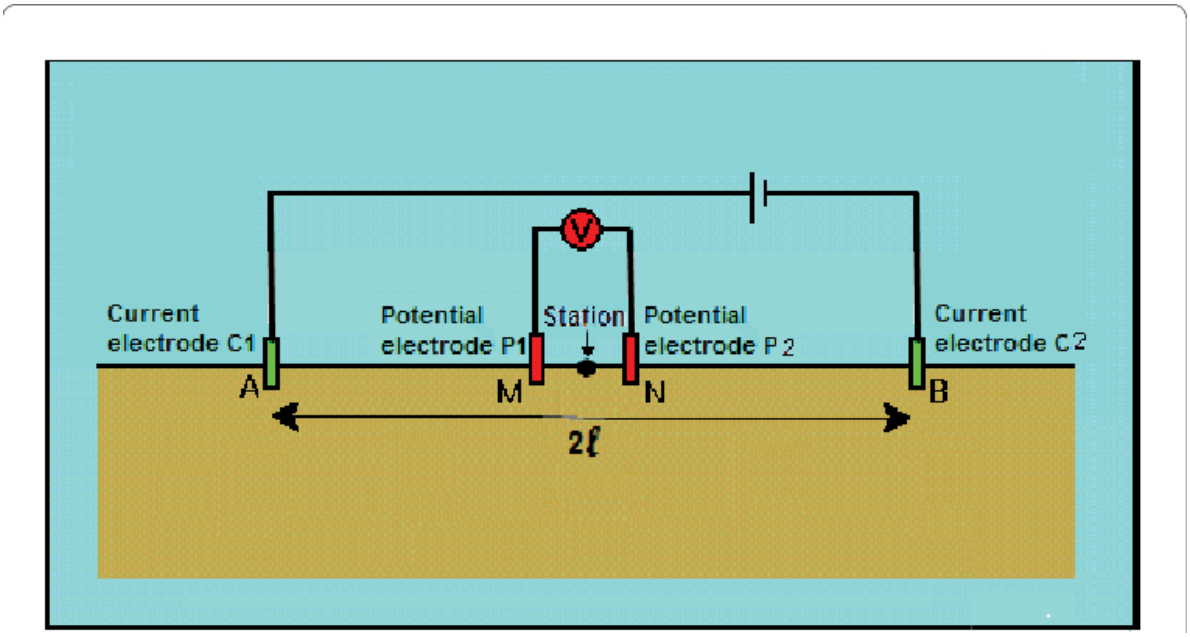


Figure5.5. Electrode configuration of Schlumberger

5.4.1 Data analysis and interpretation:

For more accurate analysis, the relationship between *ER* and *AB/2* can be converted into a relationship between electrical resistivity and actual soil depth through a software application ZondIP 1D .

ZondIP 1D program is designed for one-dimensional resistivity and induced polarization vertical electrosounding data interpretation (with taking account frequency).

Depending on the interpreter's choice, software gives different variants of data interpretation algorithms. Comfortable control system allows to choose from the great number of equivalents results that will appear to be the best in geophysical and geological point of view. Conception of multi-station interpretation is basis of the **ZondIP1D** software.

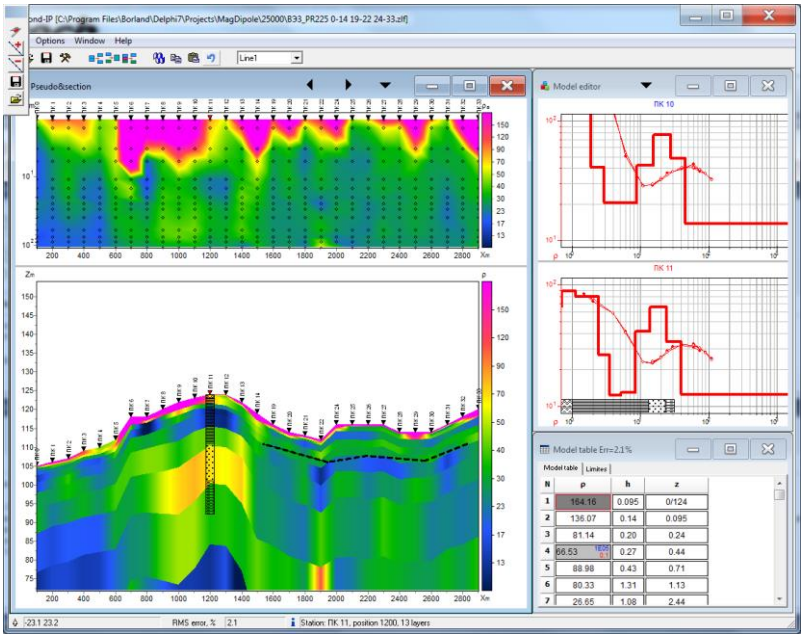


Figure5.6. Interpreted soil profile by ZOND IP 1D software

Table 5. 1: VES Field Data measured at the stduy area in Silla, Bardhaman

SCHLUMBERGER METHOD									
Sl. No.	MN/2 (m)	AB/2 (m)	R (ohm)	K (m/s)	T=K×MN/[(AB/2)^2-(MN/2)^2] (s^{-1})	Rho= K×R (Ohm-m)	Thickness (m)	Depth (m)	Current (*i*)
1	0.5	1	0.00941	2.36	3.146667	0.0222	0.26	0	484.26
2	0.5	2	0.00576	11.78	3.141333	0.0679	0.44	0.26	452.07
3	0.5	3	0.00239	27.49	3.141714	0.0657	0.74	0.71	431.02
4	1	4	0.0166	23.56	3.141333	0.3911	1.24	1.45	408.68
5	1	5	0.02463	37.7	3.141667	0.9286	2.06	2.68	379.92
6	1	6	0.05143	54.98	3.141714	2.8276	3.45	4.75	295.44
7	2	8	0.03626	47.12	3.141333	1.7086	5.76	8.20	330.92
8	2	10	0.02395	75.4	3.141667	1.8058	9.63	13.96	380.97
9	2	12	0.02266	109.96	3.141714	2.4917	16.08	23.58	388.48
10	3	14	0.04043	97.91	3.141497	3.9585	23.32	39.66	264.31
11	3	16	0.01866	129.33	3.141619	2.4133	16.38	62.98	228.06
12	3	18	0.02461	164.93	3.141524	4.0589	9.72	79.36	240.5
13	3	20	0.02177	204.73	3.141637	4.4570	5.30	89.08	231.55

14	4	22	0.00861	183.78	3.141538	1.5823	2.77	94.38	265.24
15	4	26	0.0316	259.18	3.141576	8.1901	1.41	97.15	428.26
16	4	30	0.03746	347.15	3.141629	13.0042	0.71	98.57	480.47
17	6	34	0.03062	293.22	3.141643	8.9784	0.36	99.28	366.05
18	6	42	0.02862	452.39	3.141597	12.9474	0.18	99.64	358.21
19	6	50	0.0106	645.07	3.141575	6.8377	0.09	99.82	282.68
20	8	60	0.01098	694.29	3.141584	7.6233	0.045	99.91	251.45
21	8	70	0.01742	949.55	3.141605	16.5412	0.023	99.95	287.91
22	10	80	0.00592	989.6	3.141587	5.8584	0.011	99.98	757.90
23	10	90	0.02937	1256.64	3.141600	36.9075	0.0055	99.99	196.40
24	10	100	0.03401	1555.09	3.141596	52.8886		99.99	174.83

5.5 Pumping Tests & Recuperation Test

5.5.1 Pumping Tests:

Besides the main bore well of 200 mm diameter situated 10.1 m away from the river bank (Silla site), there were three observation wells situated 9.891 m (Observation well 1: Obs-1), 19.958 m (Observation well 2: Obs-2) and 55.089 m (Observation well 3: Obs-3) away from the main well as depicted in Fig.

In order to adjudge various hydrogeological parameters, the detailed investigation was carried out from 8th February to 10th February 2024 in the presence of the representatives of the Research Team Members of SWRE, JU and officials from PHED. A long-duration pumping test was intended to be carried out for 72 hours. Since the stable drawdown had been achieved in 25.51 hours, pumping was stopped and instantly a recuperation test was started. During the withdrawal at a constant discharge, drawdowns were noted in the pumping well and three observation wells. The readings were taken at one-minute intervals only for the period of the first one hour followed by two minutes' intervals for the next half an hour duration. Gradually depending upon the rate of change of drawdown, intervals were increased from two minutes to two hours. After the cessation of pumping, a recuperation test was carried out by continuous monitoring of the augmentation of the water table with respect to time in the main as well as in the three observation wells. After continuous six hours of monitoring, it was observed that almost the original level of the water table was regained. Accordingly, the water level data as obtained from the main, as well as the observation wells, were plotted in semi-log and log-log graph papers.

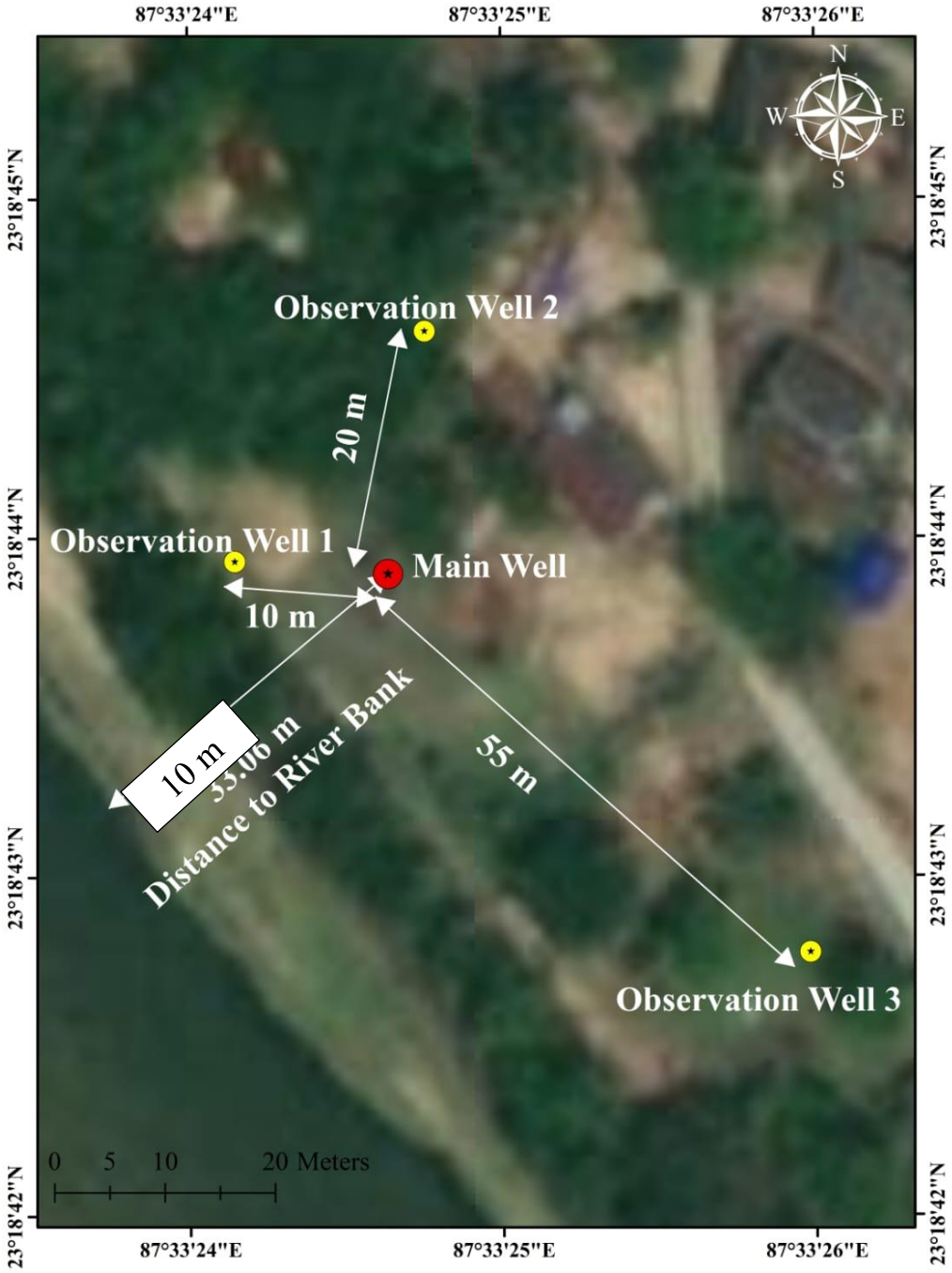


Figure.5.7: Layout of the main (pumping) well and three observation wells.



Photograph 5.2: Water level measurement in main well using in situ TLC meter with the sensor.



Photograph 5.3 **:** Measurement of pumping well discharge using volumetric method (left image) for the calibration of pumping well discharge data measured using ultrasonic flow meter

5.5.2 Recuperation Test:

At the end of the pumping test when the pump is stopped, the water level in the pumping well and three observation wells will begin to rise. This is referred to as recovery of groundwater level, while measurements of drawdown below the original static water level (prior to pumping) during this recovery period are known as residual drawdowns. In the present study, the maximum drawdown in the main well was measured 1.368 m and the residual drawdown was measured 0.0 m which suggests 100% recovery.

5.6 Estimation of sustainable withdrawal with well field design concept:

The objective of well field design is to determine the number and location of production wells required to supply water at a specific rate. For large housing complexes, pumping rate requirements are typically increasing with rapid urbanization. The primary constraint in well field design is the maximum allowable drawdown in the aquifer by well field operation. To accommodate this constraint, the following design procedure is adopted.

Step-I

Assume that each well in the well field causes a drawdown (at the well) equal to 1/2 the allowable drawdown, with the other half of the allowable drawdown caused by interference from other wells, boundary effects and well losses. Determine the pumping rate Q, at each well that would cause a drawdown (at the well) equal to one half the allowable drawdown. This can be done using Theis equation (1935) with a pumping time equal to 1 year.

Step-II

The number of wells required in the well field is equal to the required water supply rate, Q_r, divided by the pumping rate from each well Q. This ratio is rounded upward nearest integer.

Step-III

Arrange the well in such a way that the total drawdown such that total drawdown at each will does not exceed the allowable drawdown selecting the relative locations of the well will depend on the individual site characteristics, such as property boundaries, and existing pipe network, but the well should generally be aligned parallel to end and close as possible to the surface recharge boundaries.

On the basis of the above-mentioned aspect, the well field design concept is adopted for the evaluation of groundwater sustainability assessment in the Silla site.

The pumping rate from a single well that would cause a drawdown of 1.5 m, equal to one-half of the allowable drawdown of 3.0 m is estimated. The drawdown, s_w, resulting from the operation of each well can be estimated using the Theis equation which is as follows:

$$s_w = \frac{Q}{4\pi T} W(u) \ldots\ldots\ldots\ldots\ldots\ldots (5.5)$$

where, Q is the pumping rate from the well, T is the transmissivity of the aquifer, $W(u)$ is the

well function, and u is defined by the relation

$$u = \frac{r^2 S_y}{4Tt} \ldots\ldots\ldots\ldots\ldots\ldots\ldots\ldots (5.6)$$

where 'r' is the distance from the well, 'S_y' is the specific yield of the aquifer, and 't' is the time since the beginning of pumping, Since the drawdown in the wellfield will vary between zero and 2.55 m, the average transmissivity, T, to be used in the well field design obtained from the field experiment is 2375 m^2/day. But for the critical conditions in the summer season, we consider average T = 2400 m^2/day. For a single well with t = 365 days,

$$u_w = \frac{r_w^2 S_y}{4Tt} = \frac{(0.1)^2 \times 0.2}{4 \times 2400 \times 365} = 5.7 \times 10^{-10} \ldots\ldots\ldots\ldots\ldots\ldots (5.7)$$

Since $u_w \leq 0.004$, with less than 0.1% error

$W(u_w) = -0.5772 - \ln u_w$

And therefore, $W(u_w) = -0.5772 - \ln(5.7 \times 10^{-10}) = 20.71 \ldots\ldots\ldots\ldots\ldots\ldots (5.8)$

According to the Theis (1935) equation, the pumping rate Q, required to provide a drawdown, s_w, is given by the following equation:

$$Q = \frac{4\pi T s_w}{W(u_w)} \ldots\ldots\ldots\ldots\ldots\ldots\ldots\ldots (5.9)$$

For s_w = 1.257 m (one-half the allowable drawdown),

$$Qw = \frac{4\pi \times 2400 \times 1.257}{20.71} = 1745 \text{ m}^3\text{/day}$$

Hence the sustainable allowable withdrawal is 1750 m^3/day

Thus, comparing the allowable Q as obtained above from the Well Field Design Concept, the estimated value from the data provided by PHED, Q = 8000 m^3/day is a safer value of withdrawal from this study area.

The number of wells required is given by

Number of wells = $\frac{8000}{1750}$ =4.57 ≈5

Considering further sustainability and critical conditions and climatic variables in the summer season, the number of wells to be adopted is 10 numbers.

Considering the ten well fields with the arrangement shown in figure 5.8

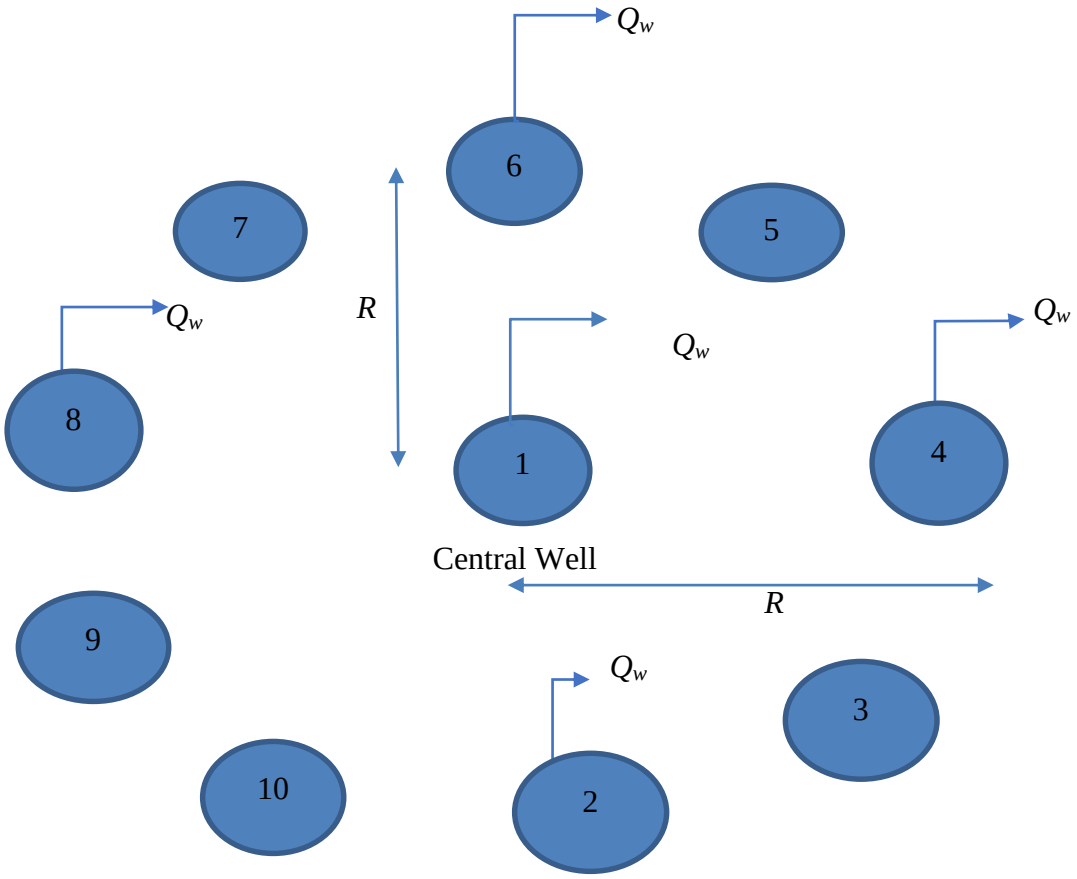


Figure5.8: Conceptual arrangement of Wells

Each of the ten wells is to operate at the same pumping rate $Q_w = \frac{8000}{10}$ = 800 m^3/day.

The arrangement consists of the central well (no. 1) surrounded by four wells (numbers. 2, 3, 4, 5, 6, 7, 8, 9, 10) at a distance from the central well. Clearly, when all five wells are in operation, the drawdown will be greatest at the central well (no.1).

According to the principle of superposition

$S_1 = \frac{Q_w}{4\pi T} \sum_{i=1}^{10} W(u_i)$; where u_i are given by $u_1 = \frac{r_w^2 S_y}{4Tt} = \frac{0.1^2 \times 0.2}{4 \times 2400 \times 365} = 5.7 \times 10^{-10}$

And $= u_3 = u_4 = u_5 \ldots\ldots\ldots\ldots = u_{10} = \frac{R^2 S_y}{4Tt} = \frac{0.2}{4 \times 2400 \times 365} R^2 = 8.56 \times 10^{-10} \times R^2$ ……..(5.10)

So, $W(u_1) = -0.5772 - \ln(5.7 \times 10^{-10}) = 20.71$

$W(u_2) = W(u_3) = W(u_4) = W(u_5) \ldots\ldots\ldots\ldots W(u_{10})$

In the present study, considering critical conditions in the summer season maximum drawdown is 0.408m for the pumping rate from the well 1280 m^3/day and the total demand is 8000 m^3/day, the projected allowable drawdown will be

$$\frac{Q_1}{Q_2} = \frac{s_{w1}}{s_{w2}} \text{.....(5.11)}$$

$$\frac{1280}{8000} = \frac{0.408}{s_{w2}}$$

s_{w2} = 2.55m

$$2.55 = \frac{800}{4\pi \times 2400}[20.371 + 9\, W(u_2)]$$

$$W(u_2) = 8.37 = W(u_3) = W(u_4) = W(u_5) \text{.....} = W(u_4)$$

$$W(u_2) = -0.5772 - \ln(u_2)$$

$$20.71 = -0.5772 - \ln(u_2)$$

$$u_2 = 0.000192$$

From equation we get,

$$0.000129 = 5.7 \times 10^{-8} \times R^2$$

$$R = 47.57 \text{ m} \approx 50m$$

5.7 Mechanical analysis :

Test Procedure:

1. Take a representative oven dried (at 105^0C for 24 hours) sample of soil that weighs about 1000 gm. (this is normally used for soil samples the greatest particle size of which is 11.2 mm.

2. If soil particles are lumped or conglomerated crush the lumped and not the particles using the pestle and mortar.

3. Determine the mass of sample accurately. Wt (gm)

4. Prepare a stack of sieves. Sieves having larger opening sizes (i.e. lower numbers) are placed above the ones having smaller opening sizes (i.e. higher numbers). In case of sandy soil, the very last sieve, is 0.075 mm and a pan is placed under it to collect the portion of soil passing 0.075 mm sieves. Here is a full set of sieves. 4.75mm and 0.075 mm should always be included).

5. Make sure sieves are clean; if many soil particles are stuck in the openings try to poke them out using brush.

6. Weigh all sieves and the pan separately. (Fill in column 3)

7. Pour the soil from step 3 into the stack of sieves from the top and place the cover, put the stack in the sieve shaker and fix the clamps, adjust the time on 5 minutes (Theoretically 10 minutes) and get the shaker going.

8. Stop the sieve shaker and measure the mass of each sieve + retained soil. (Fill in column 4)

9. Weigh the sand retained by each sieve to the nearest 0.01 gm. This is done in a cumulative way – this means that you add what is remaining on the coarsest sieve on top to the container on the scales, and measure the weight. Following this, you add the material from the second sieve down, and again note the combined weight of both samples. Continue in this way for the whole set. When finished, check that the final weight corresponds to the initial weight of the sample.

10. Clean each sieve as it is emptied and returns the soil to the stock.

11. Enter the results in Table. From this, you can calculate the percentage retained on each sieve, and correspondingly, the percentage passing.

12. Plot the results on 3 cycle logarithm graph paper.



Photograph 5.3 : Mechanical Analysis of grain-size distribution in the Laboratory

5.8 WaterGEMS:

Water GEMS is a hydraulic modeling application for water distribution systems with advanced interoperability, geospatial model building, optimization, and asset management tools. From fire flow and constituent concentration analyses, to energy consumption and capital cost management, Water GEMS provides an easy-to-use environment for engineers to analyze, design, and optimize water distribution systems. A water distribution network is an essential hydraulic infrastructure which is a part of the water supply system composed of a different set of pipes, hydraulic devices and storage reservoirs. Water distribution network connects consumers to sources of water using hydraulic components. Water distribution system infrastructure is a major component part of a water utility. A good distribution network system is essential to improve the efficiency of water supply. Water distribution network systems are designed to deliver water from a source in the adequate quantity, quality and at satisfactory pressure to all individual consumers. A distribution network may have different configurations depending upon the layout of the existing area. Generally, water distribution network has a branched and looped type of configuration of pipelines. A network is said to be an optimal network in which layout is not fixed priori but it is allowed to vary in order to obtain the optimal solution. The task to be performed in this context involves resolution of two problems which are layout and design Water GEMS software is developed for design and analysis of water supply network. The software is also used for expansion of existing water distribution network. The software provides required standard and economic environment for design, analysis and troubleshooting of new and existing supply network with minimum time duration. Water GEMS software algorithm is based on Gradient method. Water GEMS software gives optimal solution irrespective of type of network i.e. network may be branched network, looped network or combination of branched and looped network. In other words, Water GEMS software gives solution of any simple or complex network.

The hydraulic head lost by water flowing in a pipe due to friction with the pipe walls can be computed using one of three different equations:

i. Hazen-Williamsequation
ii. Darcy-Weisbach equation
iii. Chezy-Manning equation

The Hazen-Williams equation is the most commonly used headlossequationin the US. It cannot be used for liquids other than water and was originally developed for turbulent flow only. The Darcy-Weisbach equation is the most theoretically correct. It applies to all flow regimes and to all liquids. The Chezy-Manning equation is more commonly used for open channel flow. Each equation uses the followingequationt of computeheadloss between the start and end node of the pipe.ln this study HazenWilliams equation is considered during hydraulic analysis using WaterGEMS, software.

Table5.2: Pipe head loss equations for full flow

Pipe head loss equation name	Pipe head loss equation
Hazen-Williamsequation	$h_L = \frac{10.67LQ^{1.85}}{C^{1.85}d^{4.87}}$
Darcy-Weisbach equation	$h_L = \frac{8fLQ^2}{\pi^2 gd^5}$
Chezy-Manning equation	$h_L = \frac{\pi^2 LQ^2}{0.0972D^5}$

where, C = Hazen-Williams roughness coefficient
f=Darcy-Weisbach friction factor [f is a function of Reynolds number and relative roughness]
E = Darcy-Weisbach roughness coefficient
nChezy-Manning roughness coefficient
d = pipe diameter (m)
L= Pipe length (m)
Q = flow rate (m3/s)

Minor head losses (also called local losses) are caused by the added turbulence thatoccurs at bends and fittings. The importance of including such losses on the layout of the network and the degree of accuracy required. They can be accounted for by assigning the pipe a minor loss coefficient. The minor head product of this coefficient and loss becomes the the velocity head of the pipe,

i.e$h_L = K\frac{v^2}{2g}$……..(5.8.1)

where, K is minor loss coefficient,
v is flow velocity (lcngth/timc) and
g is the acceleration of gravity (length/time2).

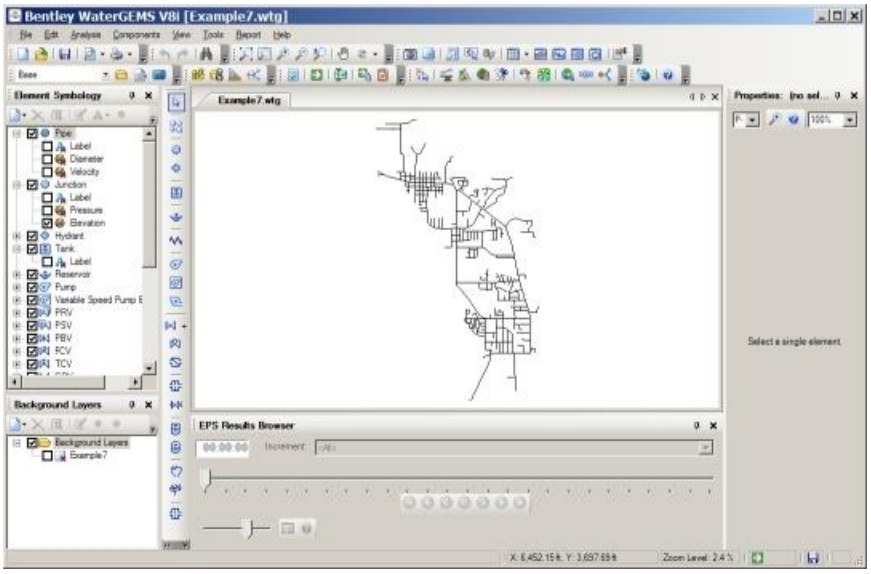


Figure5.9:WaterGEMS V8i Home screen

CHAPTER-6 RESULT AND DISCUSSION

6.1 Lithological data analysis and result

Detailed lithological information for a pumping well and observation wells (OBS-1, OBS-2, and OBS-3) is crucial for understanding groundwater resources and management strategies. Key components of such information.

From this study, it can be interpreted that the top layer of 12 m from the ground surface consists of clayey soil and below it, a 24 m thick confined or saturated layer is exhibited. Within confined or saturated layer 12 m to 36 m sand layer is available.

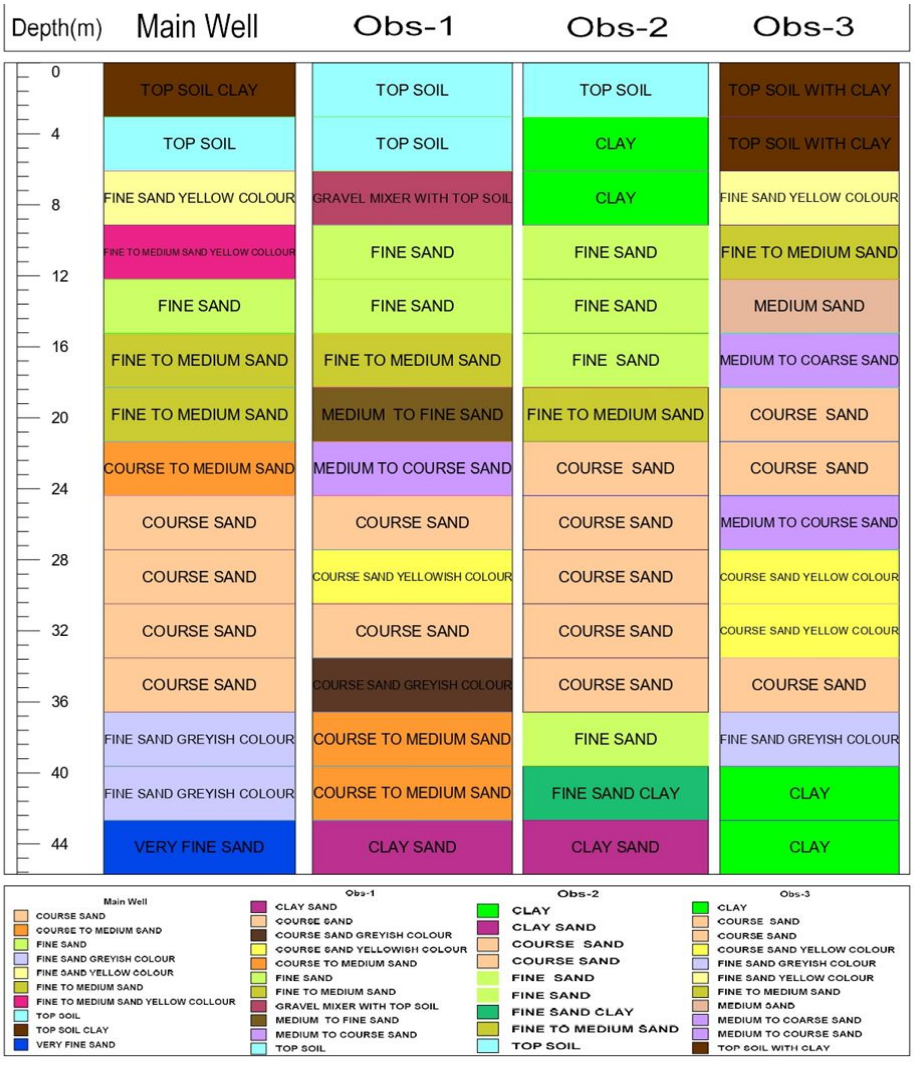


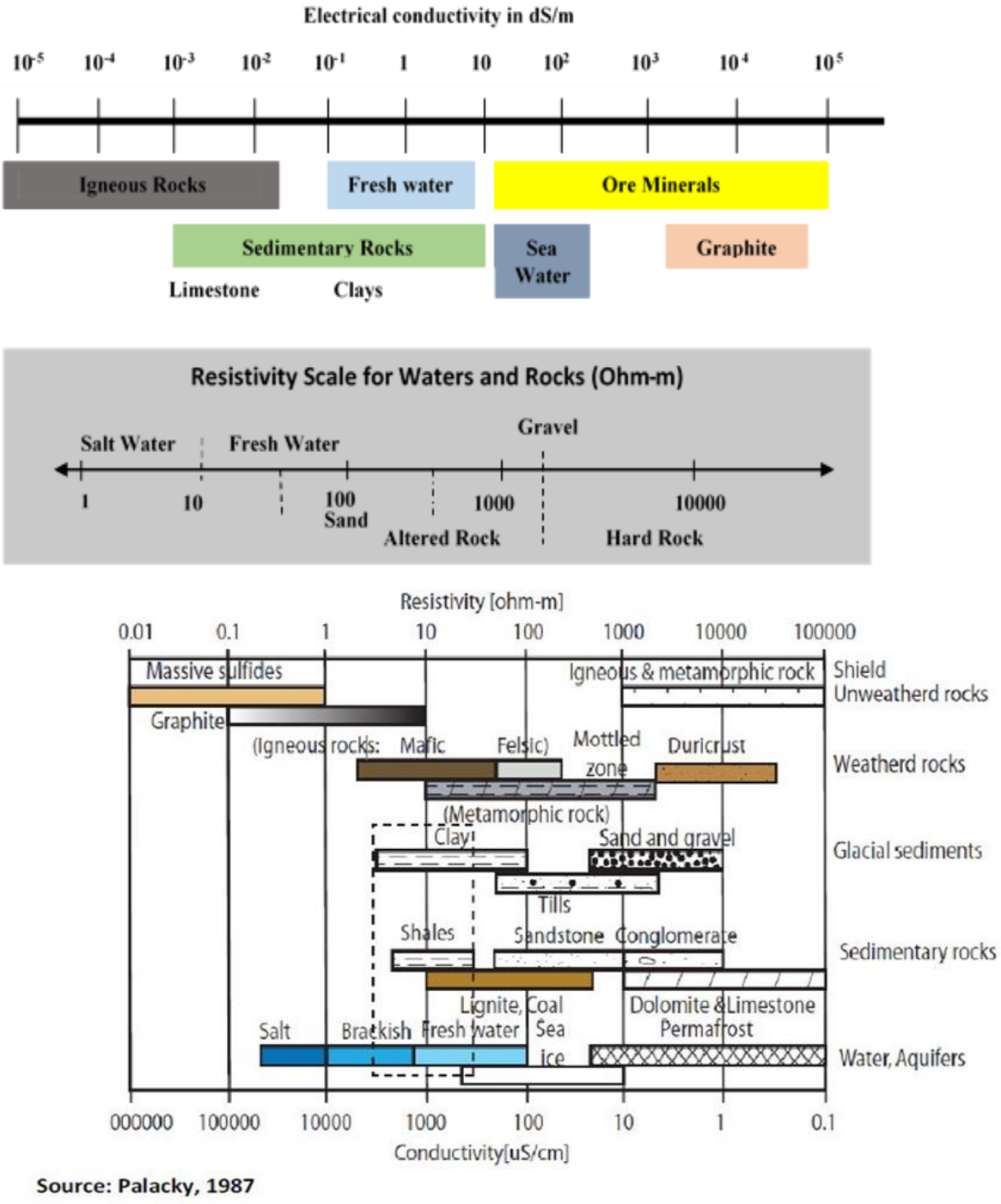
Figure 6.1 : Lithological details of the pumping well and three observation wells (OBS-1, OBS-2 and OBS-3).

6.2 Vertical Electrical Resistivity (VES) survey Result:

The interpretation of the VES data was processed using ZONDIP1D software. ZONDIP1D is a 1D Direct Current (DC) resistivity, Induced Polarization (IP), Magnetotelluric (MT) and electromagnetic sounding inversion program, which produces the actual estimation of a layered model and smooth model for DC resistivity data along with true resistivity, thickness, depth and elevation. Using this software we can fit the aquifer field data with the least RMS fitting error between the data resistivity and true resistivity by multiple iterations for both layered model and smooth model. Using this software variation of resistivity with depth for the layered model at each point is plotted and shown below. Resistivities, thickness and depth, Longitudinal Conductivity and Transverse Resistivity of the VES data are tabulated below.

Table 6.1: Interpretation of longitudinal conductivity and transverse resistivity from VES Data

Sl. No	R (ohm-m)	Thickness (m)	Depth (m)	Longitudinal conductivity (dS/m)	Transverse Resistivity (Ohm-m^2)
1	0.00941	0.26	0	11.7077	0.0058
2	0.00576	0.44	0.26	6.4846	0.0299
3	0.00239	0.74	0.71	11.2631	0.0486
4	0.0166	1.24	1.45	3.1706	0.4850
5	0.02463	2.06	2.68	2.2185	1.9128
6	0.05143	3.45	4.75	1.2201	9.7553
7	0.03626	5.76	8.20	3.3712	9.8414
8	0.02395	9.63	13.96	5.3327	17.3901
9	0.02266	16.08	23.58	6.4534	40.0664
10	0.04043	23.32	39.66	5.8911	92.3123
11	0.01866	16.38	62.98	6.7874	39.5298
12	0.02461	9.72	79.36	2.3947	39.4528
13	0.02177	5.30	89.08	1.1891	23.6220
14	0.00861	2.77	94.38	1.7506	4.3831
15	0.0316	1.41	97.15	0.1722	11.5480
16	0.03746	0.71	98.57	0.0546	9.2330
17	0.03062	0.36	99.28	0.0401	3.2322
18	0.02862	0.18	99.64	0.0139	2.3305
19	0.0106	0.09	99.82	0.0132	0.6154
20	0.01098	0.045	99.91	0.0059	0.3430
21	0.01742	0.023	99.95	0.0014	0.3804
22	0.00592	0.011	99.98	0.0019	0.0644
23	0.02937	0.0055	99.99	0.0001	0.2030

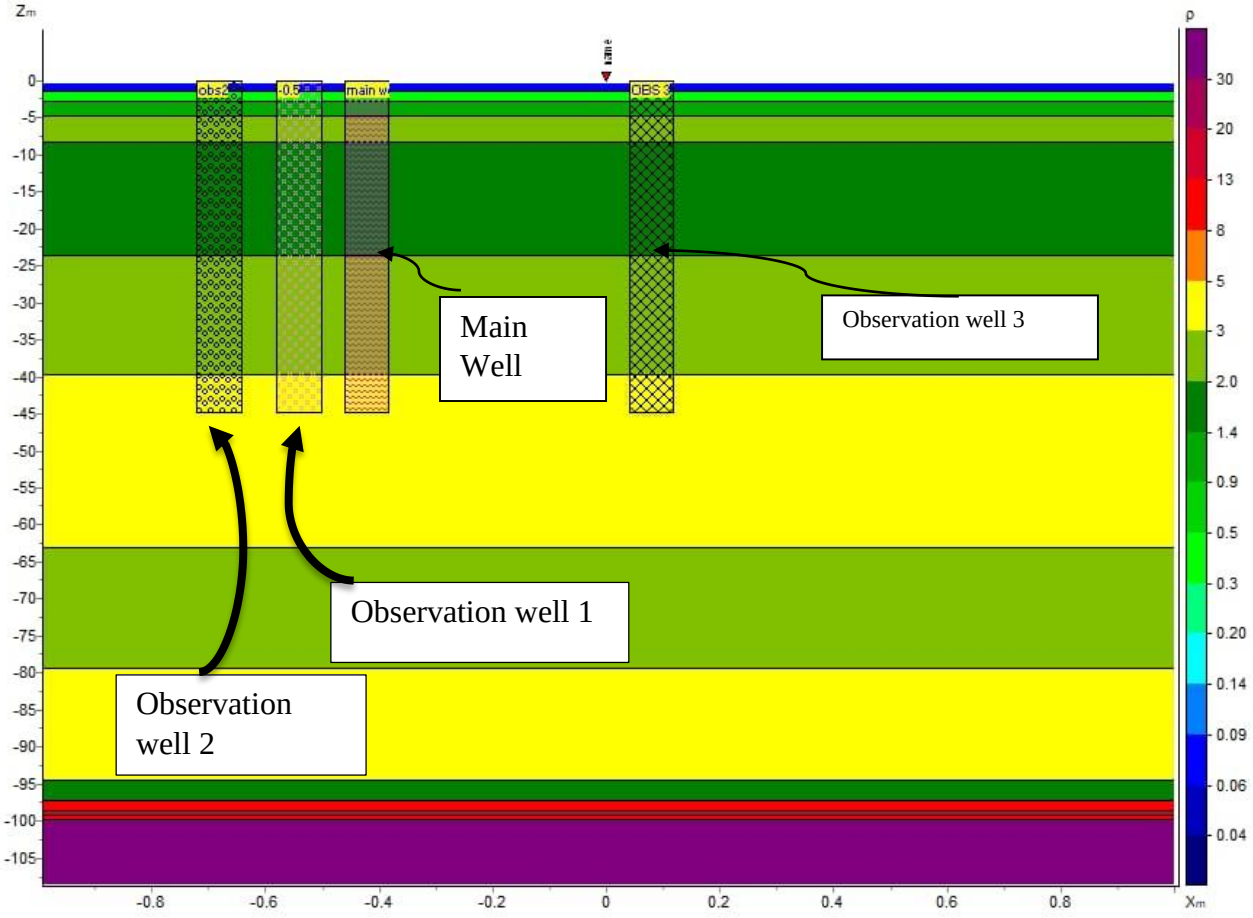


Source: Palacky, 1987

Figure6.2: Resistivity and conductivity scale for water, clay, sand, gravel and rock (Palacky, G.V, 1987, Steve Nylund, 2012)

THE INTERPRETATION OF VES BY SOFTWARE APPLICATION (ZOND IP 1D):

PSEUDO & SECTION:



X_m axis scale: 1 represents 100 m, Z_m scale: 1 represents 1 m, ρ represents resistivity in ohm-m

Figure6.2.2: Interpreted soil profile by ZOND IP 1D software

MODEL: APPARENT RESISTIVITY VERSUS DEPTH

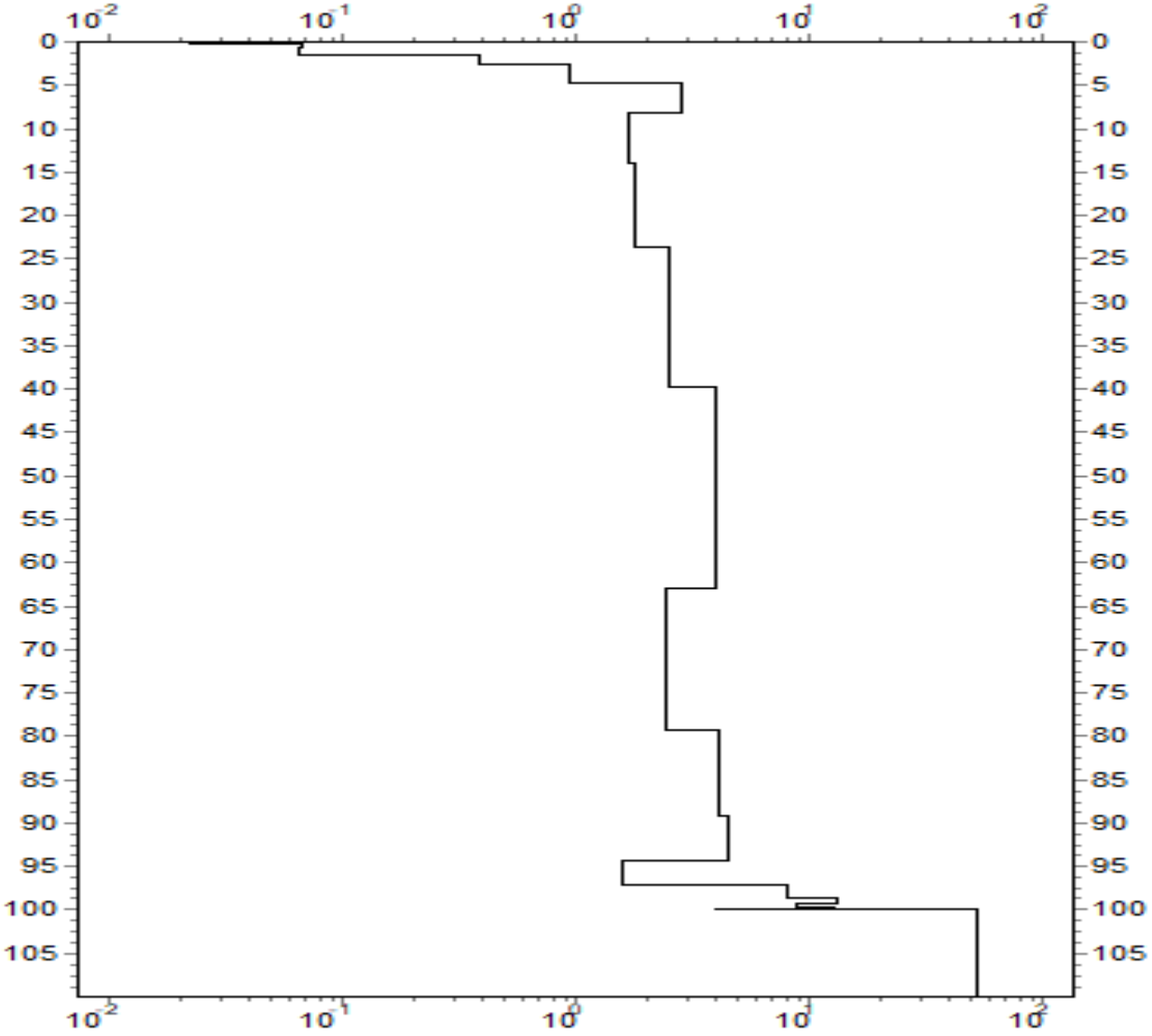


Figure6.3: A prepared smooth layer of the soil profile by ZOND IP 1D software

RESISTIVITY SCALE FROM SOFTWARE PROFILE:

Layers	Depth (m)	Resistivity (Ohm-m)	Profile Color	Probable Lithology
1	0-0.24	0-0.04		Clay Top Soil
2	0.24-1.48	0.04-0.06		Clay Top Soil
3	1.48-2.7	0.3-0.5		Clay Top Soil
4	2.7-4.8	0.9-1.4		Clayey Sand
5	4.8-8.25	2-3		Blackish Clay
6	8.25-23.8	1.4-2		Blackish Clay
7	23.8-39.8	2-3		Fine Sand
8	39.8-64.1	3-5		Sand
9	64.1-78	2-3		Sand
10	78-94	3-5		Coarse Sand
11	94-96	1.4-2		Gravel
12	96-101	8-13		Blakish Clay
13	≻ 101	≥30		Clay

Discussion: From this study, it can be interpreted that the top layer of 23.8 m from the ground surface consists of clayey soil and below it, a 70.2 m thick confined or saturated layer is exhibited. Within confined or saturated layer 39.8 m to 64.1 m and 78 m to 94 m sand layer is available.

6.3 Pumping Tests And Recuperation Test result:

All the distances of the observation wells were measured with respect to the respective main wells. The diameter of the main well was 200 mm and the depth of boring was 45 m. The diameter of the three observation wells was 50 mm each and their depth of boring was 45 m.

Table 6.2: Initial Data recorded just before starting the Pumping Test

Well Name	Distance from the main well	Duration of monitoring	Depth of water from Datum / Static Water table	MSL of bed level	Discharge of pump
	(m)	(hr)	(m)	(m)	(m^3/hr)
Main Well	--	45	7.43	96.505	80
OBS-1	10	45	8.45	96.611	--
OBS-2	20	45	7.99	96.922	--
OBS-3	55	45	9.36	97.889	--

The pump started at 03:03 pm on 8th February, 2024 and the readings of the drawdown in the main well and three observation wells were taken as depicted in the following graphs –

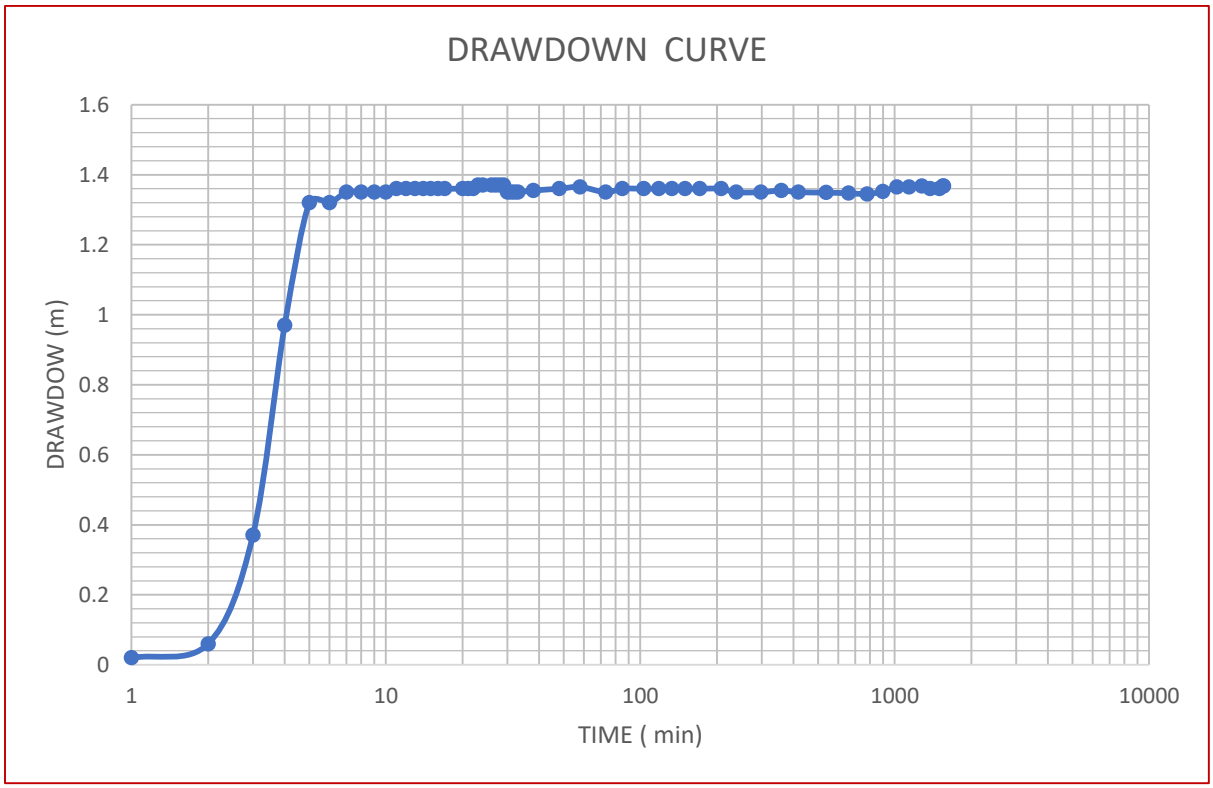


Figure 6.4 : Variation of Drawdown (*s*) at the main well with varying time (*t*) for pumping out water from the main well.

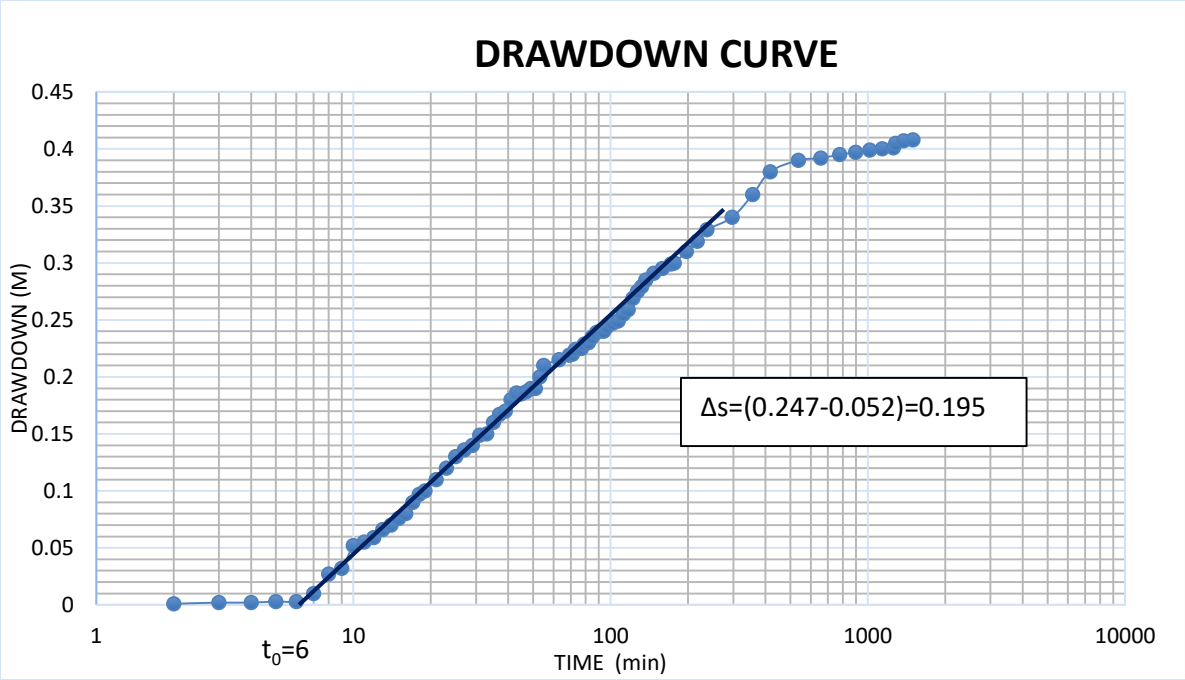


Figure 6.5 : Drawdown (*s*) versus time (*t*) data plotted for observation well-1.

Straight-line fitted through the data as shown from the basis for the calculation of hydraulic parameters.

The transmissivity (*T*) of the aquifer has been determined using equation (2).

$$T = \frac{2.3Q}{4\pi\Delta s} = \frac{2.3\times(80\times24)}{4\pi\times0.195} = 1802.12 \text{m}^2/\text{day} \approx 1800 \text{ m}^2/\text{day} \ldots\ldots\ldots\ldots\ldots\ldots (5.1)$$

The confined storativity (*S*) has been determined using equation (4).

$$S = \frac{2.25Tt_{0s}}{r^2} = \frac{2.25\times1800\times6}{10^2\times60\times24} = 0.16875 \approx 0.16 \ldots\ldots\ldots\ldots\ldots\ldots\ldots\ldots\ldots\ldots (5.2)$$

The **Radius of Influence** (*R*) has been determined by the following equation (5).

$$Q = \frac{2\pi Ts_d}{ln\left(\frac{R}{r}\right)} = \frac{2\times\pi\times1800\times0.408}{ln\left(\frac{R}{10}\right)} \quad \ldots\ldots\ldots\ldots\ldots\ldots \quad (5.3)$$

$R \approx 110$ m

The calculation for the rest of the observation wells for constant discharge and different distances from the pumping well is the same as above.

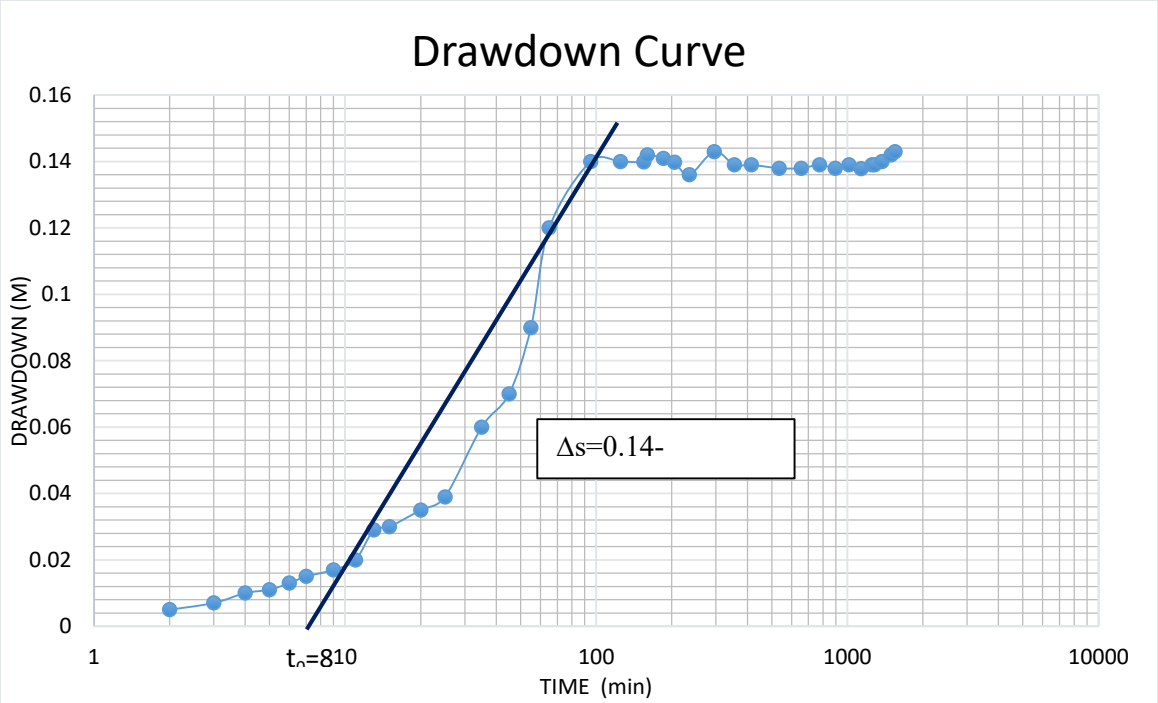
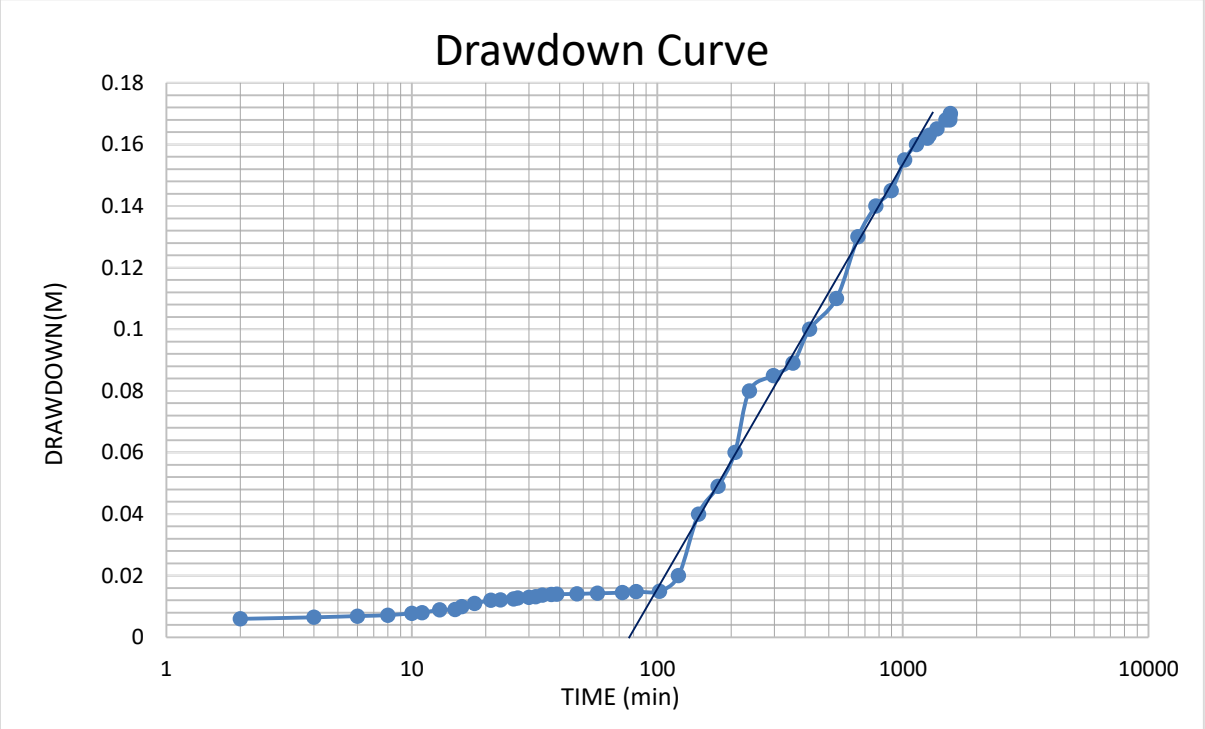


Figure.6.6: Drawdown (*s*) versus time (*t*) data for observation well-2.



Fiure.6.7: Drawdown (*s*) versus time (*t*) data for observation well-3.

A summary of observation data of Drawdown, Transmissivity, and Storativity of observation wells with respect to the main well (10 m from the left bank) is given Table 6.3.

.**Table 6.3:** Results of pumping Test

Well Name	**Distance from Main Well**	**Storativity**	**Discharge**	**Transmissivity**	**Maximum Drawdown**
	(m)		**(m^3/hr)**	**(m^2/day)**	**(m)**
Main Well (10 m from the left bank)	-	-	80		1.368
OBS-1	10	0.1690	-	1804.020	0.408
OBS-2	20	0.0904	-	2929.936	0.143
OBS-3	55	0.1033	-	2511.374	0.170
Average Transmissivity = 2414 m^2/day Critical Value of Transmissivity=1804 m^2/day					

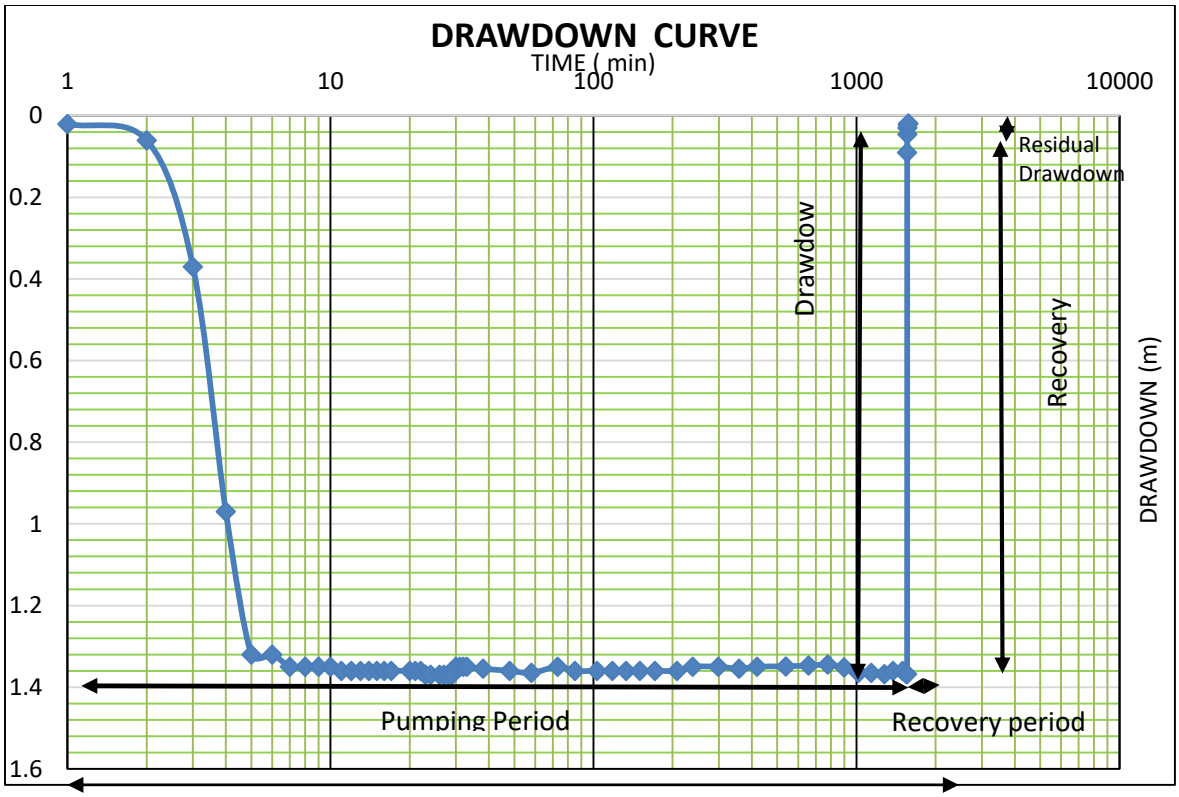


Figure.6.8 : Drawdown versus time curve representing recuperation data for Main well

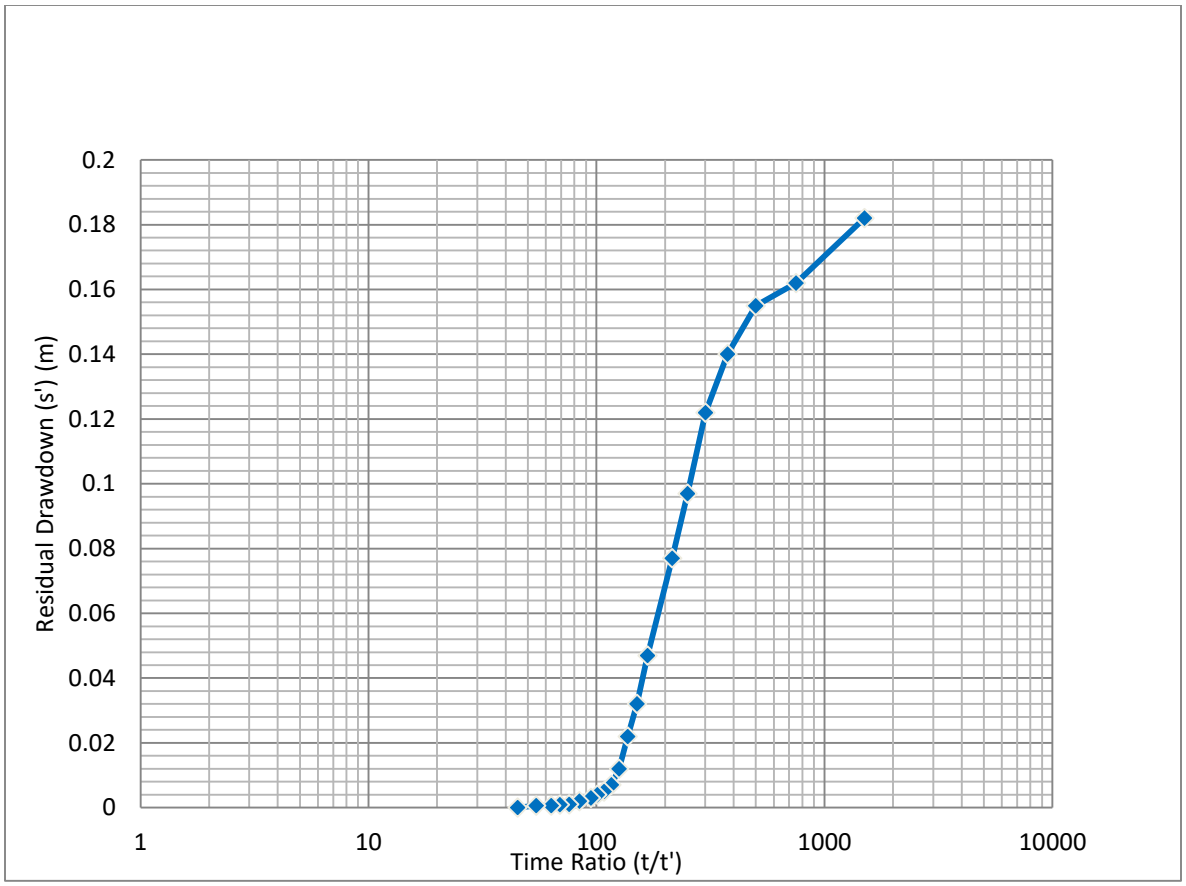


Figure.6.9: Time drawdown curve, Theis recovery for observation well-1.

The values of *S*' versus *t/t'* are plotted on semi-log paper and using the following equation, transmissivity and storage coefficient have been determined.

$T = \frac{2.3Q}{4\pi\Delta s'} = \frac{2.3\times80\times24}{4\pi(0.159)} = 2212$ m^2/d.....(5.4)

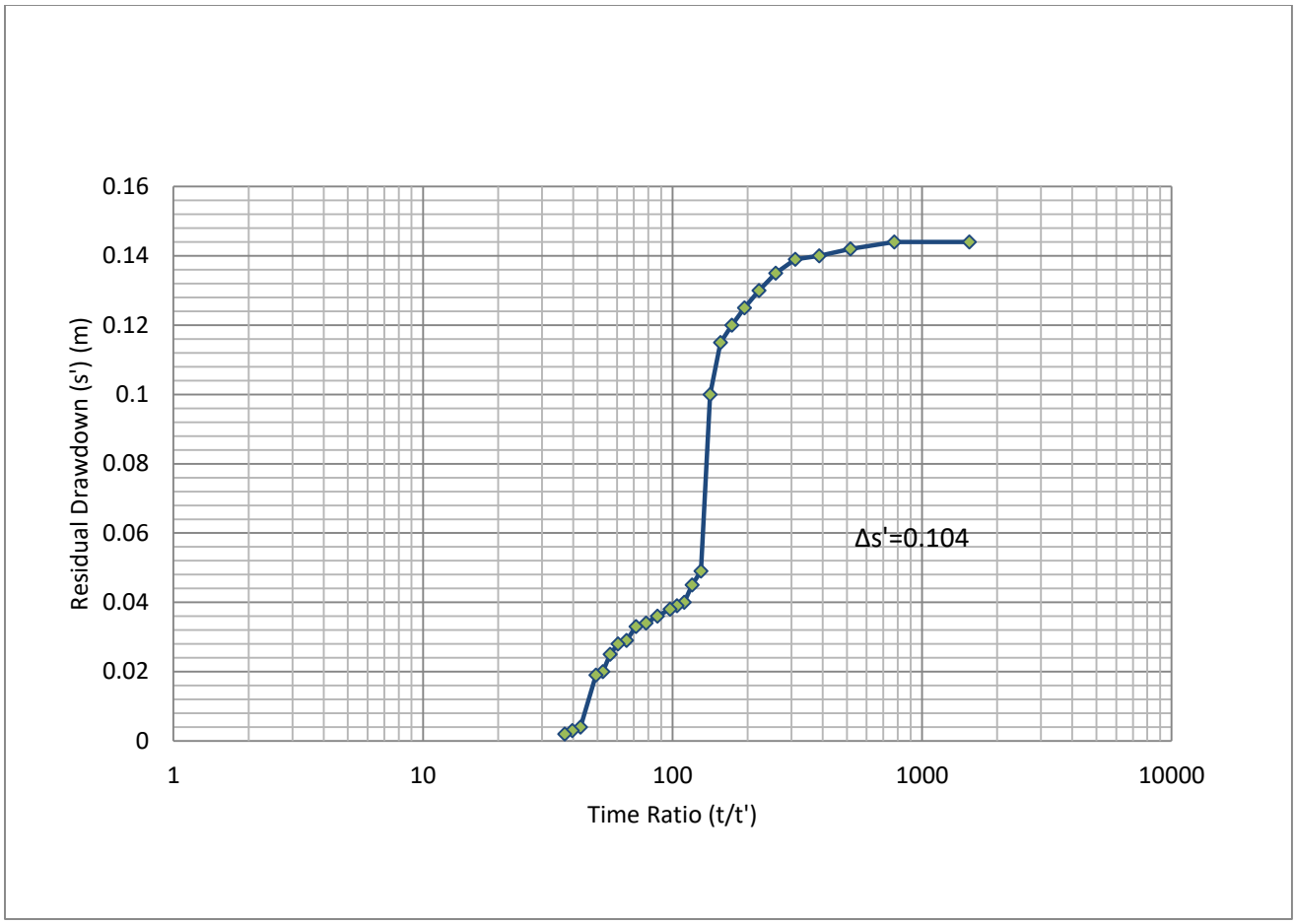


Figure 6.10**:** Time drawdown curve, Theis recovery for observation well-2.

Table 6.4 : Results of recuperation or recovery test at a glance.

Well Name	**Distance from Main Well**	**Discharge**	**Transmissivity**	**Maximum Drawdown**
	(m)	**(m^3/hr)**	**(m^2/day)**	**(m)**
Main 1 (10 m from the left bank)	-	80	-	1.368
OBS-1	10	-	2211.273	0.408
OBS-2	20	-	3380.696	0.143

6.4 Well field design result:

Therefore, a well field consisting of ten wells is arranged as shown in Figure 6.4.1with each well pumping 800 m^3/day and spaced 50 m apart from the centre well, will yield the required amount of water and produce a drawdown that will not exceed the specified maximum of 2.55 m. The arrangement of nine wells is considered at 40° from the centre well.

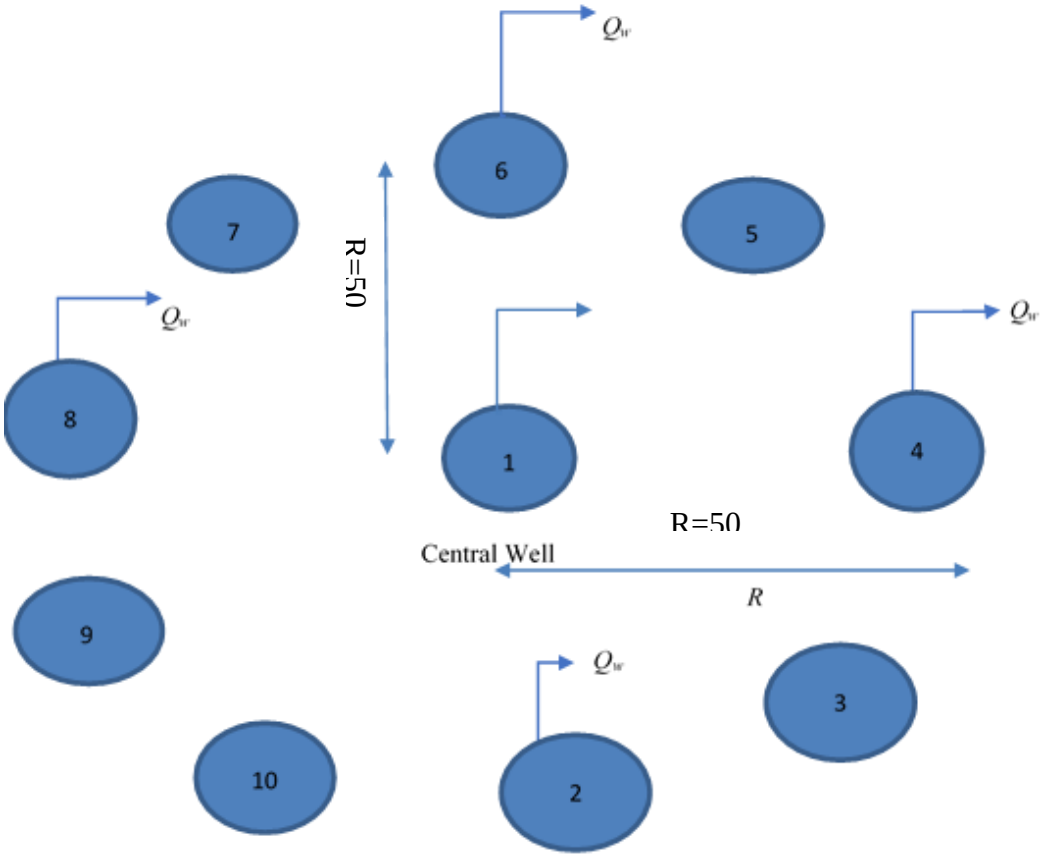


Figure6.4.1: Proposed Well Field

6.5 Mechanical Analysis Result:

A mechanical analysis is done with the bore well log material and from that the material size is determined.

Table 6.5: Mechanical Analysis of Main Well (depth 10 m to 30 m)

Sieve Size (mm)	**Weight Retained (gm)**	**Cumulative Weight Retained (gm)**	**% of Cum. Wt. Retained**	**% Finer**
11.2	1.6	1.6	0.16	99.84
4.75	12.86	14.46	1.45	98.55
3.35	6.82	21.28	2.14	97.86
2.3	14.36	35.64	3.57	96.43
1.7	56.79	92.43	9.29	90.71
0.85	381.26	473.69	47.49	52.51
0.5	327.93	801.62	80.57	19.43
0.3	192.74	994.36	99.94	0.06
0.12	0.05	994.41	99.94	0.06
0.09	0.03	994.44	99.95	0.05
Pan	0.54	994.98	100	0
CALCULATION				
D_{10} = 0.41 mm , D_{30}= 0.61 mm, D_{50} = 0.82 mm, D_{60} = 1.0 mm				
Coefficient of Uniformity, Cu (U.C)= D_{60}/D_{10} = 2.4				
Coefficient of Curvature, Cc= $D_{30}^2/(D_{60}\times D_{10})$ = 1.0				

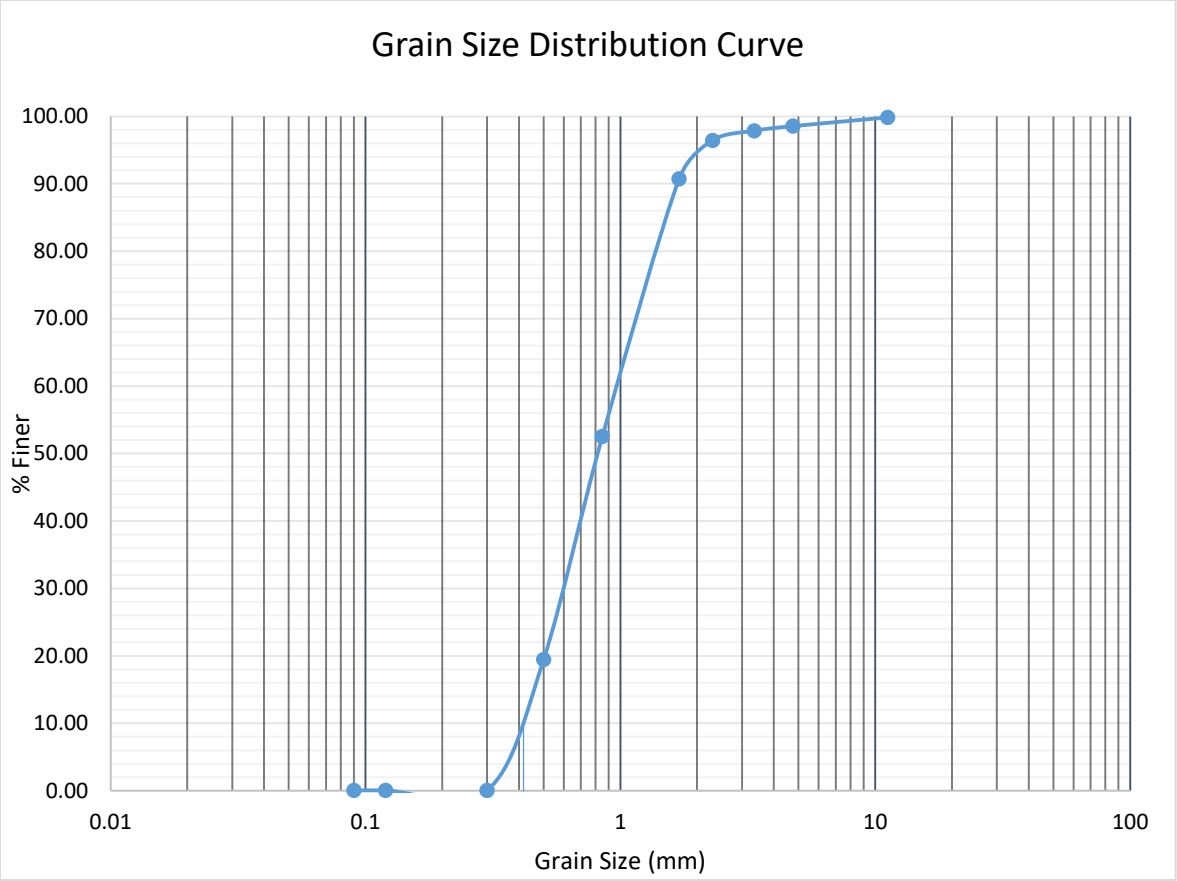


Figure 6.11: IS sieve aperture dimension (mm) versus cumulative % passing as per Sieve analysis for the main well (depth 10 m to 30 m)

Table 6.6: Mechanical Analysis of Main Well (depth 30 m to 50 m)

Sieve Size (mm)	**Weight Retained (gms)**	**Cumulative Weight Retained (gms)**	**% of Cum. Wt. Retained**	**% Finer**
11.2	0	0	0	100
4.75	35.8	35.8	3.59	96.41
3.35	25.17	60.97	6.11	93.89
2.3	31.44	92.41	9.26	90.74
1.7	31.57	123.98	12.64	87.36
0.85	150.04	274.02	27.95	72.05
0.5	172.25	446.27	45.52	54.48
0.3	528.9	975.17	99.46	0.54

0.12	0.82	975.99	99.54	0.46
0.09	0.31	976.3	99.57	0.43
Pan	4.18	980.48	100.00	0.00
CALCULATION				
D_{30}= 0.41 mm, D_{50}= 0.49 mm, D_{60}= 0.60 mm, D_{10}= 0.35 mm				
Coefficient of Uniformity, C_u= D_{60}/D_{10} = 1.82				
Coefficient of Curvature, Cc= $D_{30}^2/(D_{60}\times D_{10})$= 0.81				

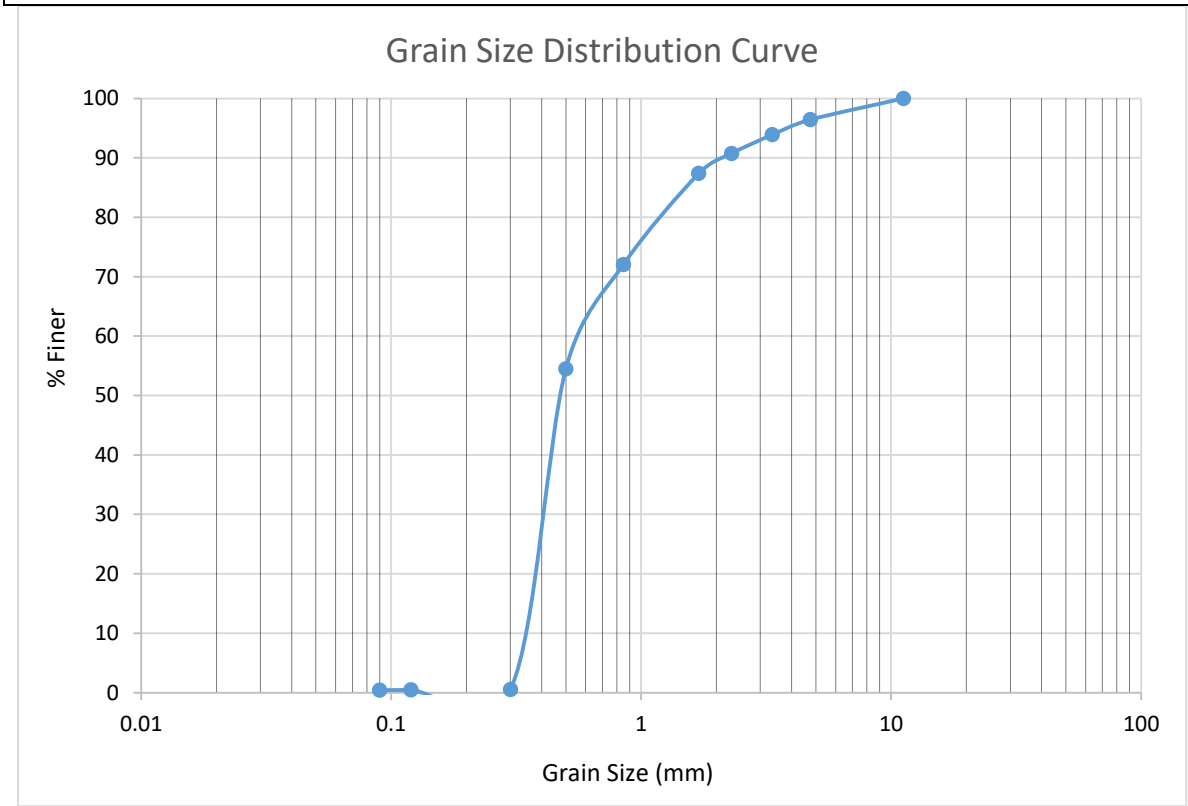


Figure 6.12: IS sieve aperture dimension (mm) versus cumulative % passing as per Sieve analysis for Main Well (depth 30 m to 50 m)

Table 6.7: Mechanical Analysis of Observation Well-1 (depth 10 m to 18 m)

Sieve Size (mm)	**Weight Retained (gms)**	**Cumulative Weight Retained (gms)**	**% of Cum. Wt. Retained**	**% Finer**
11.2	4.23	4.23	0.39	99.61
4.75	27.03	31.26	2.90	97.10

3.35	99.99	131.25	12.17	87.83
2.3	31.56	162.81	15.10	84.90
1.7	43.85	206.66	19.17	80.83
0.85	168.16	374.82	34.77	65.23
0.5	388.12	762.94	70.77	29.23
0.3	313.41	1076.35	99.84	0.16
0.12	0.16	1076.51	99.86	0.14
0.09	0.04	1076.55	99.86	0.14
Pan	1.52	1078.07	100.00	0.00
CALCULATION				
D_{30}= 0.51 mm, D_{50}=0.67 mm, D_{60}= 0.79 mm, D_{10}= 0.38 mm				
Coefficient of Uniformity, Cu= D_{60}/D_{10} = 2.17				
Coefficient of Curvature, Cc= $D_{30}^2/(D_{60}\times D_{10})$ = 0.868				

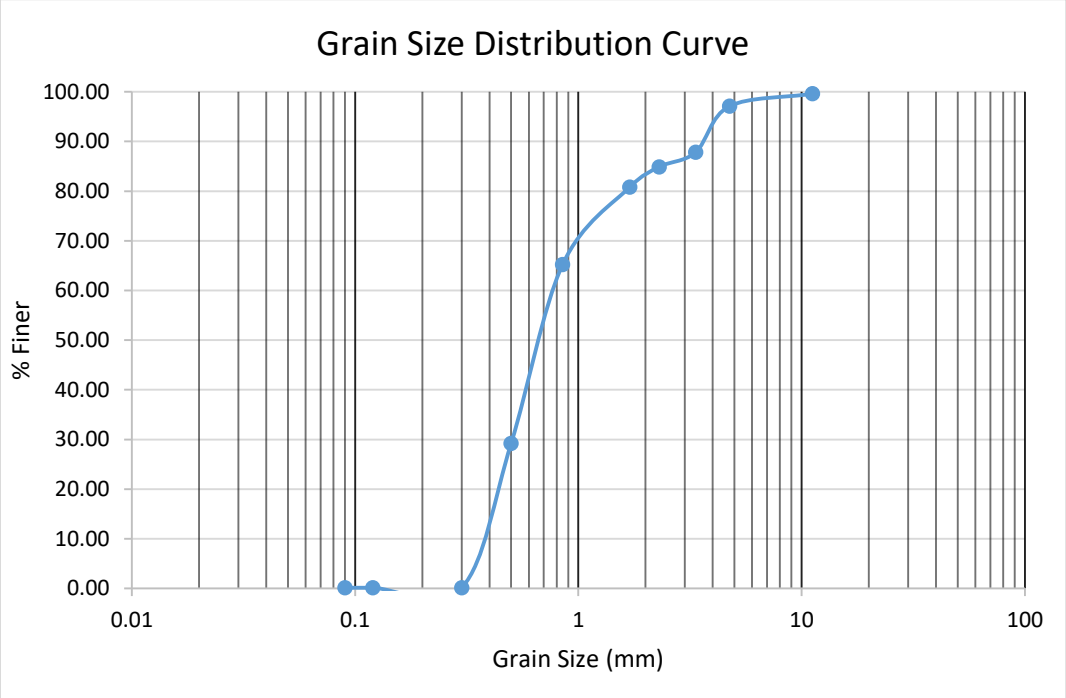


Figure 6.13: IS sieve aperture dimension (mm) versus cumulative % passing as per sieve analysis for observation well-1 (depth 10 m to 18 m).

Table 6.8: Mechanical Analysis of Observation Well-1 (depth 18 m to 30 m)

Sieve Size (mm)	**Weight Retained (gms)**	**Cumulative Weight Retained (gms)**	**% of Cum. Wt. Retained**	**% Finer**
11.2	6.38	6.38	0.64	99.36
4.75	25.76	32.14	3.22	96.78
3.35	22.51	54.65	5.47	94.53
2.3	32.65	87.3	8.74	91.26
1.7	57.55	144.85	14.50	85.50
0.85	278.15	423	42.33	57.67
0.5	327.79	750.79	75.13	24.87
0.3	247.08	997.87	99.86	0.14
0.12	0.56	998.43	99.91	0.09
0.09	0.09	998.52	99.92	0.08
Pan	0.77	999.29	100.00	0.00
CALCULATION				
D_{30}= 0.55 mm, D_{50}= 0.768 mm, D_{60}= 0.92 mm, D_{10}=0.38 mm				
Coefficient of Uniformity, Cu= D_{60}/D_{10} = 2.42				
Coefficient of Curvature, Cc= $D_{30}^2/(D_{60}\times D_{10})$ = 0.884				

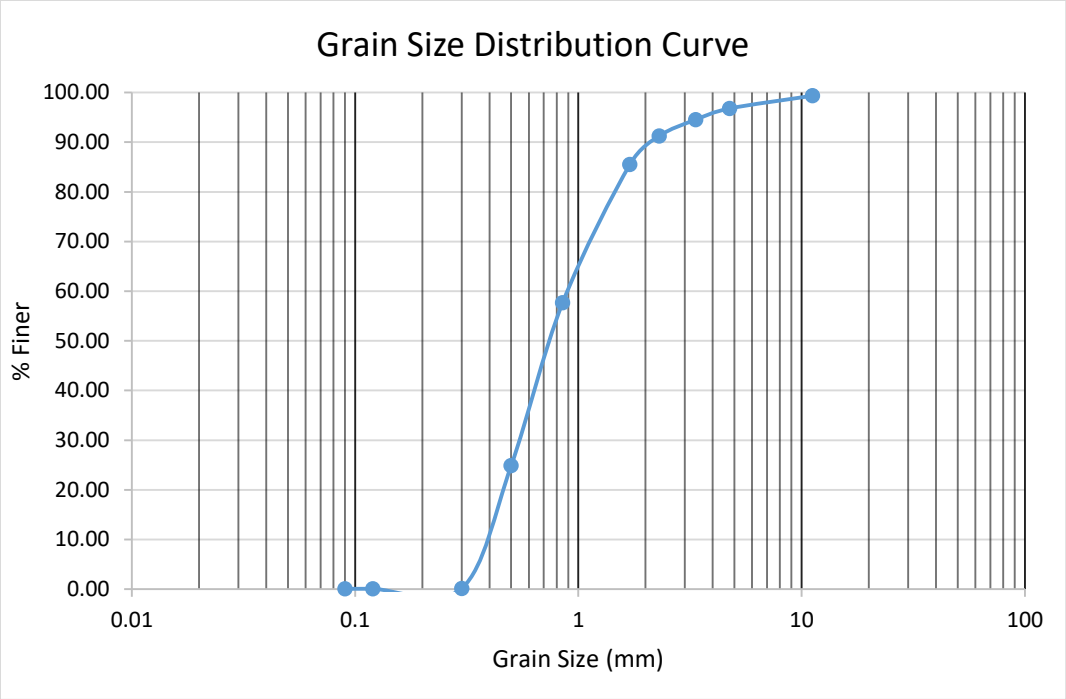


Figure 6.14: IS sieve aperture dimension (mm) versus cumulative % passing as per Sieve analysis for observation well-1 (depth 18m to 30m)

Table 6.9: Mechanical Analysis of Observation Well-1 (depth 30 m to 45 m)

Sieve Size (mm)	**Weight Retained (gms)**	**Cumulative Weight Retained (gms)**	**% of Cum. Wt. Retained**	**% Finer**
11.2	15.52	15.52	1.56	98.44
4.75	61.6	77.12	7.74	92.26
3.35	15.98	93.1	9.34	90.66
2.3	38.41	131.51	13.20	86.80
1.7	63.2	194.71	19.54	80.46
0.85	213.39	408.1	40.95	59.05
0.5	284.22	692.32	69.47	30.53
0.3	301.93	994.25	99.76	0.24
0.12	1.02	995.27	99.86	0.14
0.09	0.11	995.38	99.87	0.13
Pan	1.25	996.63	100.00	0.00

CALCULATION
D_{30}= 0.5 mm, D_{50}= 0.738 mm, D_{60}= 0.91 mm, D_{10}=0.38 mm
Coefficient of Uniformity, Cu= D_{60}/D_{10} = 2.43
Coefficient of Curvature, Cc= $D_{30}^2/(D_{60}\times D_{10})$ = 0.76

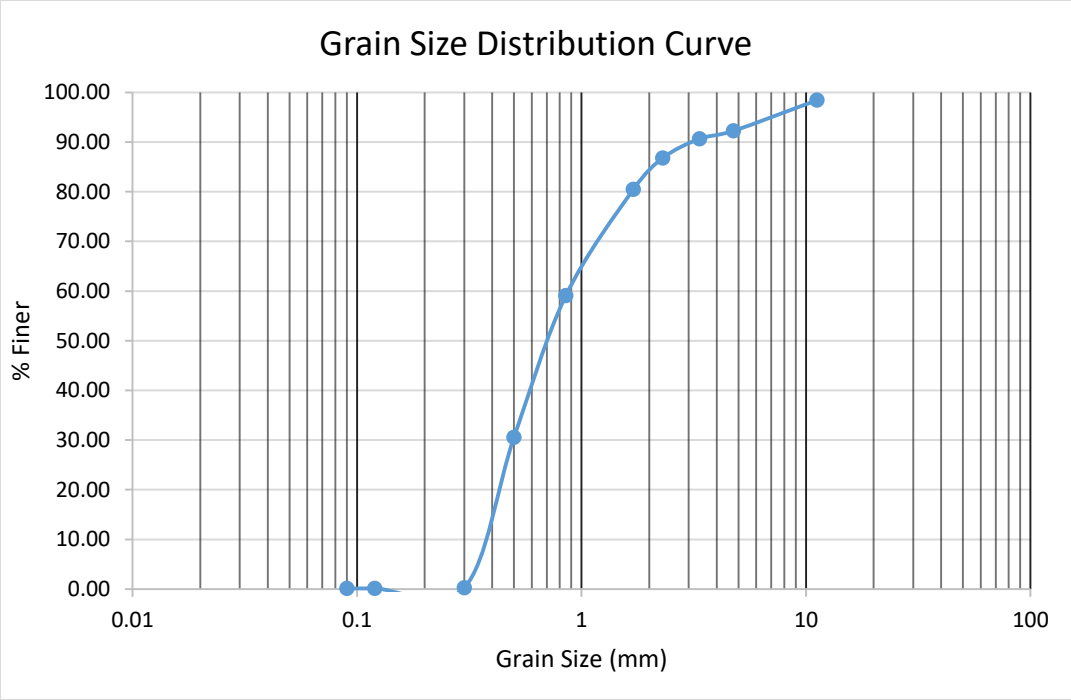


Figure 6.15: IS sieve aperture dimension (mm) versus cumulative % passing as per Sieve analysis for observation well-1 (depth 30m to 45m)

Table 6.10: Mechanical Analysis of Observation Well-2 (depth 10m to 25m)

Sieve Size (mm)	**Weight Retained (gms)**	**Cumulative Weight Retained (gms)**	**% of Cum. Wt. Retained**	**% Finer**
11.2	2.47	2.47	0.25	99.75
4.75	84.1	86.57	8.71	91.29
3.35	46.02	132.59	13.34	86.66
2.3	78.45	211.04	21.23	78.77
1.7	87.36	298.4	30.02	69.98
0.85	260.98	559.38	56.28	43.72

0.5	275.89	835.27	84.03	15.97
0.3	157.36	992.63	99.86	0.14
0.12	0.34	992.97	99.90	0.10
0.09	0.01	992.98	99.90	0.10
Pan	1.02	994	100.00	0.00
CALCULATION				
D_{30}= 0.676 mm, D_{50}=1.05mm, D_{60}= 1.37 mm, D_{10}= 0.43 mm				
Coefficient of Uniformity, Cu= D_{60}/D_{10} = 3.24				
Coefficient of Curvature, Cc= $D_{30}^2/(D_{60}\times D_{10})$ = 0.78				

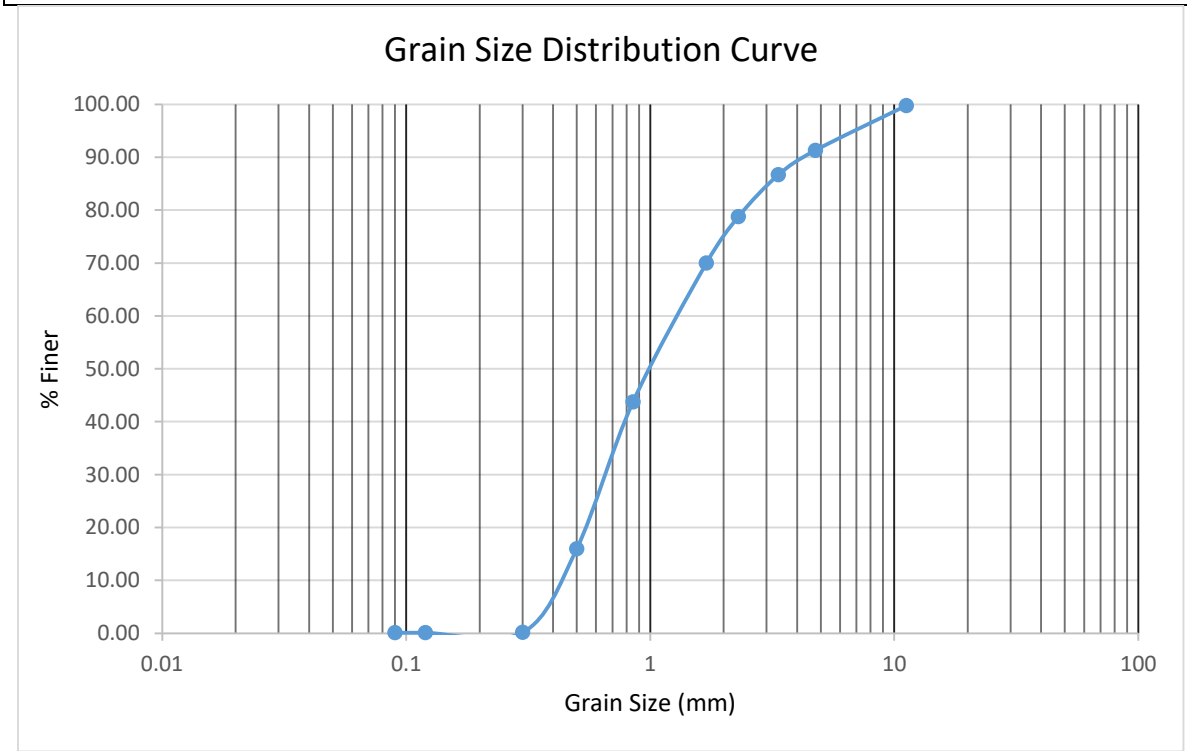


Figure 6.16: IS sieve aperture dimension (mm) versus cumulative % passing as per Sieve analysis for observation well-2 (depth 10m to 25m)

Table 6.11: Mechanical Analysis of Observation Well-2 (depth 25m to 40m)

Sieve Size (mm)	**Weight Retained (gms)**	**Cumulative Weight Retained (gms)**	**% of Cum. Wt. Retained**	**% Finer**
11.2	0	0	0.00	100.00
4.75	19.28	19.28	1.94	98.06
3.35	26.09	45.37	4.57	95.43
2.3	58.28	103.65	10.43	89.57
1.7	92.32	195.97	19.73	80.27
0.85	324.76	520.73	52.42	47.58
0.5	303.59	824.32	82.98	17.02
0.3	167.15	991.47	99.80	0.20
0.12	0.35	991.82	99.84	0.16
0.09	0.09	991.91	99.85	0.15
Pan	1.5	993.41	100.00	0.00
CALCULATION				
D_{30}= 0.648 mm, D_{50}=0.91mm, D_{60}= 1.17 mm, D_{10}= 0.43 mm				
Coefficient of Uniformity, Cu= D_{60}/D_{10} = 2.81				
Coefficient of Curvature, Cc= $D_{30}^2/(D_{60}\times D_{10})$ = 0.86				

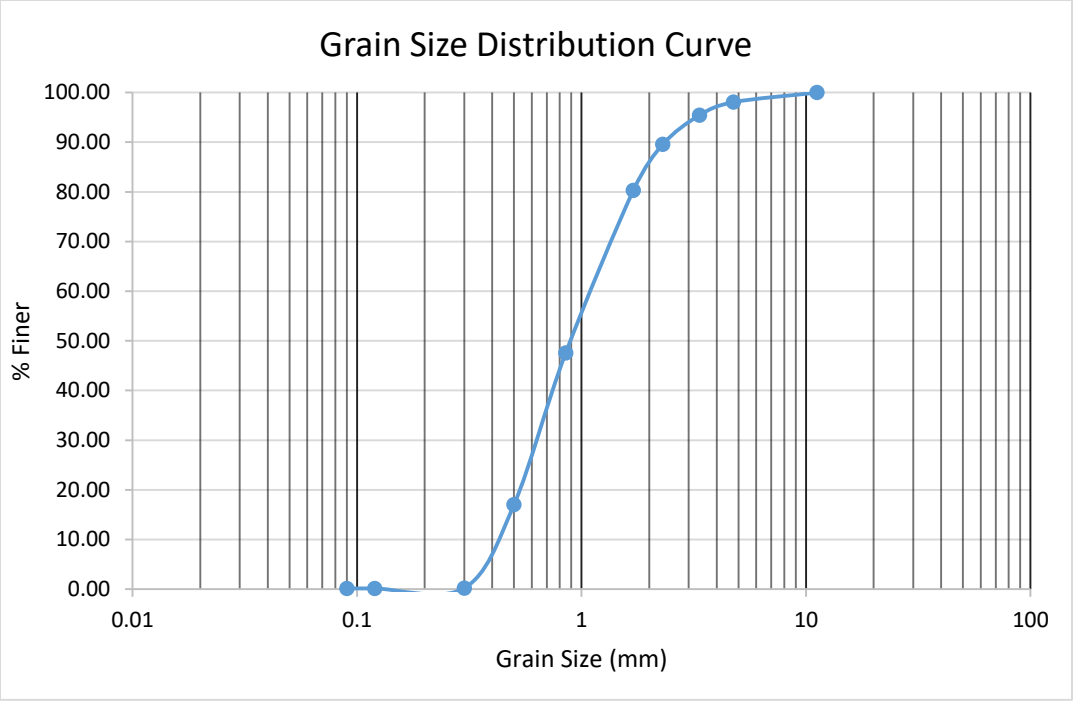


Figure 6.17: IS sieve aperture dimension (mm) versus cumulative % passing as per Sieve analysis for observation well-2 (depth 25m to 40m)

Table 6.12: Mechanical Analysis of Observation Well-3 (depth 6m to 25m)

Sieve Size (mm)	**Weight Retained (gms)**	**Cumulative Weight Retained (gms)**	**% of Cum. Wt. Retained**	**% Finer**
11.2	1.7	1.7	0.17	99.83
4.75	21.53	23.23	2.33	97.67
3.35	14.3	37.53	3.77	96.23
2.3	27.85	65.38	6.56	93.44
1.7	44.13	109.51	10.99	89.01
0.85	238.24	347.75	34.90	65.10
0.5	406.4	754.15	75.69	24.31
0.3	241.19	995.34	99.90	0.10
0.12	0.04	995.38	99.91	0.09
0.09	0.04	995.42	99.91	0.09
Pan	0.9	996.32	100.00	0.00

CALCULATION
D_{30}= 0.55 mm, D_{50}=0.72mm, D_{60}= 0.806mm, D_{10}= 0.40 mm
Coefficient of Uniformity, Cu= D_{60}/D_{10} = 2.11
Coefficient of Curvature, Cc= $D_{30}^2/(D_{60}\times D_{10})$ = 0.97

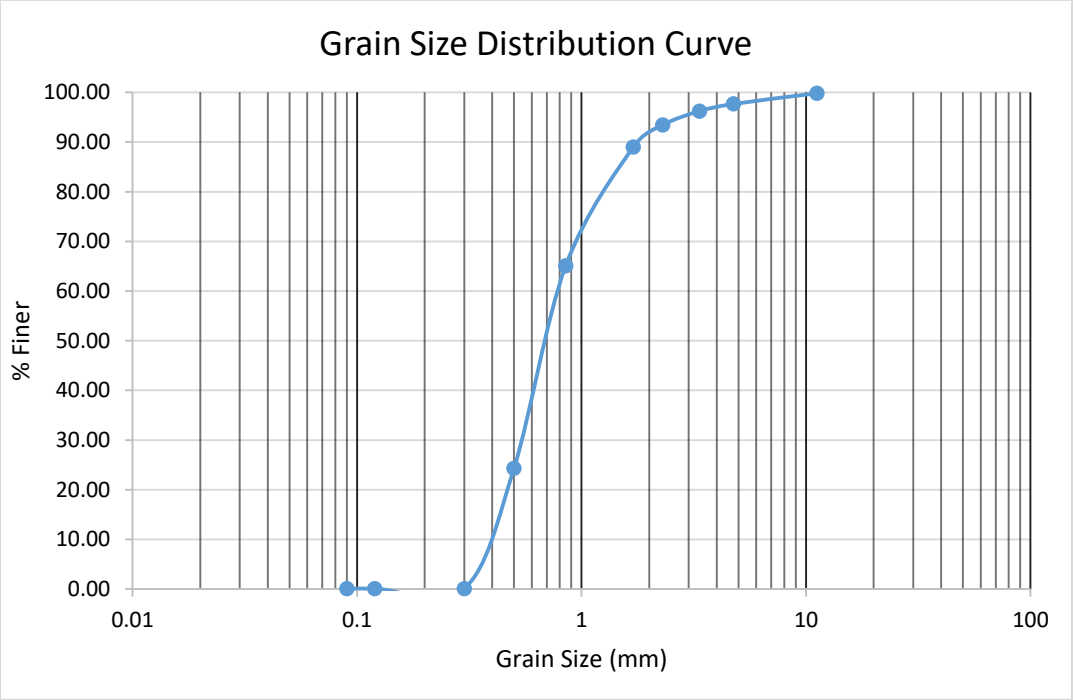


Figure 6.18: IS sieve aperture dimension (mm) versus cumulative % passing as per Sieve analysis for observation well-3 (depth 6m to 25m)

Table5 6.13: Mechanical Analysis of Observation Well-3 (depth 25m to 40m)

Sieve Size (mm)	**Weight Retained (gms)**	**Cumulative Weight Retained (gms)**	**% of Cum. Wt. Retained**	**% Finer**
11.2	0	0	0.00	100.00
4.75	17.52	17.52	1.77	98.23
3.35	22.66	40.18	4.05	95.95
2.3	54.18	94.36	9.51	90.49
1.7	82.25	176.61	17.81	82.19
0.85	290.45	467.06	47.09	52.91
0.5	274.29	741.35	74.74	25.26

0.3	247.97	989.32	99.74	0.26
0.12	0.22	989.54	99.77	0.23
0.09	0.1	989.64	99.78	0.22
Pan	2.22	991.86	100.00	0.00
CALCULATION				
D_{30}= 0.56 mm, D_{50}=0.81mm, D_{60}= 1.05mm, D_{10}= 0.38 mm				
Coefficient of Uniformity, Cu= D_{60}/D_{10} = 2.79				
Coefficient of Curvature, Cc= $D_{30}^2/(D_{60}\times D_{10})$ = 0.82				

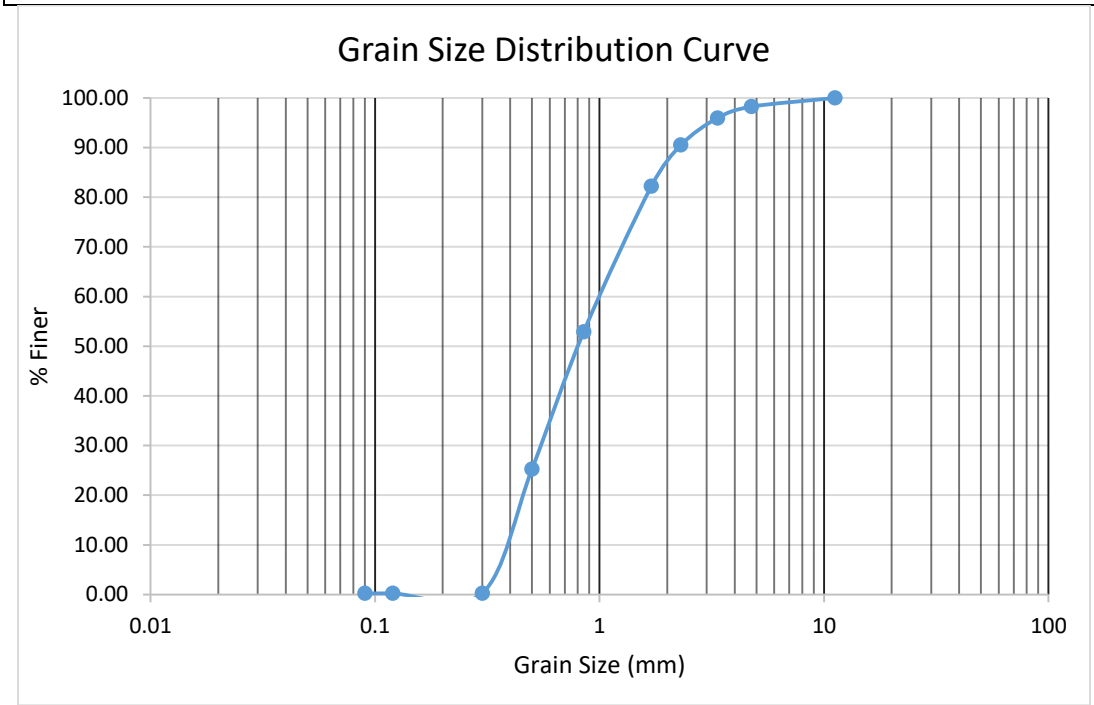


Figure 6.19: IS sieve aperture dimension (mm) versus cumulative % passing as per Sieve analysis for observation well-3 (depth 25 m to 40 m)

Based on the grain size distribution data, it is observed that the Coefficient of Uniformity (C_u) mostly varies from 1.8 to 2.4 for the main well. Based on the analysis, an artificial gravel pack around the pumping well is required as the Coefficient of Uniformity is found less than 3.0. The gravel pack materials should have a Coefficient of Uniformity less than 2.5. For determination of the gravel size, D_{30} can be considered and around 4 to 6 times of D_{30} can be selected for artificial gravel packing.

6.7: Hydraulic Analysis By WaterGEMS

The ultimate design demand of the study area has been calculated using data collected from WBPHED, BARDHAMAN. The design demand is determined considering total demand. All the calculation have been made as per CPHEEO Manual 1999 and WBPHED Schedule. . Considering 30 years design year the projected population from year 2022 to year 2052 of each Mouza are given in below table.

Table 6.14 Water demand for the water supply scheme Galsi-1 Block

BLOCK	SL NO		SCHME NAME	MOUZA NAME	JLNo	2022	2052	Water Demand (KLD)	TOTAL Demand (KLD)
GALSI-I	1	SHILLA	ZONE-I (BAMUNARA)	KARKONA	58	2903	3743	253	1120
				BAMUNARA	59	1430	1796	121	
				NABAKHANDA	60	1653	2219	150	
				BIRINGPUR	61	562	782	53	
				SILLA	62	1417	1813	122	
				RAM GOPALPUR	63	4864	6234	421	
	2		ZONE-II (PARAJ)	PARAJ (85%)	48	5268	6747	456	976
				SIHIGRAM	49	875	1100	74	
				BHIMSARA	50	596	762	51	
				RANADI	51	749	1121	76	
				BOLPUR	52	895	1167	79	
				KARAKDAL	53	997	1300	88	
				MALLATIKAR	54	471	600	41	
				KHURAJ	82	1254	1640	111	
	3		ZONE-III (LOA)	JAGULPARA	55	3265	4187	283	1033
				LOA	56	4157	5431	367	
				DHARMAPUR	57	4413	5667	383	
	4		ZONE-IV (RAKONA)	KHAMARGRAM	39	698	921	62	1283
				KHANPARA	40	1343	1807	122	
				KONDAIPUR	41	1585	2075	140	
				NURKONA	42	1198	1508	102	
				SIMNARI	44	4183	5602	378	
				RAKONA	45	1090	1445	98	
				JHARUL	46	3030	4376	296	
				JOT KOLKOL	47	40	69	5	
				PARAJ (15%)	48	930	1191	80	
				Purandargar	87	1505	1966	133	
				Uchchagram	88	5648	7752	524	
				Kutruki	93	2037	2670	180	

Water demand for the water supply scheme considering intake at Silla for Zone-I (Bamunara), Zone-II (Paraj), Zone-III (Loa) and Zone-IV(Rakona), water Supply scheme for a total demand of (1120+736+1033+1283) = 4412 KLD ≈ 4500 KLD. As per requirement from PHED, the projected water demand is considered 8000 KLD.
But we take only one Zone -1 (Bamunara) for hydraulic model analysis by WaterGEMS software.Demand of Shillya Zone-1 Bamunara village is 1120 KLD.

Table 6.15 Water Demand Shilla Zone-1 Bamunara village

DEMAND CALCULATION SHEET								
SL NO	BLOCK NAME	SCHEME NAME	MOUZA NAME NAME	JL NO	BASE YEAR POPULATION 2022	ULTIMATE YEAR POPULATION 2052	ULTIMATE YEAR WATER DEMAND(KLD)	TOTAL DEMNAD (KLD)
1	GALSI-I	SHILLA- ZONE-I (BAMUNARA)	KARKONA	58	2903	3743	253	1120
2			BAMUNARA	59	1430	1796	121	
3			NABAKHANDA	60	1653	2219	150	
4			BIRINGPUR	61	562	782	53	
5			SILLA	62	1417	1813	122	
6			RAM GOPALPUR	63	4864	6234	421	
PER CAPITA DEMAND= 55 LPCD								
ESR CAPACITY= 350 KL								

For optimal design purpose a part of water supply network of Shilla Zone-1 Bamunara village area is considered. Pipes are laid of various materials such as HDPE. for the distribution system. Primarily, reservoir was a focal point from where the pipes and nodes will be drawn through Water GEMS software. Elevation and flow direction were automatically taken from the input parameters by the software. While digitizing the pipe line and the nodes care were taken elevation was considered from the previous level was considered. Then the network is designed as

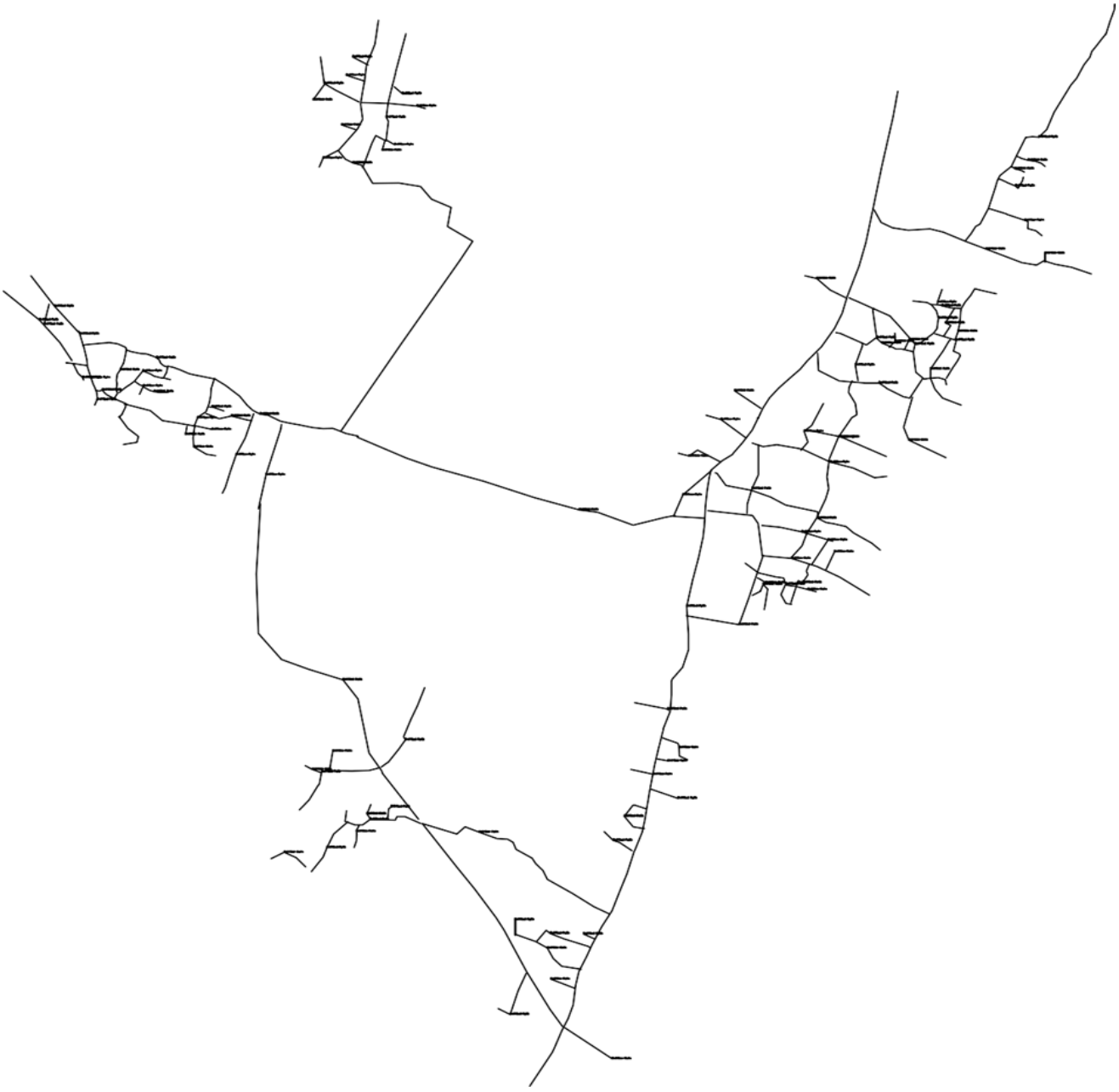


Figure 6.20: Network Water Demand Shilla Zone-1 Bamunara village

In the given network the HDPE pipe and DIK-7 are used and the different length of pipe show different diameters and for distribution of pipe the radial method is used. In the given network different diameter of pipes are shown in different length and the details are as shown in tables.

Table6.16: Details of Pipe diameter, Length and materials

PIPE SUMMARY			
Diameter (mm)	Length (HDPE) (m)	Length (DI K-7) (m)	Length (All Materials) (m)
90	21,805	0	21,805
110	4,383	0	4,383
125	4,328	0	4,328
140	728	0	728
160	548	0	548
180	565	0	565
200	688	0	688
250	0	38	38
All Diameters	33,042	38	33,080
HDPE PIPE - PE-100, PN-6			

Then the complete network is designed and finally the network is computed. After computation of network the next step is to validate the results and if there are errors in network then those errors are adjusted and further the network is validate. Finally, the results for pipe network are obtained and the table is given in annexure 1.

After finalizing, all the pipes and the nodes, inputs such as demand and the pipe material will be provided to the software. Software takes into consideration of the elevation, contour, demand, pipe material and other parameters. A simulation was carried out by the software's, were it decides the diameter of the pipe and flow direction and flow quantity along with the drawing

profile and the results of junctions are given in annexure 2.

The critical path is a path which is originated from the overhead tank T1 ended at an extreme consumer end of junction J-244. The length of the longest path is 3200m.The model result shows in Figure 6.21

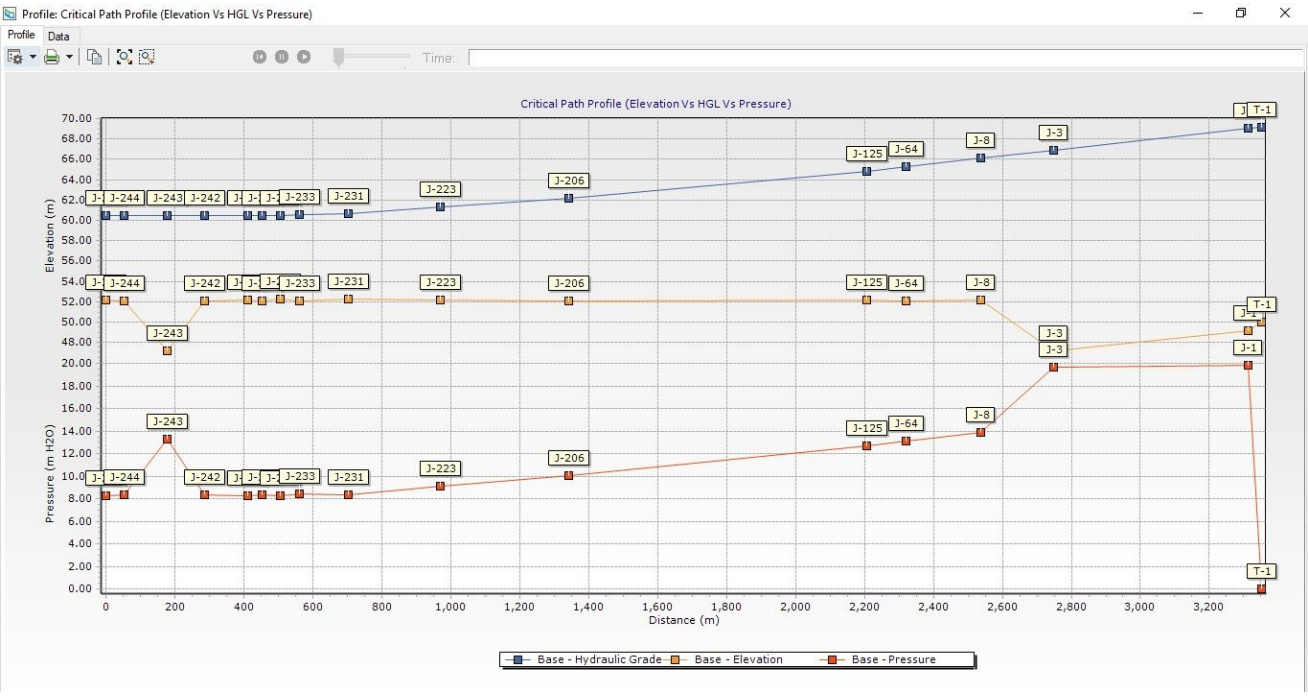


Figure 6.21: Critical Path Profile (Critical Point To OHR Path) Lowest Point -J-245 Elevation Vs Hgl Vs Pressurefor Shillya- Zone-I-Bamunara

Table 6.17: Details of Over head Reservoir

DESIGN METHOD CONSIDERATION	UNIT LINE METHOD					
TERMINAL PRESSURE	7 m H20					
TANK DETAILS						
Label	Elevation (Base) (m)	Elevation (Minimum) (m)	Elevation (Initial) (m)	Elevation (Maximum) (m)	Flow (Out net) (L/s)	Hydraulic Grade (m)
T-1	68	68.1	68.15	72	38.889	68.15
TANK HEIGHT=	20 M					
RISING MAIN LENGTH=	1790 M	150 MM DIA DI K-9 PIPE				

CHAPTER-7 CONCLUSIONS, LIMITATION AND FUTURE SCOPE

The comprehensive assessment of hydrogeological characteristics and the design of a sustainable water supply system for rural areas of Shilla village, Purba Bardhaman in the district of West Bengal have yielded significant insights and outcomes. Through pumping tests and Vertical Electrical Sounding (VES) surveys, essential aquifer properties and lithological details were determined, facilitating the development of a robust water extraction and distribution strategy. The lithological analysis revealed a stratified subsurface structure dominated by clayey soils, blackish clay thickness 12m and various sand layers thickness 12m to 36m providing crucial information for aquifer characterization and well field design. Pumping tests conducted elucidated aquifer transmissivity and storativity. The average transmissivity is 2414 m^2/day and average storativity is 0.1209 obtained from pumping test and average transmissivity in recuperation test is 2795 m^2/day ,essential parameters for understanding groundwater flow dynamics and designing efficient well fields. Based on the hydraulic parameters obtained from pumping tests, a well field design comprising ten wells spaced strategically to yield the required water volume each well having capacity of 800 m^3/day and spaced 50m apart from the center well without exceeding specified drawdown limits 2.55m was proposed. Additionally, mechanical analysis of bore well materials informed the selection of appropriate gravel pack materials, the Coefficient of Uniformity (C_u) mostly varies from 1.8 to 2.4 for the main well. Based on the analysis, an artificial gravel pack around the pumping well is required as the Coefficient of Uniformity is found less than 3.0. The gravel pack materials should have a Coefficient of Uniformity less than 2.5. for well construction.Furthermore, hydraulic analysis using Water GEMS software facilitated the simulation and optimization of the water distribution network, ensuring reliable and efficient water supply to target areas. At extreme consumer end of junction J-244 values of minimum pressure is 8.25m of H2O which is within the limit as per CPHEEO manual ($\geq$ 7m of H2O). The projected water demand for the study area of Village Shilla up to the year 2052 was estimated, guiding the sizing and planning of the water supply scheme.

Limitation:

Despite the significant insights gained from this research, certain limitations should be acknowledged:

- The accuracy and reliability of results are contingent upon the quality and representativeness of the data collected. Addressing data gaps and uncertainties is essential for robust decision-making.
- Simplifications and assumptions made in modeling approaches may introduce uncertainties and limitations in the predictive accuracy of the water supply system.
- The study's spatial and temporal scale may limit the generalizability of findings to larger regions or longer timeframes, necessitating caution in extrapolating results.

Future Scope:

- While this study provides valuable insights into hydrogeological characteristics and water supply system design, several avenues for future research and improvement exist:
- Long-term Monitoring: Continuous monitoring of groundwater levels and quality will provide insights into seasonal variations and long-term trends, aiding in sustainable groundwater management.
- Climate Change Impacts: Considering the potential impacts of climate change on groundwater resources and water demand patterns is essential for future planning and adaptation strategies.
- Advanced Modeling Techniques: Utilizing advanced modeling techniques and data analytics for predictive modeling and scenario analysis can improve the accuracy and efficiency of water distribution network optimization.

REFERENCES

1. Das, S. (2006). Study of pipeline network system and temporal decay of chlorine for the water treatment plant at Dakshin Raipur, West Bengal, M.E. Thesis. School of Water Resources Engineering, Jadavpur University, Kolkata, India.

2. Izquierdo, J., Montalvo, J., Perez, R., Herrena, M. (2008). Sensitivity analysis to assess the relative importance of pipes in water distribution networks. Mathematical and Computer Modelling, 48(1-2), 268—278.

3. Liana, V., Vlad, P. (2008). INFOWORKS WS and EPANET V2- Modelling the water distribution networks, UPB Scientific Bulletin, Seriess D, 70(4), 91-102.

4. Koppel, T.,Vassiljcv, A. (2009). Calibration of a model of an operational water distribution system containing pipes of different age. Advances in Engineering Software, 40(8), 659—664.

5.Arunkurmar, M.,Nethaji, M.V.E. (2011). Water Demand Analysis of Municipal Water Supply using EPANET Software. International Journal of Applied Bioengineering, 5(1), 9-19.

6. S., Mukherjee, B., Mazumdar, A. (2013). Analysis of Hammer Head at Increased Flow Demand in Pipe Networks: A Case Study. International Review of Mechanical Engineering, 7(4), 757-766.

7. Sarkar, P.K. (2014). Extended Period Simulations of Pipeline Distribution Network of Garfa Boosting Station by Hammer and Water GEMS Softwares. M.E.Thesis. School of Water Resources Engineering, Jadavpur University, Kolkata, India.

8.Mukherjee, B., Das, S., Mazumdar, A., Sarkar, P. (2015a). Management in Real time Operation of Drinking Water pipeline Distribution Network: A case study. 47th IWWA Annual Convention, 298-303.

9.Mukherjee, B., Das, S., Mazumdar, A. (2015b). Transient Analysis of a Pipeline Network for Drinking Purpose in Assam, India. Journal of the Institution of Public Health Engineers, India, 2014-15 (4), 26-32.

10..Mandal, S. (2015). Pipeline analysis of ash slurry disposal system of (2x520) MW Thermal Power Station by HAMMER software. M.E. Thesis. School of Water Resources Engineering, Jadavpur University, Kolkata, India.

11. Das, M. (2015). Design of Landscape Irrigation System by AutoCAD Software and Simulations of Pipeline Distribution Network of a proposed site by Hammer and WaterGEMSSoftwares. M.E. Thesis. School of Water Resources Engineering, Jadavpur University, Kolkata, India.

12. Mukherjee B., Das S. and Mondal S. (2016). A captive Power Plant Behavior of Stresses in Steam Pipelines of under Various Loading Conditions: A Case Study. 103rd Indian science Congress Conference, ISCA, University of Mysore, India.

13. Ganguly S. (2016). Hydraulic Analysis for a Composite Piped Water Supply Network

using EPANET Software: A Case Study. M.E.Thesis, School of Water Resources Engineering, Jadavpur University, Kolkata, India.
14. Saha, B.K. (2016). Transient Analysis of Purulia Piped Water Supply Line using HAMMER Software. M.E. Thesis.School of Water Resources Engineering, Jadavpur University, Kolkata, India.
15. Sarkar, K. (2016). Energy Estimation of Garden Reach Water Works and Its Water Transmission for Calcutta City Grid. M.E.Thesis. School of Water Resources Engineering, Jadavpur University, Kolkata, India.
16. Halder, K. (2016). Comparison between EPANET and LOOP Softwares using a Gravity Flow Water Supply Network. M.E. Thesis. School of Water Resources Engineering, Jadavpur University, Kolkata,India.
17.Mukherjee, B., Das, S., Mazumdar, A. (2017). Stress analysis of smart support system for a steam pipeline of Sagardighi Thermal Power Plant, West Bengal, India.
International Journal of Innovative and Emerging Research in Engineering, 4(1),137-146.
18.Debnath, K.(2019). Study of Water Distribution Network of Bhogpur G.P at Panskura in West Bengal by WATERCAD Software. M.E. Thesis. School of Water Resources Engineering, Jadavpur University, Kolkata, India.
19. Dashti, Z., Nakhaei, M., Vadiati, M., Karami, G.H., Kisi, O. (2022). A literature review on pumping test analysis. Environmental Science and Pollution Research, 30, 9184–9206, https://doi.org/10.1007/s11356-022-24440-4.
20. Kumbhar, K.S., Baride, M.V., Patil, S.N., Golekar, R.B.(2019). Characterisation of Aquifer Parameters through Pump Test in Selected Watersheds of Kolhapur District, Maharashtra. Journal of Geosciences Research, 4(1), 57-60.
21. Zahid, A., Jeffrey., Hassan, M. Q., Clark, D.W., Das, S. C.(2008).Pumping test data analysis and characterization of deep aquifer in the lower delta floodplain at madaripur ,southern bangladesh in Drinking Water Contamination. Toxicity and Treatment. ISBN 978-1-60456- 747-2 Eds: Javier D. Romero and Pablo S. Molina, pp. © 2008 Nova Science Publishers, Inc., Chapter 11, 1-15.
22. Amah E. A., Anam G. S. (2016). Determination of Aquifer Hydraulic Parameters from Pumping Test Data Analysis: A Case Study of Akpabuyo Coastal Plain Sand Aquifers, Cross River State, S-E Nigeria. IOSR Journal of Applied Geology and Geophysics (IOSR-JAGG), e-ISSN, 2321–0990, p-ISSN,2321–0982, 4(1), 01-08.
23. Merritt, M.L. (1986). Recovering fresh water stored in saline limestone aquifers. Ground Water, 24(4), 516-529.
24.Trefry, M.G., and Johnston, C.D. (1996). Hydrologic modelling and design emplacement strategies for amendment solutions. CSIRO Division of Water Resources Technical Memorandum 96.30.
25. Dillon. P., and Kookana R. (2002). ASRRI: A predictive index of contaminant attenuation during aquifer storage and recovery. In: Management of Aquifer Recharge for Sustainability, Proceedings of the 4th International Symposium on Artificial Recharge

(ISAR4), Eds: P.J. Dillon Adelaide, Swets & Zeitlinger, Lisse, ISBN. 90 5809 527 4, 69-74.
26. Fildebrandt, S., Pavelic, P., Dillon, P. and Prawoto, N. (2003). Recharge enhancement using single or dual well systems for improved groundwater management in the Bandung Basin,Indonesia.CSIROTechnicalReport29/03.
http://www.clw.csiro.au/publications/technical2003/tr29-03.pdf
27.Chandra,S ., Dewandel ,B., Dutta,S ., Ahmed,S.(2009). Geophysical model of geological discontinuities in a granitic aquifer: Analyzing small scale variability of electrical resistivity for groundwater occurrences, Journal of Applied Geophysics
journal homepage: www. e lsevier.com/locate/jappgeo, 71 (2010) ,137–148.
28.Taufiq, Maharani, H.D. Mega, Application of Vertical Electrical Sounding (VES) Resistivity Method to determine a well recommendation point at deep-groundwater exploitation, JEMT, 1(2), 71 – 76.
29.Manual on Water Supply and Treatment (1999). Central Public Health and Environmental Engineering,Govt. of India.

ANNEXURE-1

Output Parameters for Hydraulic Analysis

PIPE TABLE												
Label	Start Node	Stop Node	Length (Scaled) (m)	Diameter (mm)	Material	Headloss Gradient (m/km)	Hazen-Williams C	Flow (L/s)	Velocity (m/s)	Headloss (m)	Hydraulic Grade (Stop) (m)	Pressure (Stop) (m H2O)
P-1	T-1	J-1	38	250	DI K-7	2.368	140	38.889	0.79	0.09	68.06	18.86
P-2	J-1	J-2	337	200	HDPE	3.725	145	21.871	0.85	1.26	66.8	19.52
P-3	J-2	J-4	350	200	HDPE	3.599	145	21.467	0.84	1.26	65.54	18.42
P-4	J-3	J-1	565	180	HDPE	3.867	145	16.444	0.81	2.18	68.06	18.86
P-5	J-3	J-101	1,438	125	HDPE	1.297	145	3.488	0.36	1.87	64.01	10.88
P-6	J-4	J-5	88	160	HDPE	2.702	145	9.916	0.62	0.24	65.3	18.16
P-7	J-5	J-9	136	160	HDPE	2.636	145	9.784	0.61	0.36	64.95	17.75
P-8	J-6	J-4	110	160	HDPE	3.402	145	11.229	0.7	0.37	65.54	18.42
P-9	J-6	J-7	30	140	HDPE	1.904	145	5.832	0.47	0.06	65.11	17.99
P-10	J-7	J-9	156	90	HDPE	1.074	145	1.33	0.26	0.17	64.95	17.75
P-11	J-7	J-11	150	125	HDPE	1.915	145	4.305	0.44	0.29	64.83	17.64
P-12	J-8	J-64	215	125	HDPE	3.913	145	6.333	0.65	0.84	64.26	12.14
P-13	J-8	J-3	213	160	HDPE	3.643	145	11.653	0.73	0.78	65.88	18.68

P-14	J-9	J-12	50	140	HDPE	2.715	145	7.064	0.57	0.14	64.81	17.68
P-15	J-9	J-18	174	125	HDPE	1.481	145	3.747	0.38	0.26	64.69	17.47
P-16	J-10	J-8	108	125	HDPE	2.531	145	5.005	0.51	0.27	65.1	12.91
P-17	J-10	J-15	38	90	HDPE	2.35	145	2.03	0.4	0.09	64.74	12.56
P-18	J-11	J-18	104	90	HDPE	1.332	145	1.494	0.29	0.14	64.69	17.47
P-19	J-11	J-22	186	110	HDPE	1.455	145	2.553	0.35	0.27	64.56	17.37
P-20	J-12	J-13	132	90	HDPE	0.013	145	0.124	0.02	0	64.81	17.53
P-21	J-12	J-36	132	140	HDPE	2.5	145	6.756	0.55	0.33	64.48	12.24
P-22	J-13	J-14	39	90	HDPE	0.001	145	0.023	0	0	64.81	17.68
P-23	J-15	J-16	144	90	HDPE	0.056	145	0.269	0.05	0.01	64.73	12.61
P-24	J-16	J-17	157	90	HDPE	0.008	145	0.092	0.02	0	64.73	12.54
P-25	J-18	J-40	174	110	HDPE	1.271	145	2.374	0.32	0.22	64.47	12.29
P-26	J-18	J-61	278	110	HDPE	1.336	145	2.438	0.33	0.37	64.32	17.1
P-27	J-19	J-15	73	90	HDPE	1.532	145	1.611	0.32	0.11	64.74	12.56
P-28	J-20	J-21	187	90	HDPE	0.219	145	0.564	0.11	0.04	64.56	17.34
P-29	J-20	J-6	386	140	HDPE	1.479	145	5.088	0.41	0.57	65.17	17.97
P-30	J-21	J-24	191	90	HDPE	0.087	145	0.342	0.07	0.02	64.54	17.27
P-31	J-22	J-47	102	90	HDPE	1.861	145	1.79	0.35	0.19	64.37	17.12
P-32	J-23	J-22	69	90	HDPE	0.212	145	0.553	0.11	0.01	64.56	17.37
P-33	J-23	J-29	121	90	HDPE	0.078	145	0.323	0.06	0.01	64.53	17.29
P-34	J-24	J-26	54	90	HDPE	0.04	145	0.226	0.04	0	64.54	17.26
P-35	J-24	J-23	21	90	HDPE	0.002	145	0.041	0.01	0	64.54	17.35
P-36	J-25	J-23	56	90	HDPE	0.001	145	0.033	0.01	0	64.54	17.35
P-37	J-26	J-28	104	90	HDPE	0.004	145	0.061	0.01	0	64.54	17.35
P-38	J-27	J-26	61	90	HDPE	0.001	145	0.036	0.01	0	64.54	17.26
P-39	J-29	J-30	103	90	HDPE	0.003	145	0.06	0.01	0	64.53	17.34
P-40	J-29	J-31	112	90	HDPE	0.004	145	0.066	0.01	0	64.53	17.35

P-41	J-32	J-10	193	110	HDPE	1.699	145	2.776	0.38	0.33	64.83	12.71
P-42	J-33	J-34	59	90	HDPE	0.001	145	0.035	0.01	0	64.49	12.29
P-43	J-33	J-32	113	110	HDPE	0.071	145	0.499	0.07	0.01	64.5	12.32
P-44	J-35	J-19	101	90	HDPE	1.357	145	1.509	0.3	0.14	64.63	12.5
P-45	J-35	J-33	27	110	HDPE	0.036	145	0.347	0.05	0	64.49	12.29
P-46	J-36	J-37	115	90	HDPE	0.015	145	0.133	0.03	0	64.48	17.2
P-47	J-36	J-40	51	90	HDPE	0.254	145	0.61	0.12	0.01	64.47	12.29
P-48	J-36	J-65	130	140	HDPE	1.861	145	5.76	0.47	0.24	64.24	12
P-49	J-37	J-38	56	90	HDPE	0.001	145	0.033	0.01	0	64.48	17.35
P-50	J-39	J-35	34	110	HDPE	0.731	145	1.761	0.24	0.02	64.49	12.32
P-51	J-40	J-68	157	110	HDPE	1.68	145	2.759	0.37	0.26	64.2	11.94
P-52	J-41	J-42	64	90	HDPE	0.001	145	0.037	0.01	0	64.44	12.21
P-53	J-41	J-43	83	90	HDPE	0.019	145	0.151	0.03	0	64.44	12.31
P-54	J-41	J-39	32	110	HDPE	0.702	145	1.723	0.23	0.02	64.47	12.34
P-55	J-43	J-44	87	90	HDPE	0.003	145	0.051	0.01	0	64.44	12.27
P-56	J-45	J-46	38	90	HDPE	0	145	0.023	0	0	64.41	12.28
P-57	J-45	J-41	27	90	HDPE	1.203	145	1.414	0.28	0.03	64.44	12.21
P-58	J-47	J-50	66	90	HDPE	0.512	145	0.891	0.18	0.03	64.33	17.21
P-59	J-47	J-56	111	90	HDPE	0.357	145	0.734	0.14	0.04	64.33	17.11
P-60	J-48	J-32	174	110	HDPE	0.922	145	1.996	0.27	0.16	64.5	12.32
P-61	J-48	J-63	56	110	HDPE	0.77	145	1.81	0.25	0.04	64.3	12.06
P-62	J-49	J-48	43	90	HDPE	0.001	145	0.025	0	0	64.34	12.2
P-63	J-50	J-52	9	90	HDPE	0.267	145	0.628	0.12	0	64.33	17.15
P-64	J-51	J-50	82	90	HDPE	0.024	145	0.172	0.03	0	64.33	17.21
P-65	J-52	J-54	112	90	HDPE	0.028	145	0.184	0.04	0	64.33	17.05
P-66	J-52	J-58	56	90	HDPE	0.086	145	0.34	0.07	0	64.32	17.14
P-67	J-53	J-51	105	90	HDPE	0.004	145	0.062	0.01	0	64.33	17.09

P-68	J-54	J-55	17	90	HDPE	0	145	0.01	0	0	64.33	17.17
P-69	J-56	J-54	80	90	HDPE	0.003	145	0.051	0.01	0	64.33	17.05
P-70	J-56	J-61	76	90	HDPE	0.137	145	0.437	0.09	0.01	64.32	17.1
P-71	J-57	J-56	163	90	HDPE	0.008	145	0.096	0.02	0	64.33	17.11
P-72	J-58	J-59	80	90	HDPE	0.002	145	0.047	0.01	0	64.32	17.05
P-73	J-58	J-60	182	90	HDPE	0.01	145	0.107	0.02	0	64.32	17.2
P-74	J-61	J-62	266	90	HDPE	0.02	145	0.156	0.03	0.01	64.31	17.19
P-75	J-61	J-99	222	110	HDPE	1.126	145	2.223	0.3	0.25	64.07	16.85
P-76	J-63	J-67	111	110	HDPE	0.694	145	1.712	0.23	0.08	64.22	12.11
P-77	J-64	J-125	115	125	HDPE	3.694	145	6.139	0.63	0.43	63.83	11.69
P-78	J-65	J-66	121	90	HDPE	0.005	145	0.071	0.01	0	64.24	11.18
P-79	J-65	J-148	400	125	HDPE	2.82	145	5.306	0.54	1.13	63.11	10.94
P-80	J-67	J-88	169	90	HDPE	0.472	145	0.854	0.17	0.08	64.14	11.94
P-81	J-68	J-69	78	90	HDPE	0.032	145	0.2	0.04	0	64.2	10.97
P-82	J-68	J-99	109	110	HDPE	1.255	145	2.357	0.32	0.14	64.07	16.85
P-83	J-69	J-70	131	90	HDPE	0.005	145	0.077	0.02	0	64.2	11.94
P-84	J-71	J-67	81	90	HDPE	0.282	145	0.646	0.13	0.02	64.22	12.11
P-85	J-72	J-45	238	90	HDPE	0.906	145	1.213	0.24	0.22	64.41	12.18
P-86	J-72	J-75	49	90	HDPE	0.388	145	0.767	0.15	0.02	64.18	11.94
P-87	J-73	J-72	236	90	HDPE	0.016	145	0.139	0.03	0	64.2	12.01
P-88	J-74	J-76	76	90	HDPE	0.126	145	0.419	0.08	0.01	64.17	11.96
P-89	J-74	J-71	95	90	HDPE	0.204	145	0.542	0.11	0.02	64.2	12.17
P-90	J-75	J-84	54	90	HDPE	0.328	145	0.701	0.14	0.02	64.16	12.04
P-91	J-75	J-74	24	90	HDPE	0	145	0.008	0	0	64.18	12.06
P-92	J-76	J-77	36	90	HDPE	0.024	145	0.172	0.03	0	64.17	12.03
P-93	J-76	J-78	50	90	HDPE	0.019	145	0.151	0.03	0	64.17	12.04

P-94	J-77	J-79	4	90	HDPE	0.018	145	0.148	0.03	0	64.17	11.9
P-95	J-78	J-83	104	90	HDPE	0.004	145	0.061	0.01	0	64.17	12.05
P-96	J-79	J-81	44	90	HDPE	0.007	145	0.084	0.02	0	64.17	12.03
P-97	J-79	J-80	31	90	HDPE	0	145	0.018	0	0	64.17	11.96
P-98	J-81	J-82	50	90	HDPE	0.001	145	0.029	0.01	0	64.17	11.9
P-99	J-84	J-85	25	90	HDPE	0.289	145	0.654	0.13	0.01	64.15	11.89
P-100	J-85	J-86	60	90	HDPE	0.001	145	0.035	0.01	0	64.15	11.89
P-101	J-87	J-85	52	90	HDPE	0.202	145	0.539	0.11	0.01	64.15	11.89
P-102	J-88	J-90	77	90	HDPE	0.075	145	0.316	0.06	0.01	64.13	11.87
P-103	J-89	J-91	139	90	HDPE	0.05	145	0.254	0.05	0.01	64.13	12
P-104	J-89	J-88	49	90	HDPE	0.098	145	0.364	0.07	0	64.14	11.94
P-105	J-90	J-87	49	90	HDPE	0.163	145	0.48	0.09	0.01	64.14	12.02
P-106	J-90	J-93	50	90	HDPE	0.32	145	0.692	0.14	0.02	64.12	11.85
P-107	J-91	J-92	146	90	HDPE	0.007	145	0.086	0.02	0	64.13	12.01
P-108	J-93	J-95	76	90	HDPE	0.002	145	0.045	0.01	0	64.12	11.85
P-109	J-93	J-94	27	90	HDPE	0	145	0.016	0	0	64.12	11.97
P-110	J-93	J-96	182	90	HDPE	0.135	145	0.434	0.09	0.02	64.09	11.97
P-111	J-96	J-98	195	90	HDPE	0.012	145	0.115	0.02	0	64.09	11.91
P-112	J-97	J-96	83	90	HDPE	0.002	145	0.049	0.01	0	64.09	11.97

P-113	J-99	J-100	217	90	HDPE	0.014	145	0.128	0.03	0	64.06	16.94
P-114	J-99	J-117	101	125	HDPE	1.727	145	4.071	0.42	0.17	63.89	10.66
P-115	J-101	J-102	169	110	HDPE	0.164	145	0.785	0.11	0.03	63.98	10.75
P-116	J-101	J-104	40	110	HDPE	0.712	145	1.736	0.24	0.03	63.98	10.56
P-117	J-102	J-103	39	90	HDPE	0	145	0.023	0	0	63.98	10.56
P-118	J-102	J-105	8	110	HDPE	0.111	145	0.636	0.09	0	63.98	10.75
P-119	J-104	J-114	74	110	HDPE	0.662	145	1.669	0.23	0.05	63.93	10.87
P-120	J-105	J-106	36	90	HDPE	0.001	145	0.021	0	0	63.98	10.75
P-121	J-105	J-107	89	110	HDPE	0.081	145	0.537	0.07	0.01	63.98	10.74
P-122	J-107	J-108	128	110	HDPE	0.049	145	0.409	0.06	0.01	63.97	10.91
P-123	J-108	J-109	49	90	HDPE	0.004	145	0.064	0.01	0	63.97	10.74
P-124	J-108	J-111	205	90	HDPE	0.013	145	0.12	0.02	0	63.97	10.84
P-125	J-109	J-110	30	90	HDPE	0	145	0.018	0	0	63.97	10.91
P-126	J-112	J-113	135	90	HDPE	0.006	145	0.079	0.02	0	63.96	16.69
P-127	J-112	J-20	390	125	HDPE	1.638	145	3.957	0.4	0.64	64.6	17.41
P-128	J-114	J-115	62	90	HDPE	0.006	145	0.079	0.02	0	63.93	10.51

P-129	J-114	J-120	102	110	HDPE	0.51	145	1.45	0.2	0.05	63.88	10.65
P-130	J-115	J-116	37	90	HDPE	0.001	145	0.021	0	0	63.93	10.87
P-131	J-117	J-119	188	90	HDPE	0.011	145	0.111	0.02	0	63.89	11.72
P-132	J-117	J-143	248	110	HDPE	2.654	145	3.532	0.48	0.66	63.23	11.05
P-133	J-118	J-117	96	90	HDPE	0.003	145	0.057	0.01	0	63.89	10.66
P-134	J-120	J-121	57	90	HDPE	0.001	145	0.033	0.01	0	63.88	10.46
P-135	J-120	J-122	113	110	HDPE	0.392	145	1.257	0.17	0.04	63.84	10.78
P-136	J-122	J-123	200	90	HDPE	0.02	145	0.154	0.03	0	63.83	10.8
P-137	J-122	J-126	150	90	HDPE	0.067	145	0.297	0.06	0.01	63.83	10.8
P-138	J-122	J-129	84	90	HDPE	0.166	145	0.485	0.1	0.01	63.82	10.76
P-139	J-123	J-124	31	90	HDPE	0	145	0.018	0	0	63.83	10.7
P-140	J-126	J-127	75	90	HDPE	0.002	145	0.044	0.01	0	63.83	10.8
P-141	J-126	J-128	103	90	HDPE	0.004	145	0.061	0.01	0	63.83	10.7
P-142	J-129	J-130	69	90	HDPE	0.002	145	0.041	0.01	0	63.82	10.4
P-143	J-129	J-131	66	90	HDPE	0.074	145	0.315	0.06	0	63.82	10.59
P-144	J-131	J-132	58	90	HDPE	0.001	145	0.034	0.01	0	63.82	10.4

P-145	J-131	J-133	177	90	HDPE	0.01	145	0.104	0.02	0	63.82	10.69
P-146	J-134	J-135	80	90	HDPE	0.013	145	0.124	0.02	0	63.69	16.65
P-147	J-134	J-112	103	110	HDPE	2.622	145	3.509	0.48	0.27	63.96	16.72
P-148	J-135	J-136	65	90	HDPE	0.001	145	0.038	0.01	0	63.69	16.47
P-149	J-137	J-138	44	90	HDPE	0.001	145	0.026	0.01	0	63.5	16.37
P-150	J-137	J-134	85	110	HDPE	2.245	145	3.227	0.44	0.19	63.69	16.48
P-151	J-139	J-137	62	110	HDPE	2.072	145	3.09	0.42	0.13	63.5	16.36
P-152	J-140	J-139	81	90	HDPE	0.002	145	0.048	0.01	0	63.37	16.24
P-153	J-141	J-142	106	90	HDPE	0.004	145	0.062	0.01	0	63.27	16.13
P-154	J-141	J-139	56	110	HDPE	1.872	145	2.925	0.4	0.11	63.37	16.24
P-155	J-143	J-145	23	110	HDPE	2.135	145	3.14	0.43	0.05	63.18	10.98
P-156	J-144	J-143	198	90	HDPE	0.012	145	0.116	0.02	0	63.23	11.05
P-157	J-145	J-151	73	90	HDPE	1.925	145	1.822	0.36	0.14	63.04	9.81
P-158	J-146	J-149	103	90	HDPE	0.644	145	1.009	0.2	0.07	63.07	15.94
P-159	J-146	J-141	79	110	HDPE	1.637	145	2.721	0.37	0.13	63.27	16.05
P-160	J-147	J-145	68	90	HDPE	0.917	145	1.221	0.24	0.06	63.18	10.98

P-161	J-148	J-150	116	90	HDPE	0.497	145	0.877	0.17	0.06	63.05	10.85
P-162	J-148	J-174	139	110	HDPE	3.411	145	4.044	0.55	0.48	62.64	10.45
P-163	J-149	J-152	87	90	HDPE	0.518	145	0.897	0.18	0.05	63.02	15.88
P-164	J-150	J-147	88	90	HDPE	0.794	145	1.129	0.22	0.07	63.12	9.89
P-165	J-150	J-153	61	90	HDPE	1.98	145	1.851	0.36	0.12	62.93	9.9
P-166	J-151	J-159	125	90	HDPE	1.704	145	1.706	0.34	0.21	62.83	10.57
P-167	J-152	J-146	77	90	HDPE	1.443	145	1.56	0.31	0.11	63.14	15.99
P-168	J-153	J-155	28	90	HDPE	1.629	145	1.666	0.33	0.05	62.89	9.86
P-169	J-154	J-153	113	90	HDPE	0.004	145	0.066	0.01	0	62.93	9.9
P-170	J-155	J-156	31	90	HDPE	1.566	145	1.631	0.32	0.05	62.84	9.71
P-171	J-156	J-157	28	90	HDPE	0.003	145	0.053	0.01	0	62.84	9.61
P-172	J-156	J-162	54	90	HDPE	1.36	145	1.511	0.3	0.07	62.76	9.7
P-173	J-157	J-158	31	90	HDPE	0	145	0.018	0	0	62.84	9.71
P-174	J-159	J-160	169	90	HDPE	0.057	145	0.273	0.05	0.01	62.82	9.59
P-175	J-159	J-164	92	90	HDPE	0.898	145	1.207	0.24	0.08	62.75	10.64
P-176	J-160	J-161	148	90	HDPE	0.007	145	0.087	0.02	0	62.82	15.64

P-177	J-162	J-172	33	90	HDPE	1.198	145	1.411	0.28	0.04	62.72	10.61
P-178	J-163	J-162	42	90	HDPE	0.001	145	0.025	0	0	62.76	9.7
P-179	J-164	J-165	30	90	HDPE	0.174	145	0.498	0.1	0.01	62.74	10.6
P-180	J-165	J-167	167	90	HDPE	0.009	145	0.098	0.02	0	62.74	10.48
P-181	J-165	J-166	73	90	HDPE	0.002	145	0.043	0.01	0	62.74	10.56
P-182	J-168	J-165	169	90	HDPE	0.009	145	0.099	0.02	0	62.74	10.6
P-183	J-169	J-170	87	90	HDPE	0.01	145	0.106	0.02	0	62.74	15.61
P-184	J-169	J-152	95	90	HDPE	2.971	145	2.304	0.45	0.28	63.02	15.88
P-185	J-170	J-171	47	90	HDPE	0.001	145	0.028	0.01	0	62.74	15.5
P-186	J-172	J-164	114	90	HDPE	0.224	145	0.571	0.11	0.03	62.75	10.64
P-187	J-173	J-172	30	90	HDPE	2.034	145	1.877	0.37	0.06	62.72	10.61
P-188	J-173	J-176	79	90	HDPE	1.008	145	1.285	0.25	0.08	62.58	9.45
P-189	J-174	J-173	315	90	HDPE	0.087	145	0.343	0.07	0.03	62.66	10.43
P-190	J-174	J-175	173	90	HDPE	0.009	145	0.102	0.02	0	62.63	10.43
P-191	J-174	J-204	357	110	HDPE	2.901	145	3.706	0.5	1.04	61.6	9.42
P-192	J-176	J-178	38	90	HDPE	0.345	145	0.72	0.14	0.01	62.57	10.37

P-193	J-176	J-177	63	90	HDPE	0.15	145	0.459	0.09	0.01	62.57	9.15
P-194	J-177	J-179	59	90	HDPE	0.109	145	0.387	0.08	0.01	62.57	10.34
P-195	J-178	J-181	68	90	HDPE	0.048	145	0.25	0.05	0	62.57	9.15
P-196	J-178	J-185	48	90	HDPE	0.106	145	0.38	0.07	0.01	62.56	9.54
P-197	J-179	J-180	68	90	HDPE	0.002	145	0.04	0.01	0	62.57	10.31
P-198	J-179	J-182	21	90	HDPE	0.052	145	0.26	0.05	0	62.57	9.51
P-199	J-181	J-184	66	90	HDPE	0.024	145	0.171	0.03	0	62.56	10.36
P-200	J-182	J-183	62	90	HDPE	0.001	145	0.037	0.01	0	62.57	9.44
P-201	J-182	J-184	63	90	HDPE	0.016	145	0.137	0.03	0	62.56	10.36
P-202	J-184	J-187	22	90	HDPE	0.038	145	0.219	0.04	0	62.56	10.43
P-203	J-185	J-186	38	90	HDPE	0.013	145	0.124	0.02	0	62.56	9.15
P-204	J-186	J-187	90	90	HDPE	0.002	145	0.049	0.01	0	62.56	10.43
P-205	J-187	J-189	172	90	HDPE	0.009	145	0.101	0.02	0	62.56	10.45
P-206	J-188	J-185	175	90	HDPE	0.009	145	0.103	0.02	0	62.56	9.54
P-207	J-190	J-191	359	90	HDPE	0.036	145	0.211	0.04	0.01	62.17	15.05
P-208	J-190	J-169	258	90	HDPE	2.159	145	1.939	0.38	0.56	62.74	15.53

P-209	J-192	J-193	45	90	HDPE	0.001	145	0.026	0.01	0	62.07	14.83
P-210	J-192	J-190	110	90	HDPE	1.029	145	1.3	0.26	0.11	62.18	15
P-211	J-194	J-195	154	90	HDPE	0.119	145	0.405	0.08	0.02	62.02	14.89
P-212	J-194	J-192	37	90	HDPE	0.834	145	1.16	0.23	0.03	62.07	14.93
P-213	J-195	J-197	74	90	HDPE	0.056	145	0.271	0.05	0	62.02	14.75
P-214	J-196	J-198	154	90	HDPE	0.006	145	0.078	0.02	0	62.02	14.89
P-215	J-196	J-194	91	90	HDPE	0.238	145	0.59	0.12	0.02	62.04	14.77
P-216	J-197	J-199	78	90	HDPE	0.011	145	0.114	0.02	0	62.02	14.75
P-217	J-198	J-197	47	90	HDPE	0.002	145	0.04	0.01	0	62.02	14.75
P-218	J-199	J-200	58	90	HDPE	0.001	145	0.034	0.01	0	62.02	14.89
P-219	J-201	J-202	92	90	HDPE	0.003	145	0.054	0.01	0	62.01	14.77
P-220	J-201	J-196	77	90	HDPE	0.078	145	0.323	0.06	0.01	62.02	14.75
P-221	J-203	J-201	145	90	HDPE	0.007	145	0.085	0.02	0	62.01	14.8
P-222	J-204	J-207	376	110	HDPE	1.647	145	2.73	0.37	0.62	60.98	8.84
P-223	J-204	J-205	464	90	HDPE	0.057	145	0.273	0.05	0.03	61.57	9.43
P-224	J-206	J-125	865	125	HDPE	3.078	145	5.563	0.57	2.66	63.83	11.69

P-225	J-207	J-208	79	90	HDPE	0.209	145	0.55	0.11	0.02	60.96	7.95
P-226	J-207	J-212	152	90	HDPE	1.926	145	1.823	0.36	0.29	60.69	8.43
P-227	J-208	J-209	225	90	HDPE	0.101	145	0.371	0.07	0.02	60.94	7.88
P-228	J-209	J-210	30	90	HDPE	0	145	0.018	0	0	60.94	7.52
P-229	J-209	J-211	173	90	HDPE	0.009	145	0.101	0.02	0	60.94	8.76
P-230	J-212	J-213	137	90	HDPE	0.031	145	0.195	0.04	0	60.68	8.26
P-231	J-212	J-215	122	90	HDPE	1.16	145	1.386	0.27	0.14	60.54	7.42
P-232	J-213	J-214	98	90	HDPE	0.003	145	0.057	0.01	0	60.68	8.42
P-233	J-215	J-216	127	90	HDPE	0.005	145	0.075	0.01	0	60.54	8.32
P-234	J-215	J-217	68	90	HDPE	0.788	145	1.125	0.22	0.05	60.49	7.44
P-235	J-217	J-218	49	90	HDPE	0.001	145	0.029	0.01	0	60.49	7.44
P-236	J-217	J-219	48	90	HDPE	0.632	145	0.999	0.2	0.03	60.46	8.33
P-237	J-219	J-220	113	90	HDPE	0.004	145	0.066	0.01	0	60.46	8.33
P-238	J-219	J-221	123	90	HDPE	0.387	145	0.766	0.15	0.05	60.41	8
P-239	J-221	J-222	590	90	HDPE	0.089	145	0.347	0.07	0.05	60.36	8.22
P-240	J-223	J-224	145	90	HDPE	0.087	145	0.341	0.07	0.01	60.28	8.16

P-241	J-223	J-206	372	125	HDPE	2.375	145	4.835	0.49	0.88	61.17	9.05
P-242	J-223	J-226	178	90	HDPE	0.179	145	0.506	0.1	0.03	60.26	8.13
P-243	J-224	J-225	218	90	HDPE	0.014	145	0.128	0.03	0	60.27	8.05
P-244	J-226	J-227	75	90	HDPE	0.002	145	0.044	0.01	0	60.26	8.14
P-245	J-226	J-228	33	90	HDPE	0.065	145	0.293	0.06	0	60.25	8.13
P-246	J-228	J-229	65	90	HDPE	0.002	145	0.038	0.01	0	60.25	8.13
P-247	J-228	J-230	168	90	HDPE	0.009	145	0.099	0.02	0	60.25	8.06
P-248	J-231	J-223	267	110	HDPE	2.504	145	3.423	0.47	0.67	60.29	8.09
P-249	J-231	J-233	139	90	HDPE	0.712	145	1.065	0.21	0.1	59.52	7.41
P-250	J-231	J-246	689	90	HDPE	1.364	145	1.513	0.3	0.94	58.68	11.42
P-251	J-232	J-231	171	90	HDPE	0.009	145	0.1	0.02	0	59.62	7.39
P-252	J-233	J-234	67	90	HDPE	0.002	145	0.039	0.01	0	59.52	7.41
P-253	J-233	J-235	58	90	HDPE	0.49	145	0.87	0.17	0.03	59.49	7.27
P-254	J-235	J-236	28	90	HDPE	0.004	145	0.062	0.01	0	59.49	7.38
P-255	J-235	J-238	52	90	HDPE	0.352	145	0.728	0.14	0.02	59.47	7.35
P-256	J-236	J-237	39	90	HDPE	0.001	145	0.023	0	0	59.49	7.27

P-257	J-238	J-239	89	90	HDPE	0.003	145	0.052	0.01	0	59.47	7.25
P-258	J-238	J-240	41	90	HDPE	0.222	145	0.568	0.11	0.01	59.46	7.27
P-259	J-240	J-242	125	90	HDPE	0.121	145	0.41	0.08	0.02	59.45	7.33
P-260	J-240	J-241	51	90	HDPE	0.001	145	0.03	0.01	0	59.46	7.27
P-261	J-242	J-243	109	90	HDPE	0.057	145	0.272	0.05	0.01	59.44	12.26
P-262	J-243	J-244	124	90	HDPE	0.016	145	0.135	0.03	0	59.44	7.33
P-263	J-244	J-245	53	90	HDPE	0.001	145	0.031	0.01	0	59.44	7.25
P-264	J-246	J-247	174	90	HDPE	0.021	145	0.159	0.03	0	58.68	11.55
P-265	J-246	J-249	249	90	HDPE	0.328	145	0.701	0.14	0.08	58.6	11.34
P-266	J-247	J-248	48	90	HDPE	0.001	145	0.028	0.01	0	58.68	11.41
P-267	J-249	J-250	212	90	HDPE	0.013	145	0.125	0.02	0	58.6	11.47
P-268	J-251	J-249	260	90	HDPE	0.019	145	0.153	0.03	0.01	58.6	11.34

ANNEXURE-2

Output Parameters for Hydraulic Analysis

JUNCTION TABLE				
Label	Elevation (m)	Demand (L/s)	Hydraulic Grade (m)	Pressure (m H2O)
J-1	49.16	0.575	68.06	18.86
J-2	47.24	0.404	66.8	19.52
J-3	47.16	1.303	65.88	18.68
J-4	47.09	0.322	65.54	18.42
J-5	47.11	0.132	65.3	18.16
J-6	47.16	0.309	65.17	17.97
J-7	47.09	0.197	65.11	17.99
J-8	52.16	0.315	65.1	12.91
J-9	47.16	0.303	64.95	17.75
J-10	52.09	0.199	64.83	12.71
J-11	47.15	0.258	64.83	17.64
J-12	47.09	0.184	64.81	17.68
J-13	47.24	0.101	64.81	17.53
J-14	47.09	0.023	64.81	17.68
J-15	52.15	0.149	64.74	12.56
J-16	52.1	0.177	64.73	12.61
J-17	52.16	0.092	64.73	12.54
J-18	47.18	0.429	64.69	17.47

J-19	52.1	0.102	64.63	12.5
J-20	47.15	0.566	64.6	17.41
J-21	47.18	0.223	64.56	17.34
J-22	47.15	0.21	64.56	17.37
J-23	47.16	0.157	64.54	17.35
J-24	47.24	0.156	64.54	17.27
J-25	47.16	0.033	64.54	17.35
J-26	47.24	0.129	64.54	17.26
J-27	47.24	0.036	64.54	17.26
J-28	47.15	0.061	64.54	17.35
J-29	47.21	0.197	64.53	17.29
J-30	47.16	0.06	64.53	17.34
J-31	47.15	0.066	64.53	17.35
J-32	52.16	0.282	64.5	12.32
J-33	52.18	0.117	64.49	12.29
J-34	52.18	0.035	64.49	12.29
J-35	52.15	0.095	64.49	12.32
J-36	52.21	0.252	64.48	12.24
J-37	47.24	0.1	64.48	17.2
J-38	47.09	0.033	64.48	17.35
J-39	52.1	0.038	64.47	12.34
J-40	52.15	0.225	64.47	12.29
J-41	52.21	0.121	64.44	12.21
J-42	52.21	0.037	64.44	12.21
J-43	52.11	0.1	64.44	12.31
J-44	52.15	0.051	64.44	12.27
J-45	52.21	0.178	64.41	12.18

J-46	52.11	0.023	64.41	12.28
J-47	47.21	0.164	64.37	17.12
J-48	52.12	0.16	64.34	12.2
J-49	52.15	0.025	64.34	12.17
J-50	47.09	0.092	64.33	17.21
J-51	47.21	0.11	64.33	17.09
J-52	47.15	0.104	64.33	17.15
J-53	47.09	0.062	64.33	17.2
J-54	47.24	0.123	64.33	17.05
J-55	47.12	0.01	64.33	17.17
J-56	47.18	0.253	64.33	17.11
J-57	47.12	0.096	64.33	17.17
J-58	47.15	0.186	64.32	17.14
J-59	47.24	0.047	64.32	17.05
J-60	47.09	0.107	64.32	17.2
J-61	47.18	0.495	64.32	17.1
J-62	47.09	0.156	64.31	17.19
J-63	52.21	0.098	64.3	12.06
J-64	52.1	0.194	64.26	12.14
J-65	52.21	0.383	64.24	12
J-66	53.04	0.071	64.24	11.18
J-67	52.09	0.212	64.22	12.11
J-68	52.24	0.202	64.2	11.94
J-69	53.21	0.123	64.2	10.97
J-70	52.24	0.077	64.2	11.94
J-71	52	0.104	64.2	12.17
J-72	52.16	0.307	64.2	12.01

J-73	52.12	0.139	64.19	12.05
J-74	52.09	0.115	64.18	12.06
J-75	52.21	0.075	64.18	11.94
J-76	52.18	0.096	64.17	11.96
J-77	52.11	0.024	64.17	12.03
J-78	52.1	0.09	64.17	12.04
J-79	52.24	0.046	64.17	11.9
J-80	52.18	0.018	64.17	11.96
J-81	52.11	0.055	64.17	12.03
J-82	52.24	0.029	64.17	11.9
J-83	52.09	0.061	64.17	12.05
J-84	52.1	0.046	64.16	12.04
J-85	52.24	0.08	64.15	11.89
J-86	52.24	0.035	64.15	11.89
J-87	52.1	0.059	64.14	12.02
J-88	52.18	0.174	64.14	11.94
J-89	52.1	0.111	64.13	12.01
J-90	52.24	0.104	64.13	11.87
J-91	52.1	0.168	64.13	12
J-92	52.09	0.086	64.13	12.01
J-93	52.24	0.197	64.12	11.85
J-94	52.12	0.016	64.12	11.97
J-95	52.24	0.045	64.12	11.85
J-96	52.1	0.271	64.09	11.97
J-97	52.24	0.049	64.09	11.83
J-98	52.16	0.115	64.09	11.91
J-99	47.18	0.382	64.07	16.85

J-100	47.09	0.128	64.06	16.94
J-101	53.11	0.968	64.01	10.88
J-102	53.21	0.126	63.98	10.75
J-103	53.4	0.023	63.98	10.56
J-104	53.4	0.067	63.98	10.56
J-105	53.21	0.078	63.98	10.75
J-106	53.21	0.021	63.98	10.75
J-107	53.21	0.128	63.98	10.74
J-108	53.04	0.224	63.97	10.91
J-109	53.21	0.046	63.97	10.74
J-110	53.04	0.018	63.97	10.91
J-111	53.11	0.12	63.97	10.84
J-112	47.21	0.369	63.96	16.72
J-113	47.24	0.079	63.96	16.69
J-114	53.04	0.14	63.93	10.87
J-115	53.4	0.058	63.93	10.51
J-116	53.04	0.021	63.93	10.87
J-117	53.21	0.372	63.89	10.66
J-118	52.15	0.057	63.89	11.72
J-119	52.15	0.111	63.89	11.72
J-120	53.21	0.159	63.88	10.65
J-121	53.4	0.033	63.88	10.46
J-122	53.04	0.321	63.84	10.78
J-123	53.01	0.136	63.83	10.8
J-124	53.11	0.018	63.83	10.7
J-125	52.12	0.576	63.83	11.69
J-126	53.01	0.193	63.83	10.8

J-127	53.01	0.044	63.83	10.8
J-128	53.11	0.061	63.83	10.7
J-129	53.04	0.129	63.82	10.76
J-130	53.4	0.041	63.82	10.4
J-131	53.21	0.177	63.82	10.59
J-132	53.4	0.034	63.82	10.4
J-133	53.11	0.104	63.82	10.69
J-134	47.18	0.158	63.69	16.48
J-135	47	0.086	63.69	16.65
J-136	47.18	0.038	63.69	16.47
J-137	47.11	0.112	63.5	16.36
J-138	47.1	0.026	63.5	16.37
J-139	47.1	0.117	63.37	16.24
J-140	47.21	0.048	63.37	16.13
J-141	47.18	0.142	63.27	16.05
J-142	47.1	0.062	63.27	16.13
J-143	52.16	0.275	63.23	11.05
J-144	52.09	0.116	63.23	11.12
J-145	52.18	0.096	63.18	10.98
J-146	47.11	0.153	63.14	15.99
J-147	53.21	0.092	63.12	9.89
J-148	52.15	0.385	63.11	10.94
J-149	47.1	0.112	63.07	15.94
J-150	52.18	0.156	63.05	10.85
J-151	53.21	0.116	63.04	9.81
J-152	47.11	0.153	63.02	15.88
J-153	53.01	0.119	62.93	9.9

J-154	52.11	0.066	62.93	10.8
J-155	53.01	0.035	62.89	9.86
J-156	53.11	0.067	62.84	9.71
J-157	53.21	0.035	62.84	9.61
J-158	53.11	0.018	62.84	9.71
J-159	52.24	0.226	62.83	10.57
J-160	53.21	0.186	62.82	9.59
J-161	47.15	0.087	62.82	15.64
J-162	53.04	0.075	62.76	9.7
J-163	53.21	0.025	62.76	9.53
J-164	52.09	0.138	62.75	10.64
J-165	52.12	0.258	62.74	10.6
J-166	52.16	0.043	62.74	10.56
J-167	52.24	0.098	62.74	10.48
J-168	52.24	0.099	62.74	10.48
J-169	47.18	0.259	62.74	15.53
J-170	47.1	0.078	62.74	15.61
J-171	47.21	0.028	62.74	15.5
J-172	52.09	0.104	62.72	10.61
J-173	52.21	0.25	62.66	10.43
J-174	52.16	0.579	62.64	10.45
J-175	52.18	0.102	62.63	10.43
J-176	53.11	0.106	62.58	9.45
J-177	53.4	0.072	62.57	9.15
J-178	52.18	0.09	62.57	10.37
J-179	52.21	0.087	62.57	10.34
J-180	52.24	0.04	62.57	10.31

J-181	53.4	0.079	62.57	9.15
J-182	53.04	0.086	62.57	9.51
J-183	53.11	0.037	62.57	9.44
J-184	52.18	0.089	62.56	10.36
J-185	53.01	0.153	62.56	9.54
J-186	53.4	0.075	62.56	9.15
J-187	52.11	0.167	62.56	10.43
J-188	52.09	0.103	62.56	10.45
J-189	52.09	0.101	62.56	10.45
J-190	47.15	0.428	62.18	15
J-191	47.09	0.211	62.17	15.05
J-192	47.11	0.113	62.07	14.93
J-193	47.21	0.026	62.07	14.83
J-194	47.24	0.165	62.04	14.77
J-195	47.1	0.134	62.02	14.89
J-196	47.24	0.189	62.02	14.75
J-197	47.24	0.117	62.02	14.75
J-198	47.1	0.118	62.02	14.89
J-199	47.24	0.08	62.02	14.75
J-200	47.1	0.034	62.02	14.89
J-201	47.18	0.184	62.01	14.8
J-202	47.21	0.054	62.01	14.77
J-203	47.24	0.085	62.01	14.75
J-204	52.16	0.704	61.6	9.42
J-205	52.12	0.273	61.57	9.43
J-206	52.1	0.727	61.17	9.05
J-207	52.12	0.357	60.98	8.84

J-208	53	0.179	60.96	7.95
J-209	53.04	0.252	60.94	7.88
J-210	53.4	0.018	60.94	7.52
J-211	52.16	0.101	60.94	8.76
J-212	52.24	0.241	60.69	8.43
J-213	52.4	0.138	60.68	8.26
J-214	52.24	0.057	60.68	8.42
J-215	53.11	0.186	60.54	7.42
J-216	52.21	0.075	60.54	8.32
J-217	53.04	0.097	60.49	7.44
J-218	53.04	0.029	60.49	7.44
J-219	52.11	0.167	60.46	8.33
J-220	52.11	0.066	60.46	8.33
J-221	52.4	0.419	60.41	8
J-222	52.12	0.347	60.36	8.22
J-223	52.18	0.566	60.29	8.09
J-224	52.1	0.213	60.28	8.16
J-225	52.21	0.128	60.27	8.05
J-226	52.11	0.168	60.26	8.13
J-227	52.1	0.044	60.26	8.14
J-228	52.11	0.156	60.25	8.13
J-229	52.11	0.038	60.25	8.13
J-230	52.18	0.099	60.25	8.06
J-231	52.21	0.744	59.62	7.39
J-232	52.24	0.1	59.62	7.36
J-233	52.1	0.155	59.52	7.41
J-234	52.1	0.039	59.52	7.41

J-235	52.21	0.081	59.49	7.27
J-236	52.1	0.039	59.49	7.38
J-237	52.21	0.023	59.49	7.27
J-238	52.11	0.107	59.47	7.35
J-239	52.21	0.052	59.47	7.25
J-240	52.18	0.128	59.46	7.27
J-241	52.18	0.03	59.46	7.27
J-242	52.1	0.138	59.45	7.33
J-243	47.16	0.137	59.44	12.26
J-244	52.1	0.104	59.44	7.33
J-245	52.18	0.031	59.44	7.25
J-246	47.24	0.653	58.68	11.42
J-247	47.1	0.131	58.68	11.55
J-248	47.24	0.028	58.68	11.41
J-249	47.24	0.424	58.6	11.34
J-250	47.1	0.125	58.6	11.47
J-251	47.15	0.153	58.59	11.42